Better Decisions, Better Products
Through Simulation & Innovation

Simulation of Electron Kinetics in Gas Discharges

by

Vladimir Kolobov and Robert Arslanbekov

2005 Workshop on Nonlocal, Collisionless Electron Transport in Plasmas

Princeton, NJ
August 4, 2005

CFD Research Corporation
www.cfdrc.com
215 Wynn Drive • Huntsville, Alabama 35805 • Tel: (256) 726-4800 • FAX: (256) 726-4806 • info@cfdrc.com

Outline

- An overview of basic models for simulations of electron kinetics in gas discharges
- Examples of simulations using CFD-ACE+
  - Inductively Coupled Plasmas
  - Capacitively Coupled Plasmas
  - Direct current glow discharges with different electrodes
  - Physical phenomena in Positive Column of rare gases
  - Ionization Waves (Striations) in rare gases
- Simulations using UFS collisionless effects with Vlasov & PIC codes

From Boltzmann to FPE for electrons

Hierarchy of transport models for electrons

6D : $f(\vec{v},\vec{r},t)$
Boltzman Kinetic equation

$$\frac{\partial f}{\partial t} + div_r(\vec{u}f) + div_v(\vec{a}f) = S(f)$$

$vt > \lambda$ ↓ velocity correlation time

4D : $f_0(v,\vec{r},t)$
Fokker-Planck equation

$$\frac{\partial f_0}{\partial t} + div\vec{\Gamma} = S_0(f_0)$$

$$\Gamma_\alpha = V_\alpha f_0 + D_{\alpha\beta}\frac{\partial f_0}{\partial x_\beta} \qquad \alpha,\beta = 1..4$$

$v_d t > \lambda_u$ ↓ energy correlation time

3D : $n(\vec{r},t)$
Drift-Diffusion model

$$\frac{\partial n}{\partial t} + div(\vec{v}_d n - D\nabla n) = I$$

Two-terms Spherical Harmonics Expansion

$$\mathbf{f}(\mathbf{r},\mathbf{v}.t) = f_0(\mathbf{r},v.t) + \frac{\mathbf{v}}{v}\cdot\mathbf{f}_1(\mathbf{r},v,t)$$

$$\frac{\partial f_0}{\partial t} + \frac{v}{3}\mathrm{div}(\mathbf{f}_1) + \frac{1}{3v^2}\frac{\partial}{\partial v}\left(v^2\frac{e\mathbf{E}}{m}\cdot\mathbf{f}_1\right) = S_0[f_0]$$

$$\frac{\partial \mathbf{f}_1}{\partial t} + v_m\mathbf{f}_1 + \mathbf{f}_1\times\boldsymbol{\omega}_B = -v\nabla f_0 - \frac{e\mathbf{E}}{m}\frac{\partial f_0}{\partial v}$$

momentum equation with a scalar pressure term

$$\frac{\partial n\mathbf{v}}{\partial t} + n(v_m\mathbf{v} + \mathbf{v}\times\boldsymbol{\omega}_B) = -\nabla(\frac{1}{3}nv^2) - \frac{ne\mathbf{E}}{m}$$

Limitation: in this approximation, the mean electron velocity is a *local* function of the electric field.

FPE for Electrons in Collisional Plasmas

$$\mathrm{v}\frac{\partial f_0}{\partial t} - \nabla \cdot \left[\chi \left(\nabla f_0 + \nabla \phi \frac{\partial f_0}{\partial u} \right) \right] -$$

(a)

$$\frac{\partial}{\partial u}\left[\chi \nabla \phi \cdot \left(\nabla \phi \frac{\partial f_0}{\partial u} + \nabla f_0 \right) + Y_{ee}\left(C f_0 + D \frac{\partial f_0}{\partial u} \right) + \mathrm{v} V_T f_0 + \mathrm{v} D_E \frac{\partial f_0}{\partial u} \right] = \mathrm{v} S$$

(b) (c) (d) (e) (f)

a) Transport in Configuration Space
b) Heating/Cooling by the Electrostatic Field
c) Coulomb Collisions
d) Quasi-elastic Collisions
e) Heating by alternating electromagnetic fields
f) Inelastic Collisions

Total Energy as Independent Variable

$$\varepsilon = u - \phi(\vec{\mathbf{r}}, t)$$

$$\frac{\partial}{\partial t}(vf) - \frac{\partial \phi}{\partial t}\frac{\partial}{\partial \varepsilon}(vf) - \nabla \cdot \chi \nabla f - \frac{\partial}{\partial \varepsilon}\left[Y_{ee}\left(Cf + D\frac{\partial f}{\partial u}\right) + vV_T f + vD_E \frac{\partial f}{\partial u}\right] = vS$$

- using *total* energy as independent variable eliminates complicated cross-terms in FPE and facilitates numerical solution
- the price for this simplification is more complicated boundary conditions for the trapped electrons which have to be defined on the surface of zero *kinetic* energy $\varepsilon = -\phi(\vec{\mathbf{r}}, t)$
- the energy range may substantially increase to reflect the entire range of $\phi(\vec{\mathbf{r}}, t)$ variation in computational domain

Direct Current Glow Discharges

SPICE circuit

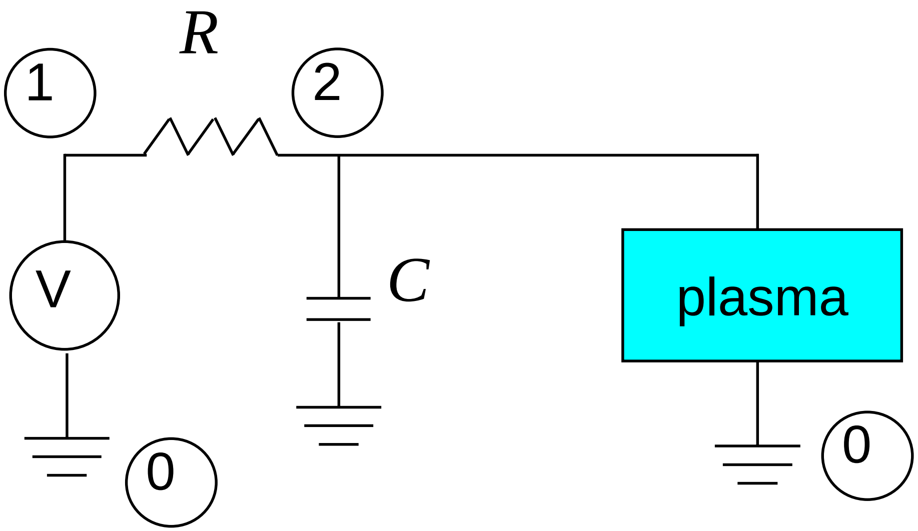

SPICE .cir file

```
abnormal DC Discharge

.model ccp ACE
+ model="twsd.2D.3Torr.100Ohm.1pF.500V.fine.DTF"
+ pin1="electric:grounded"
+ pin2="electric:RF"
+ tol=1e-2 zero=1e-12
+ minTimeStep=1ns
+ maxvoltchg=50.0
+ trace=2 minIter=2 maxIter=5
+ deriv=(0,0)
+ noCurrentUntil=5ns

.options RELTOL=0.01 VNTOL=0.5V ABSTOL=0.01A ITL4=20

Vsrc 1 0 500V
R1   2 1 100Ohm
C1   2 0 1pF

Accp 0 2 ccp

.IC V(1)=500 V(2)=500

.TRAN 1ns 50us 0ns 1ns UIC
```

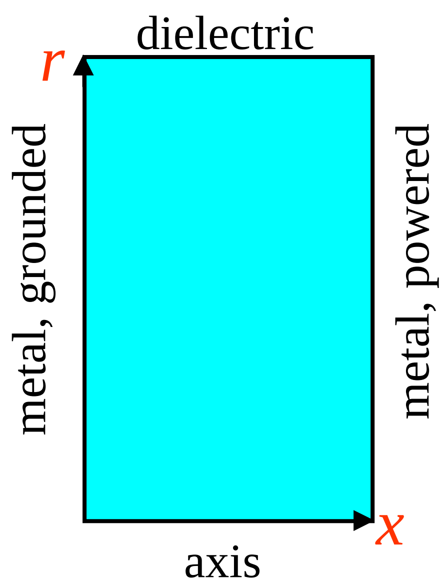

- 2D discharge geometry: R = 1.5 cm and L = 1 cm
- Ar gas at pressures of 3 and 6 Torr
- Discharge current I = 1μA-1A, voltage U = 200-400 V

Current Voltage Characteristics

Direct Current (DC) glow discharges have been studied for over a century. These discharges exist in different modes (Townsend, subnormal, normal, abnormal, etc). The transition between these modes is accompanied by redistribution of electric fields and spatial parameters of the plasma.

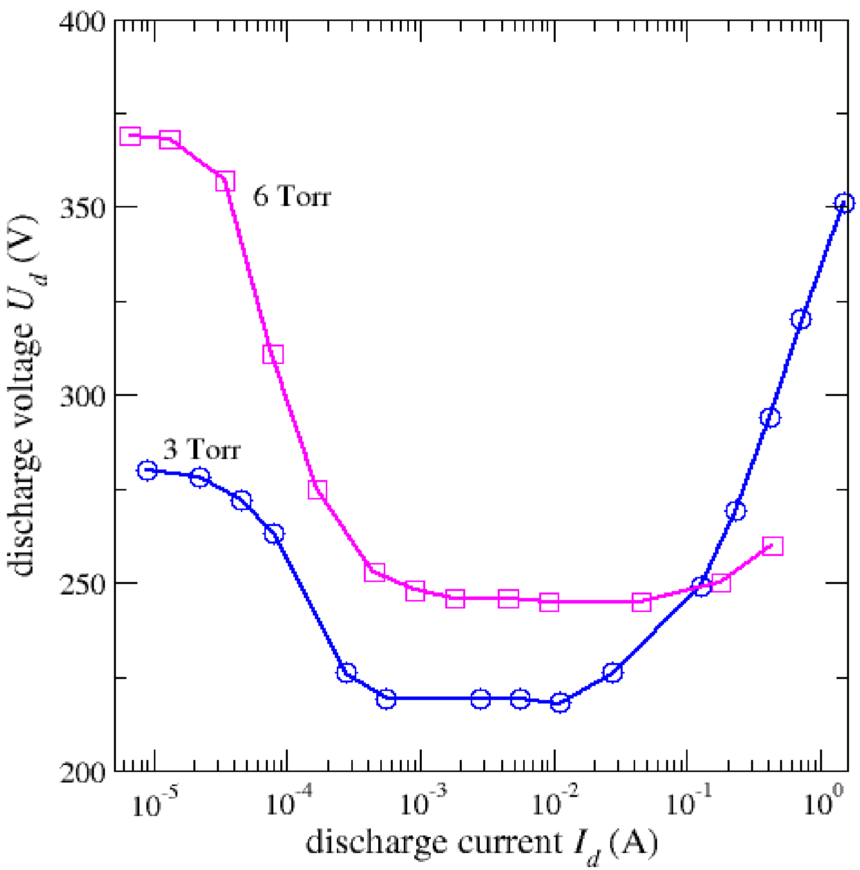

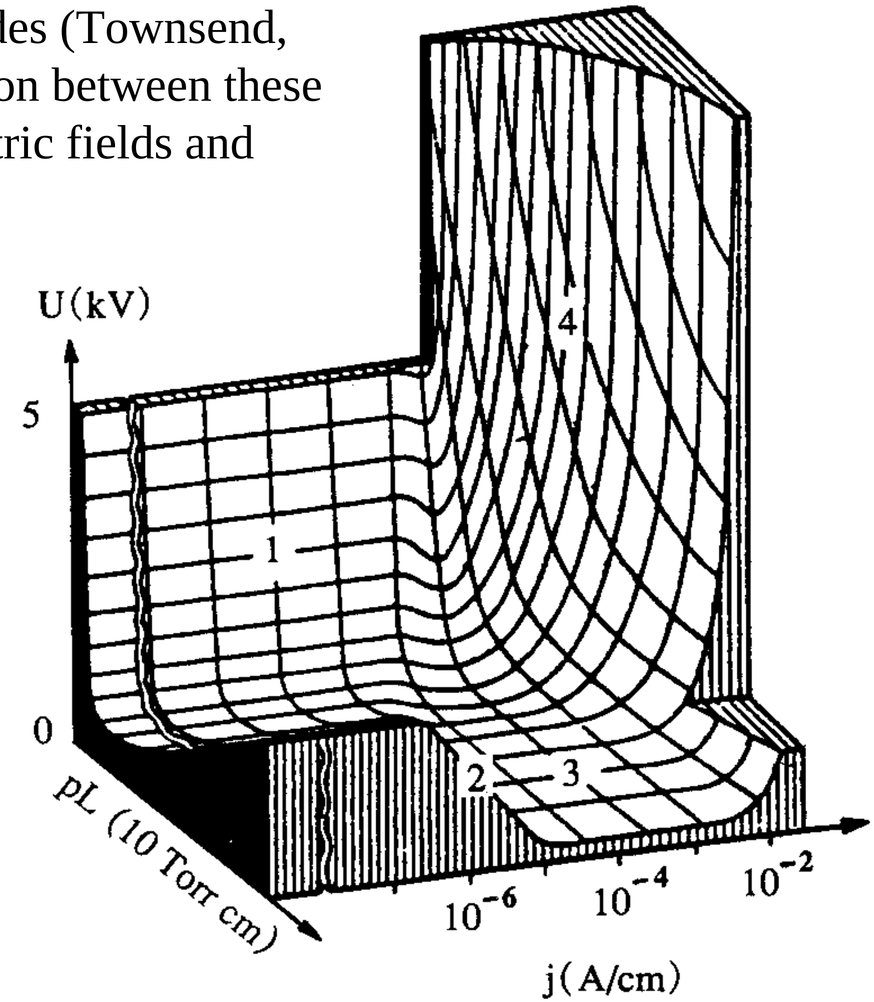

R.Arslanbekov & V.Kolobov, J. Phys. D 36, (2003)

Subnormal Oscillations

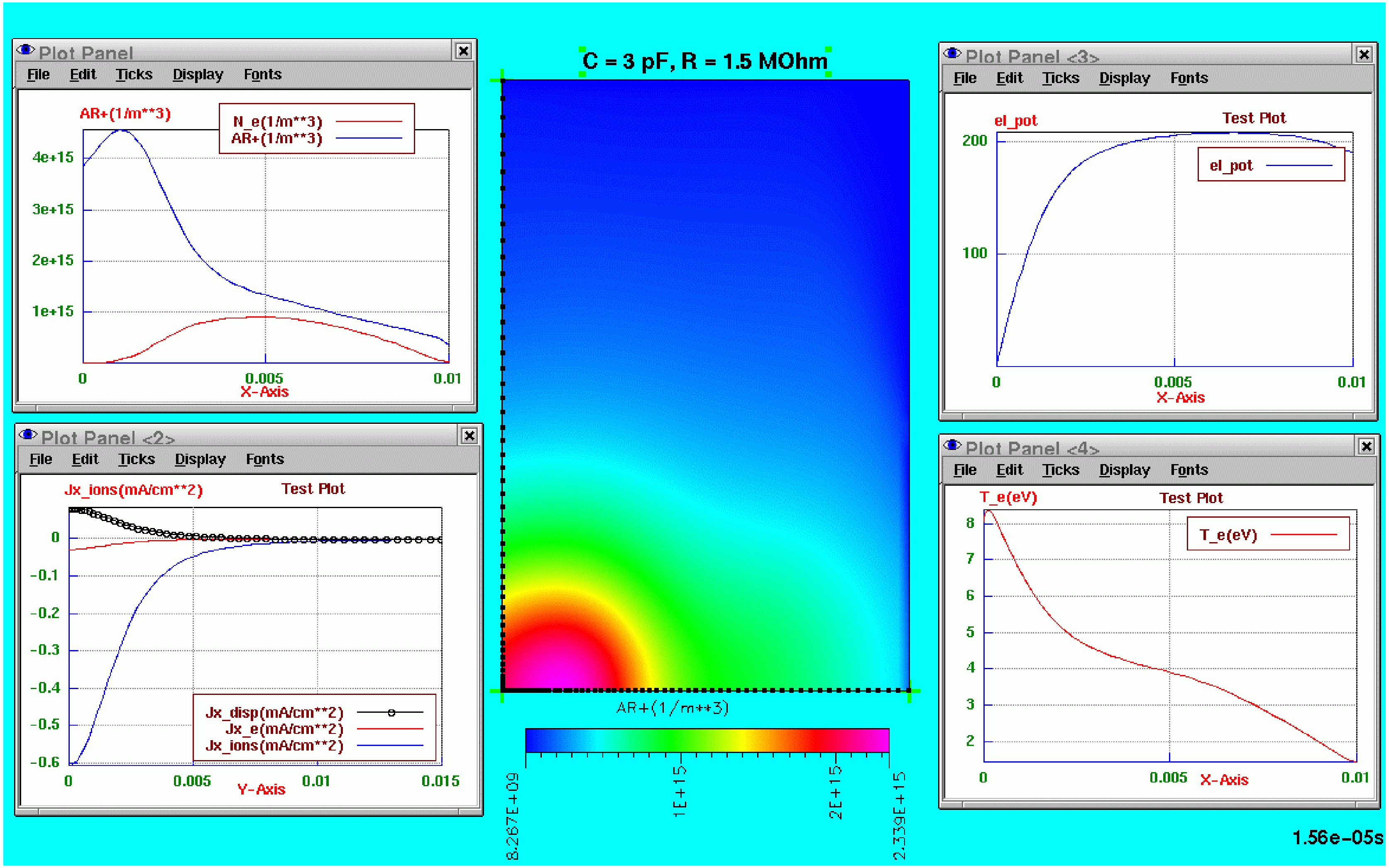

Simulations of positive column in rare gases

Electron density, temperature & potential profiles: Ar, 1 mA

⊗ E_z = 6.9, 6.2, 12.1, 31.3, 64.9, and 131.7 V/cm for p = 1, 5, 10, 25, 50 and 100 Torr.

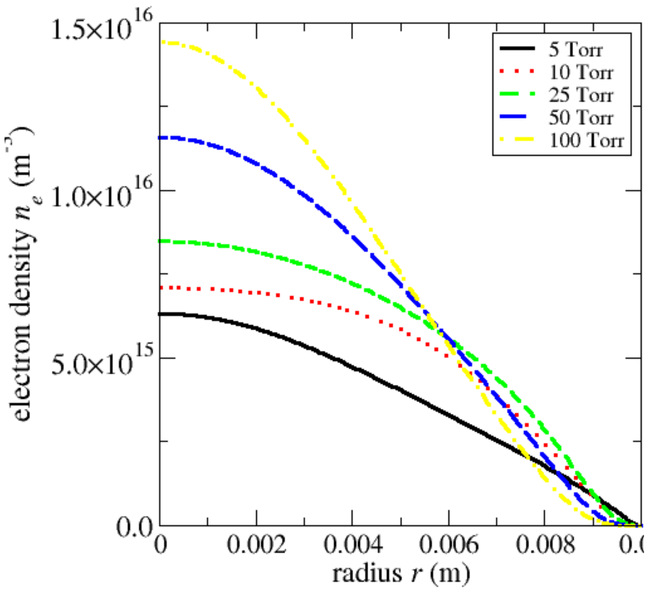

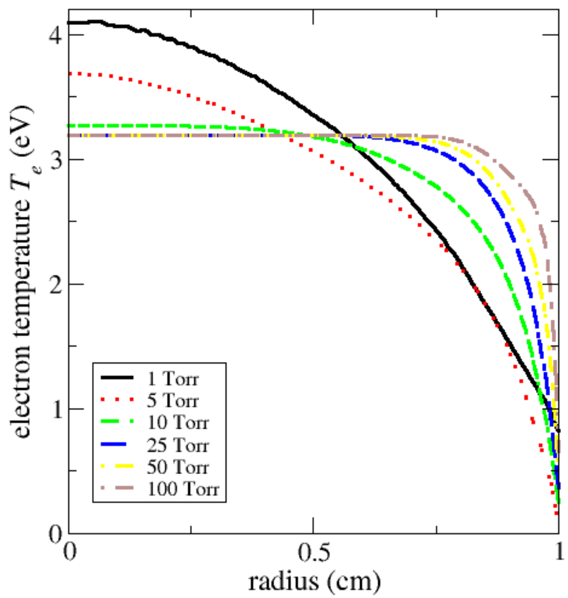

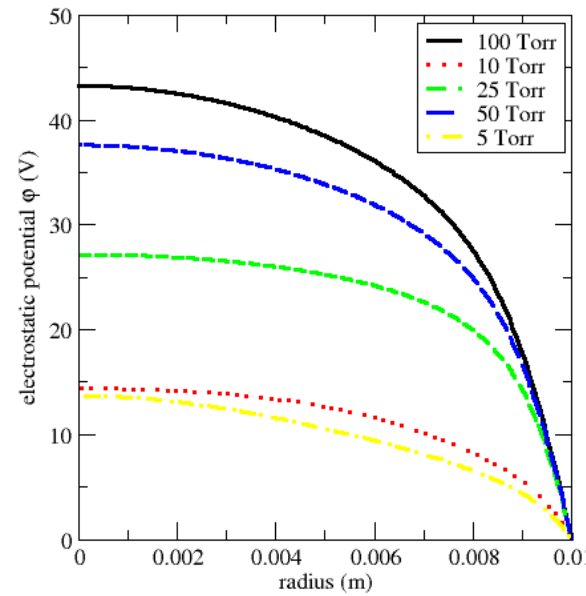

- ♦ Electron density profiles resemble a Bessel distribution
- ♦ Electron temperature profiles become more flat as pressure increases.
- ♦ potential well depth increases with pressure

Simulations of positive column in rare gases

Density of excited species: Ar, 1 mA

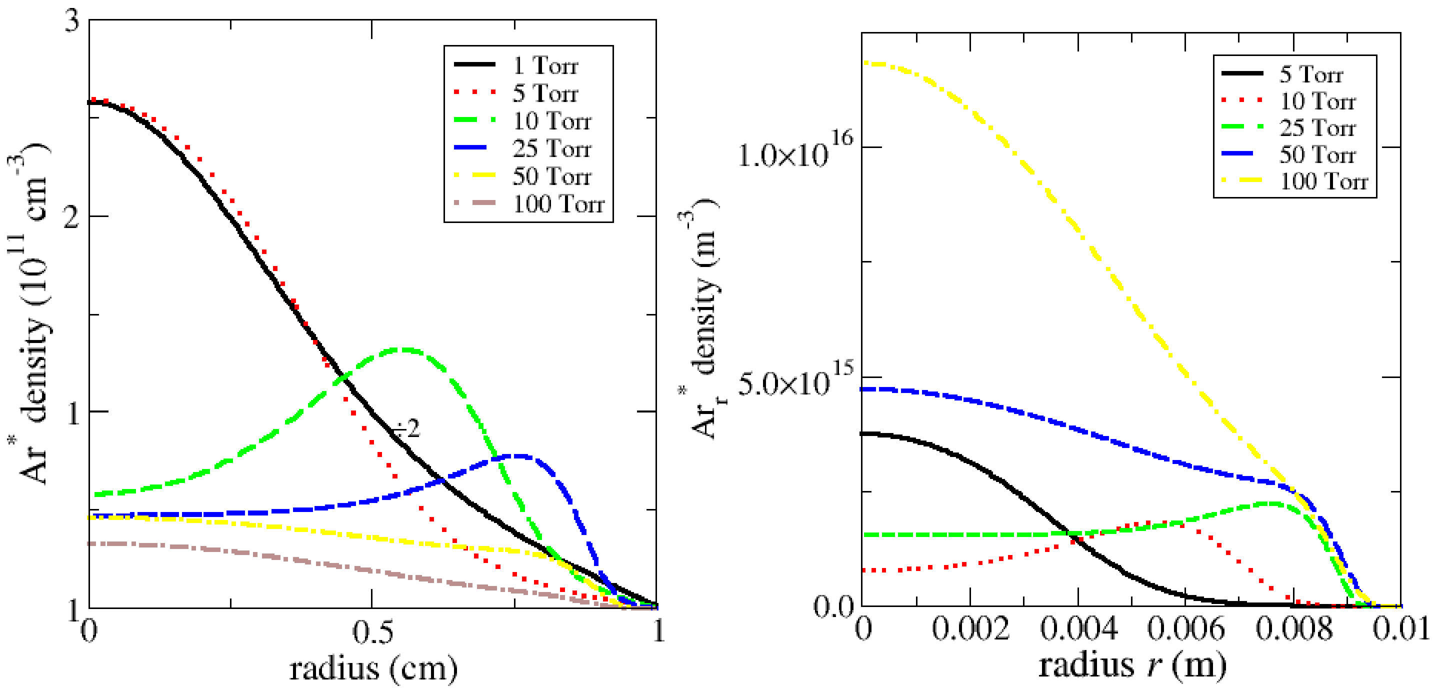

♦ non-monotonic distribution is more pronounced for Ar* than for Ar_r^*

♦ at pressures < 5 Torr and > 50 Torr, the density maximum is on axis

potential well depth increases with pressure

Simulations of positive column in rare gases

Excitation rates: Ar, 1 mA

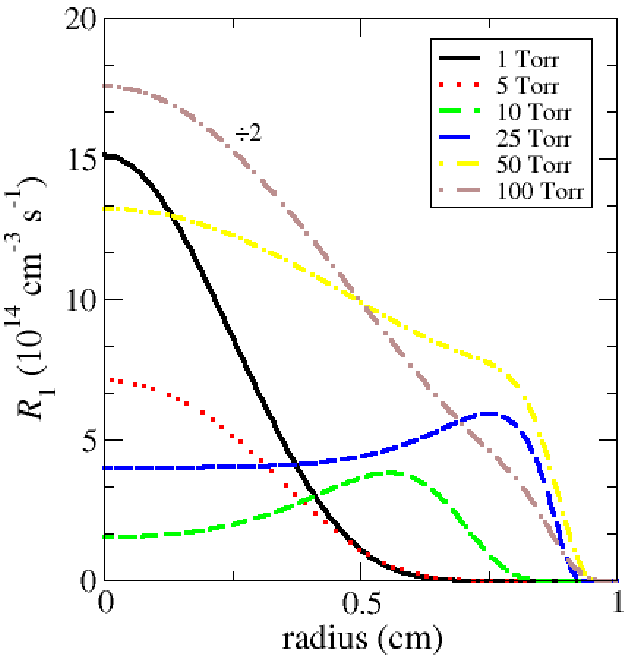

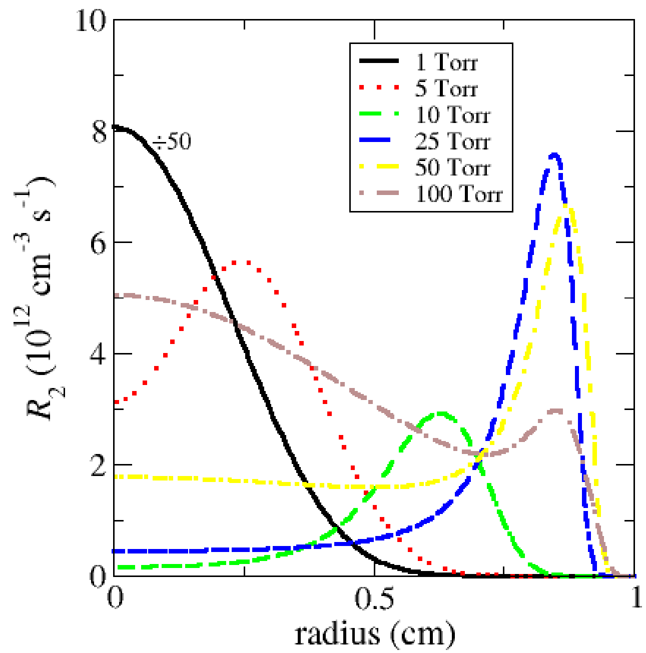

- ♦ Excitation rates have on axis maximum at p < 5 Torr and p > 50 Torr

R.Arslanbekov et al., Applied Physics Letters 85 (15), October (2004)

Moving Striations in Rare Gases

Striations = Ionization Waves

- **Striations have been studied for more than a century. They were observed at pressures 10^{-3}-10^{3} Torr and currents 10^{-4}-10 A in almost all gases**
- **Striations as a test bead for advanced plasma models: accuracy of kinetic models of gas discharges can be checked versus experimental observations accumulated over a century of studies**
- **Striations as a research tool: detailed information about the high energy part of the EEDF can be obtained, cross section set can be verified**
- **Striations as nonlinear systems: ideal object for studies of nonlinear phenomena and self-organization.**

Standing striations in Hydrogen

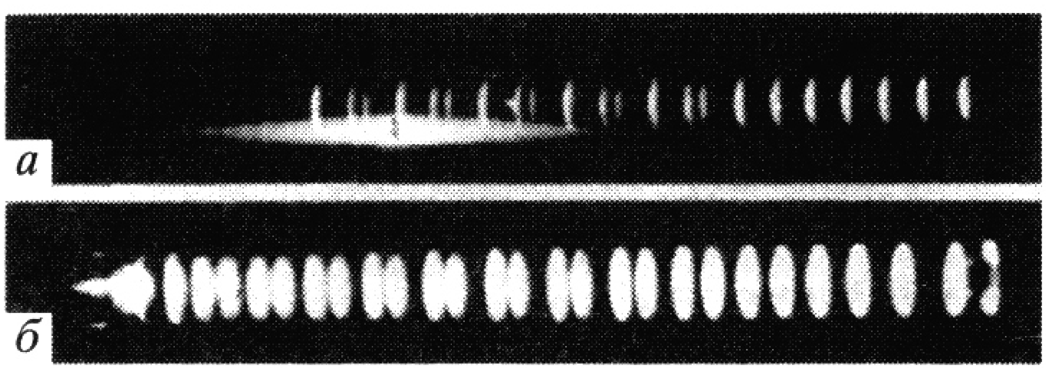

p=0.66 Torr, i=17 mA, R=2.5 cm

p=0.3 Torr, i=80 mA, R=2.75 cm

cathode is on the left

Different States of PC in Neon

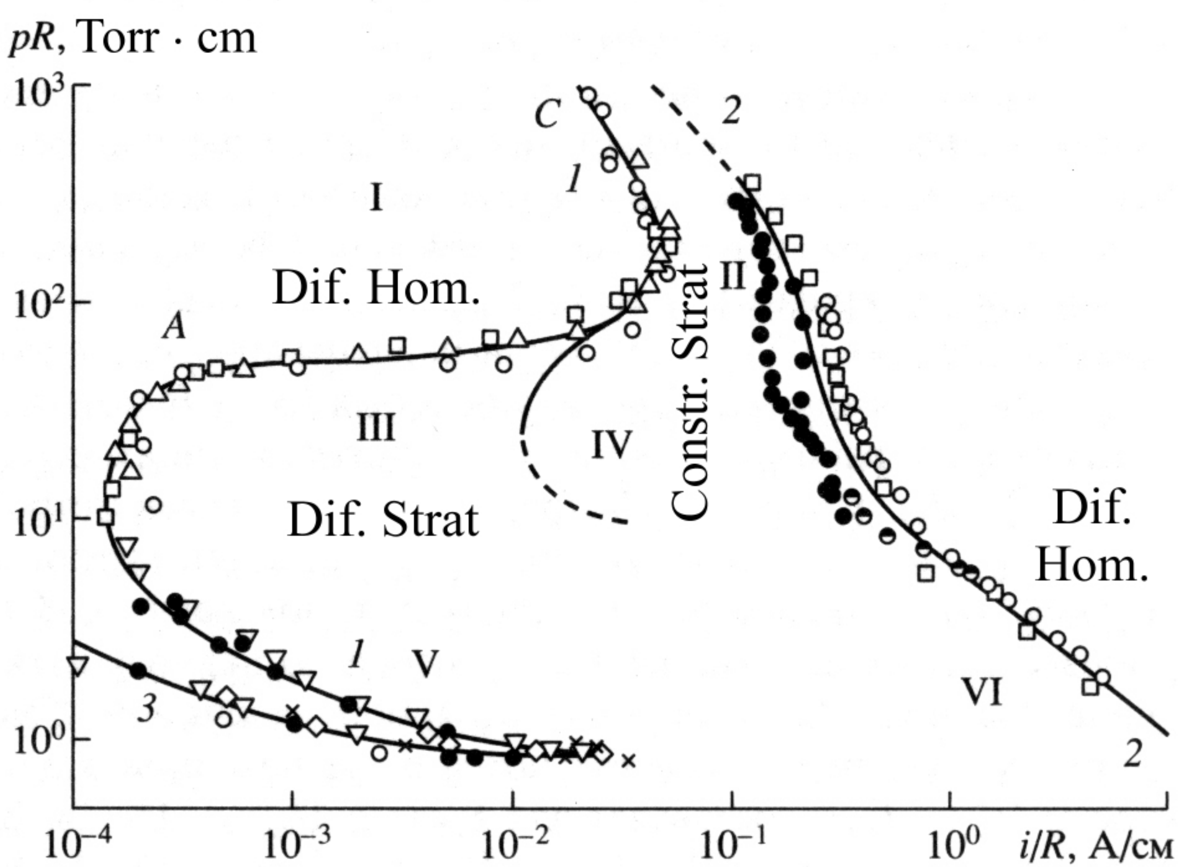

Symbols denote experimental data for different R

- ***Curve 1: Low Current Boundary***
- ***Curve 2: High Current (Pupp's) Boundary***
- ***Curve 3:* Low Pressure Boundary**
- **Area II: Current Constriction**
- **Area IV: Optical Constriction**
- **Area III: regular or chaotic striations (depending on tube length)**
- **Area V: Kinetic Striations (P, R, S types)**
- **Area VI: Hydrodynamic striations: ωk=const**

2D Simulations of Striations in Argon

• 2 Torr, 100 mA, cylindrical tube of length $L = 20$ cm and radius $R = 1$ cm, cathode on the left, anode on the right. The tube wall is dielectric. Simulation takes about 30 hours on a 1 GHz computer.

• Negative-glow region near the cathode with a large plasma density, about 3-4 striations excited along the tube.

• Striations are self-excited; they initially appear near the cathode and propagate towards the anode, group velocity is directed from cathode to anode. The phase velocity is directed from the anode to the cathode ("backward waves")

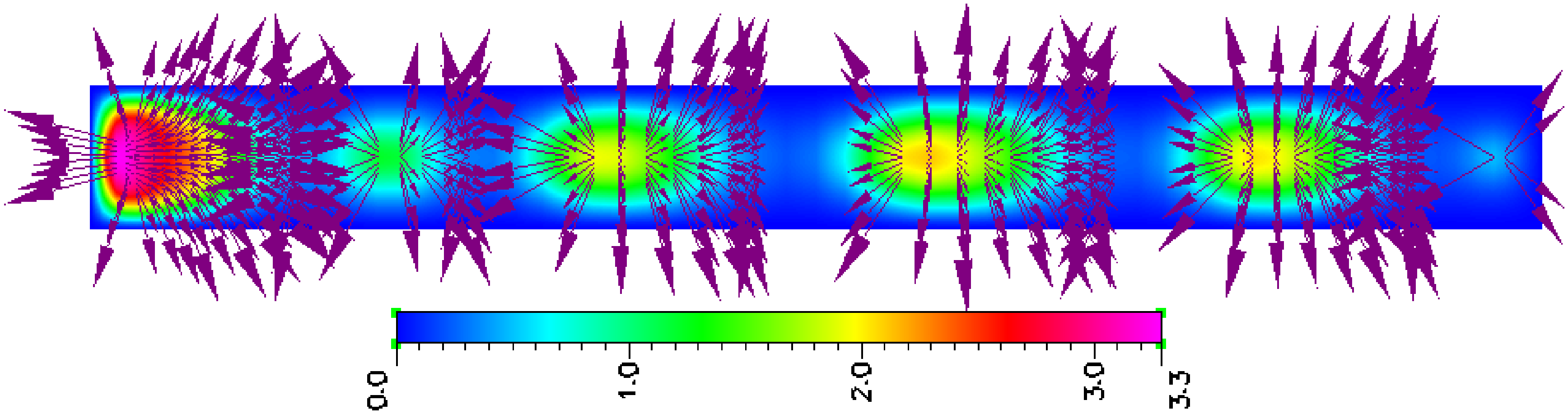

Moving Striations in Dynamics

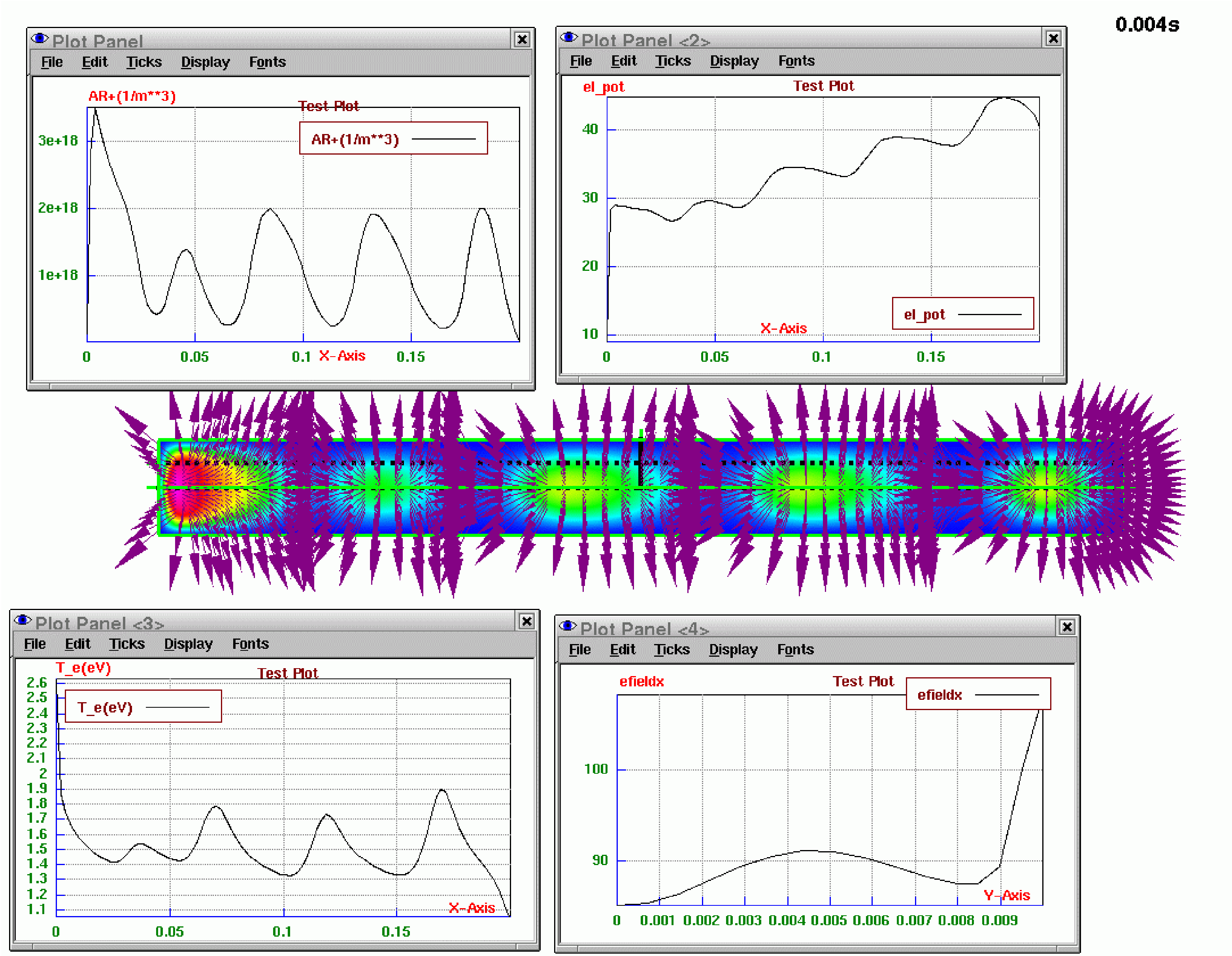

Distributions of Various Parameters

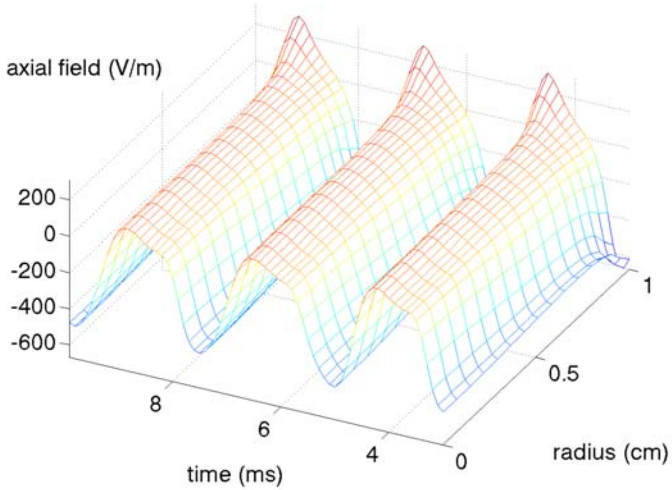

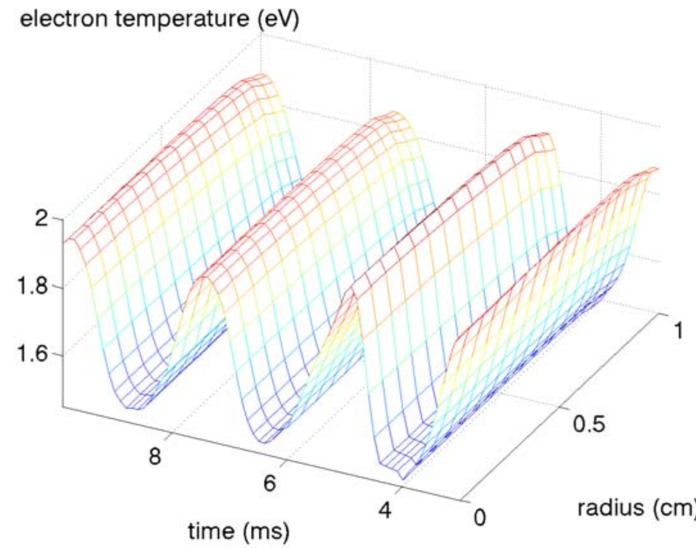

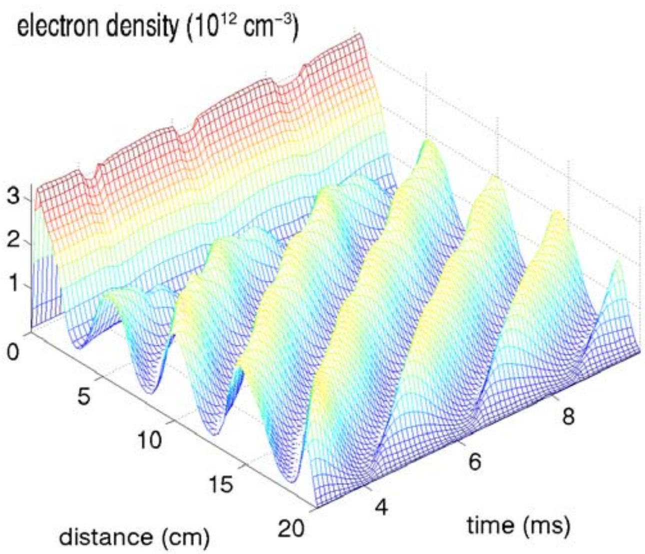

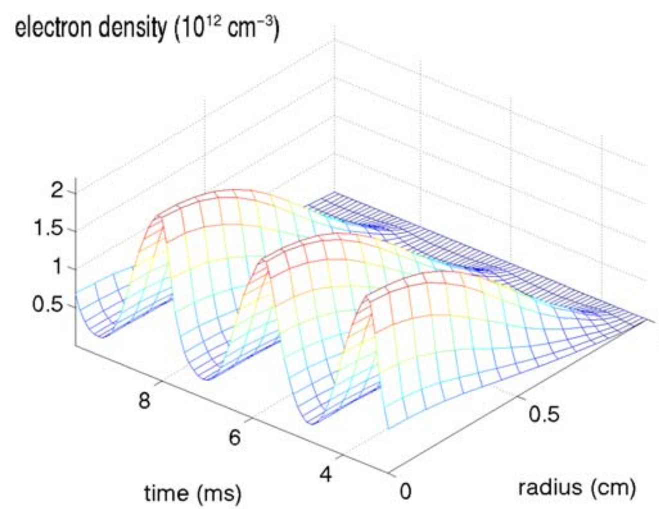

Inductively Coupled Plasmas

An Overview of Hybrid Discharge Model

- Deterministic Boltzmann solver for electrons based on two-term SHE, coupled to continuum ICP model
- Implicit Poisson solver and non-uniform mesh resolving sheath regions
- Drift-diffusion or momentum equation for ions
- Continuum model for neutral species, gas phase and surface reactions
- Gas heating (in the entire reactor) with temperature jump conditions at plasma boundaries
- Continuum gas flow model with slip wall boundary conditions, maintaining constant gas pressure in the reactor
- Maxwell solver for vector magnetic potential in time and frequency domains

Chemistry & Cross Section Data

No.	Reaction	Notes	Af	nf	pf	(E/R)f
1	E+AR->AR+E	Mom. Transfer	0	0	0	0
2	AR+E->AR*+E	Ar* excitation	0	0	0	0
3	AR+E->AR**+E	Ar** excitation	0	0	0	0
4	AR+E->AR++2E	Direct Ionization	0	0	0	0
5	AR*+E->AR++2E	stepwise ionization 1	0	0	0	0
6	AR*+E->AR+E	superelastic 1	0	0	0	0
7	AR*+E->AR**+E	excitation	0	0	0	0
8	AR**+E->AR+E	superelastic 2	0	0	0	0
9	AR**+E->AR++2E	stepwise ionization 2	0	0	0	0
10	AR**+E->AR*+E	de-excitation	0	0	0	0
11	2AR*->AR++AR+E	Penning Ionization	1E-015	0	0	0
12	2AR**->AR++AR+E	Penning Ionization	1E-015	0	0	0
13	AR**+AR*->AR++AR+E	Penning Ionization	1E-015	0	0	0
14	AR**->AR*	Penning Ionization	100000	0	0	0

Reaction mechanism and electron collision cross section data are from Vasenkov & Kushner, Phys. Rev. E 66, 66411 (2002)

Ar* denotes Ar(4s) with excitation threshold 11.6 eV
Ar** denotes Ar(4p)

The simulated Osram Sylvania ICP

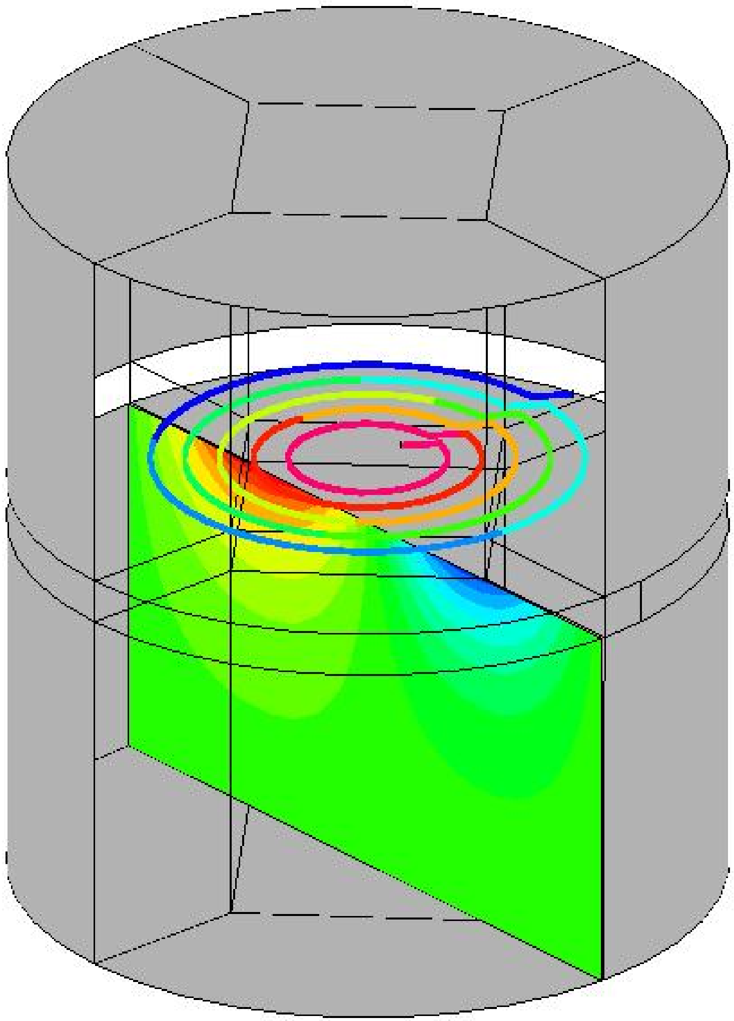

- Faraday shield eliminates capacitive coupling in the plasma
- Spatially resolved experimental EEPF measurements are performed on the axis of the reactor and at r=4 cm

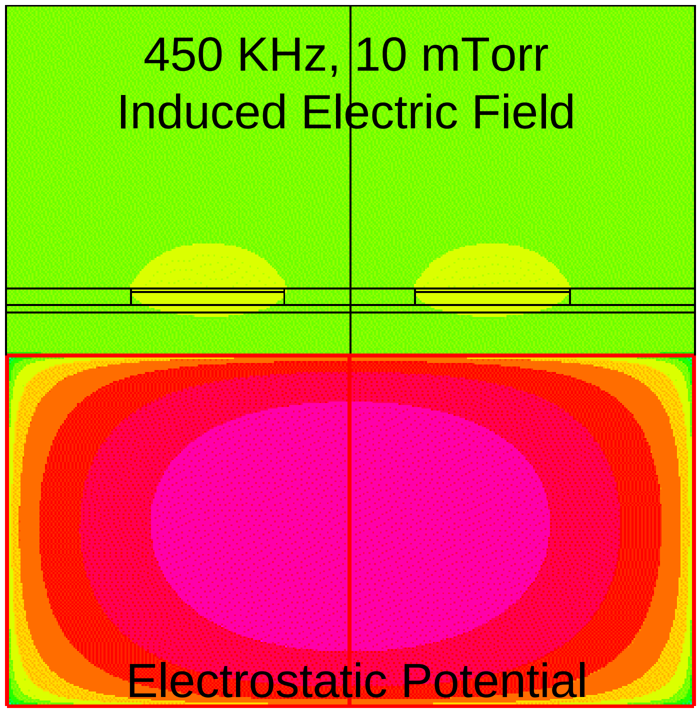

Effect of Ion Inertia

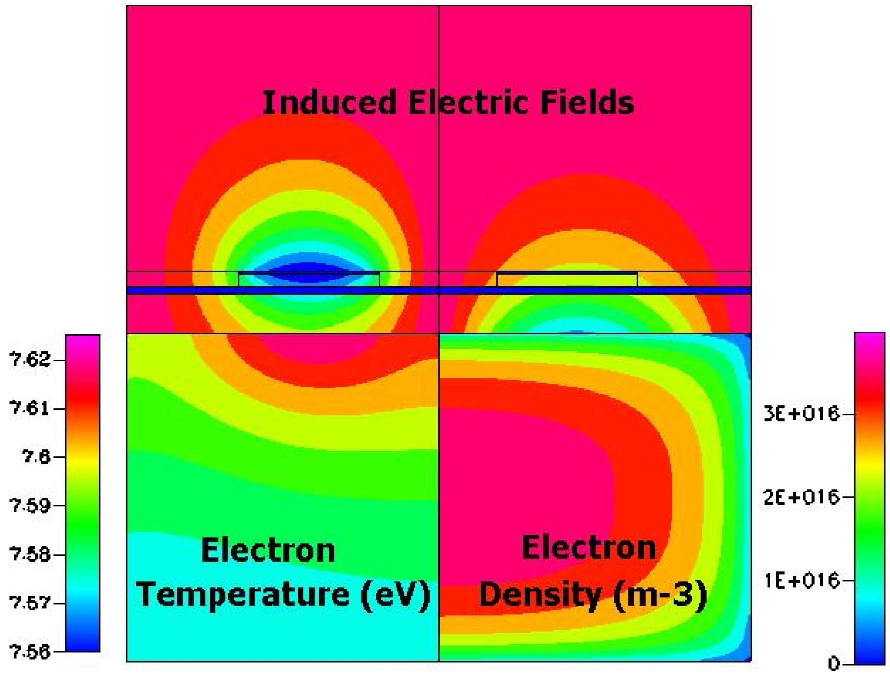

ICP in Argon, 0.3 mTorr, 100W

Solving momentum equations for ions allows simulations of plasma sources at very low gas pressures

Ion inertia becomes crucial at gas pressures below 10 mTorr

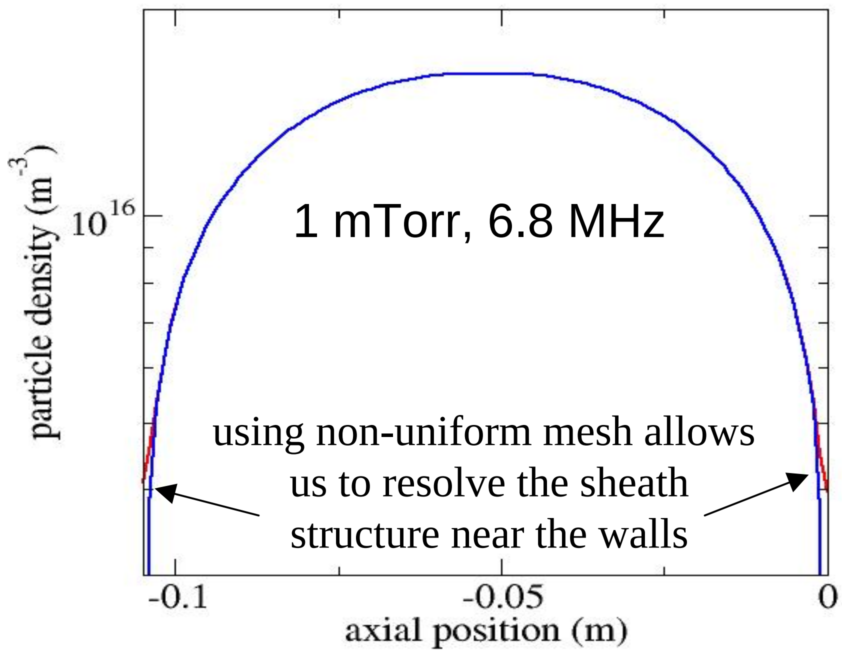

1 mT, Without Gas Heating

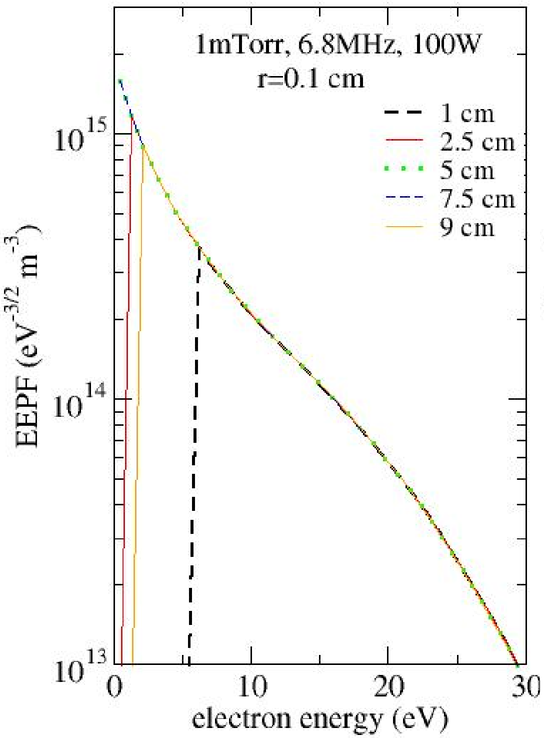

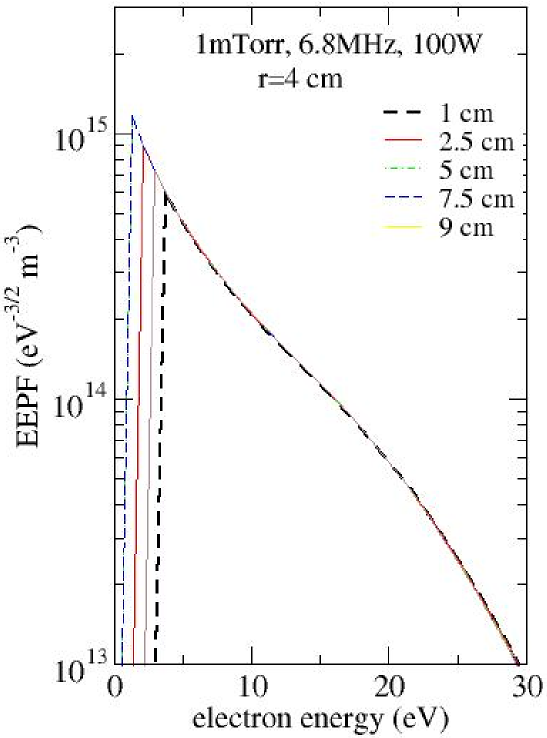

Electron (left) and metastable atom densities

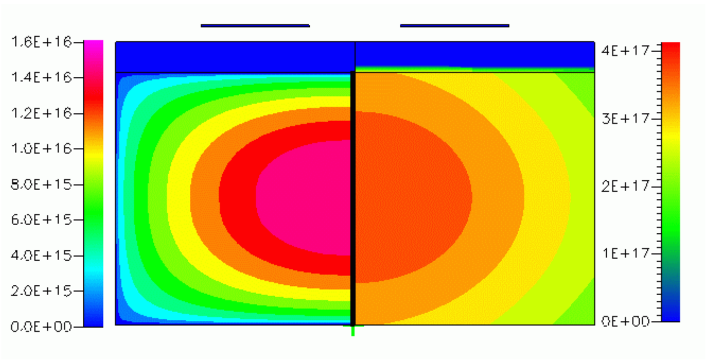

Electron temperature (left) and electrostatic potential (right)

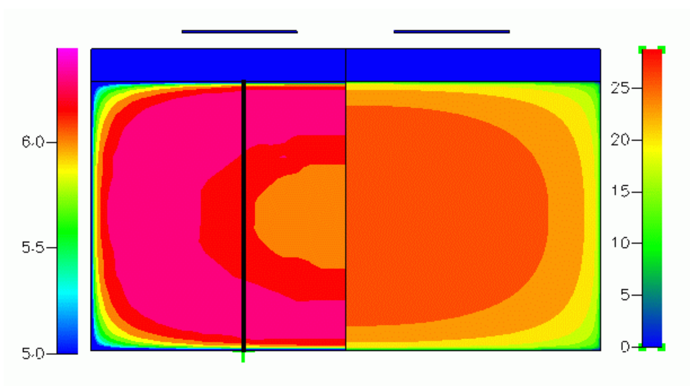

EEPF depends solely on total electron energy, no explicit dependence on spatial position

10mT, 6.8 MHz

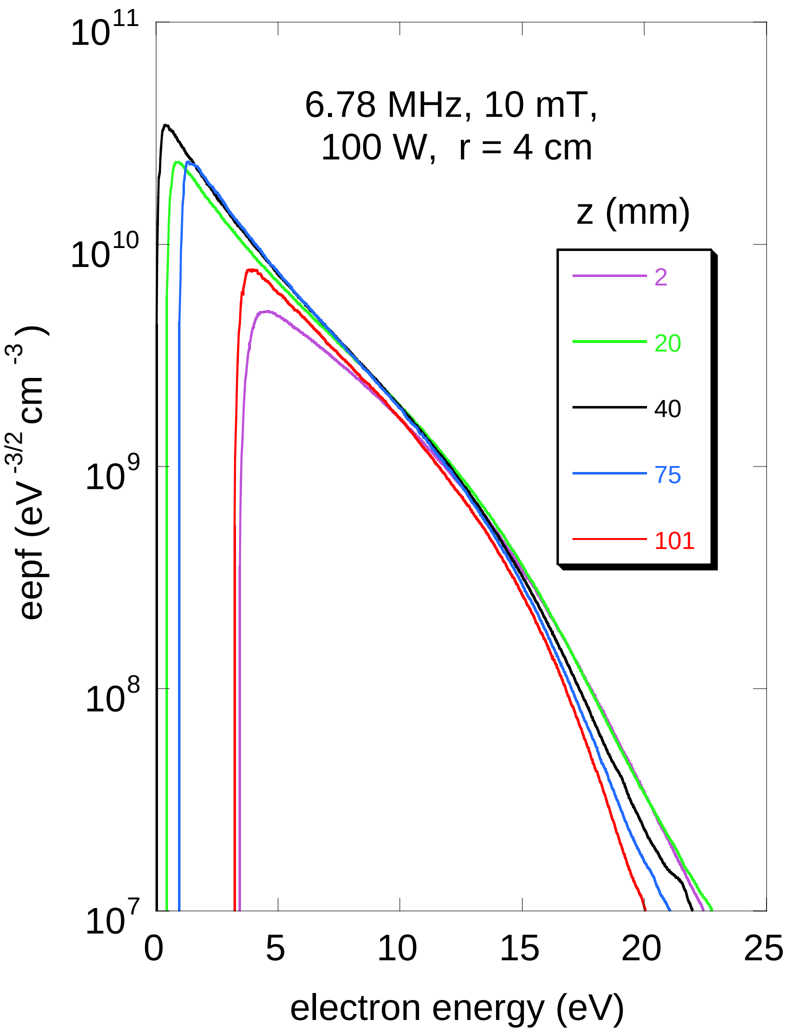

without gas heating

Electron temperature (left) and electrostatic potential (right)

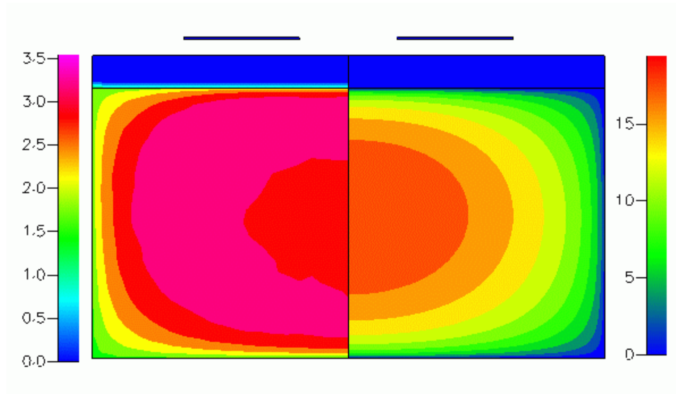

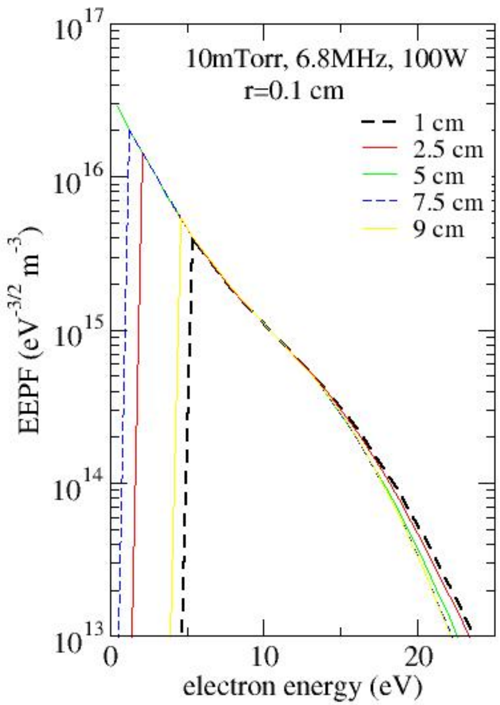

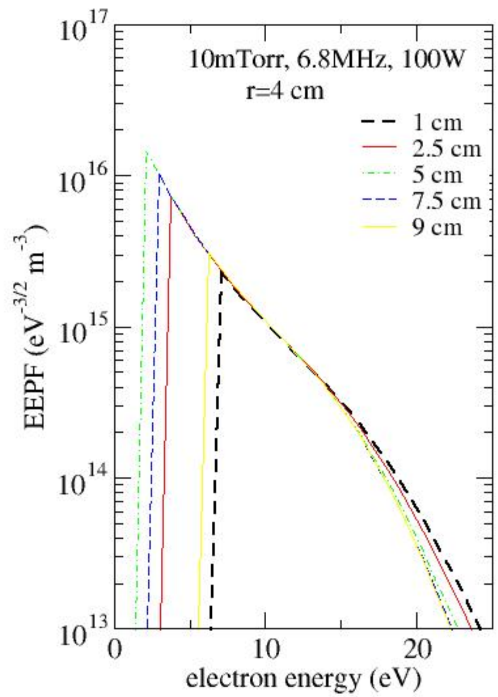

100mT, 6.8 MHz

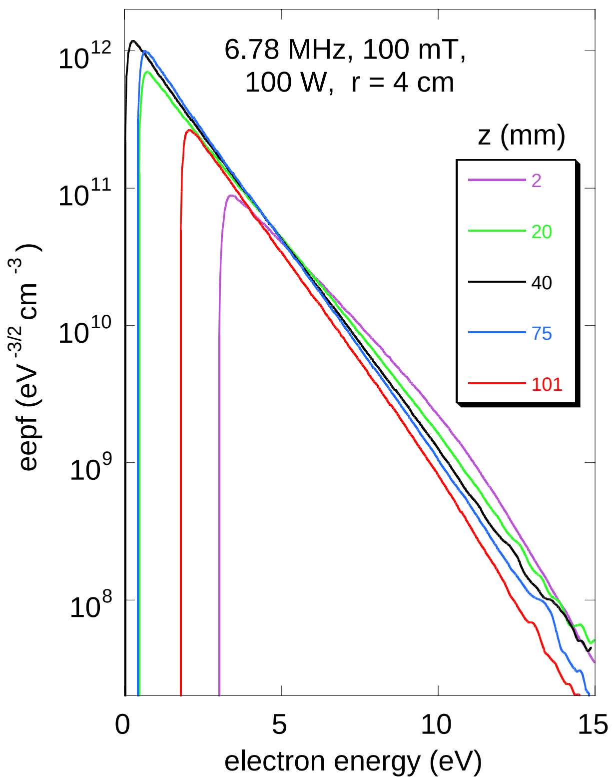

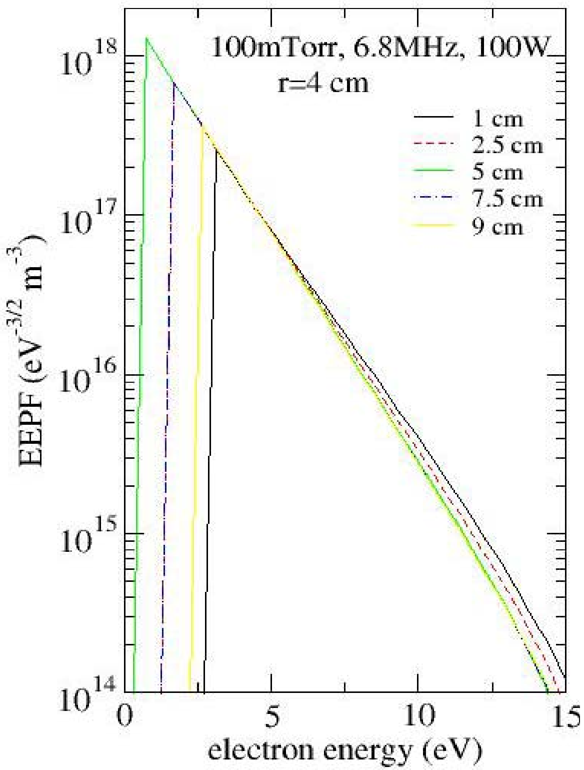

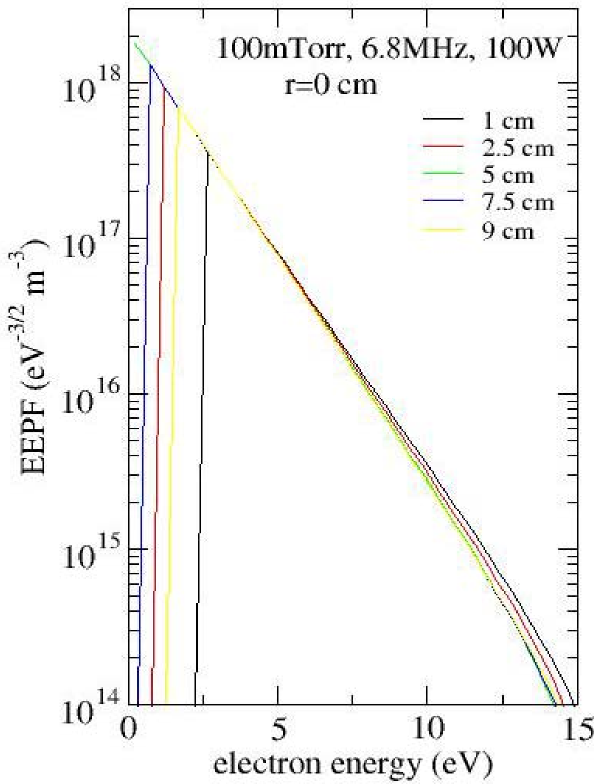

no gas heating

Time-resolved ICP Simulations

Motivation:

- **Time (RF cycle) resolved data are important for insight into ICP reactor operation. For example, recent time resolved light emission data show interesting behavior in (2D) space and time**

Simulation reactor and operation conditions:

- **Osram-Sylvania ICP reactor: Ar gas, 10 mTorr**
- **RF frequency from 450 kHz to 13.6 MHz. Simulations are presented for frequency of 450 kHz.**
- **Coil currents up to 200 A and RF powers 50 – 400 W**

Pulsed ICP Simulations

- **Osram-Sylvania ICP reactor: Ar gas, 10 mTorr, 6.8 MHz**
- **Pulsed (square) coil current: 50-400 A**
- **Pulse length: 30 and 50 μs**
- **Repetition rate : 100 μs**

- **fluid model for heavy particles (ions and neutrals)**
- **Boltzmann solver (2D space and 1D energy) for electrons. Total energy formulation is used.**

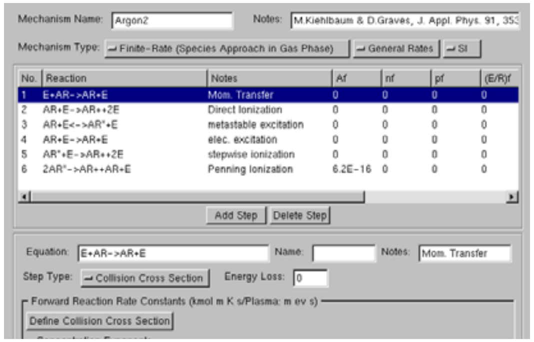

- **5-step mechanism with Ar ions and metastables.**
- **simulations take 1-2 days of computational time on 1 GHz processor**

50 μs pulse, low coil current: time evolution

Electron density, reactor center

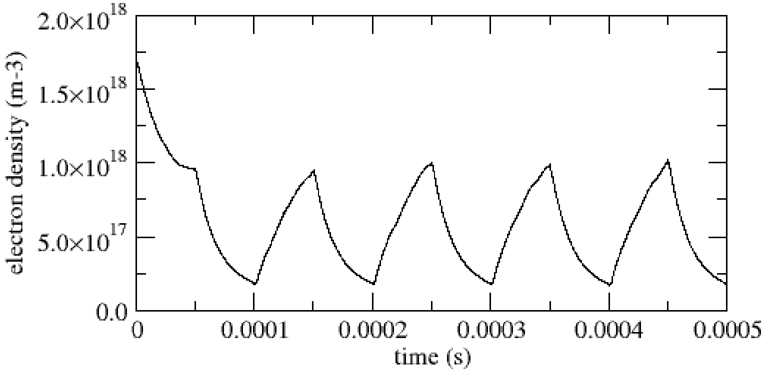

Electron temperature, reactor center

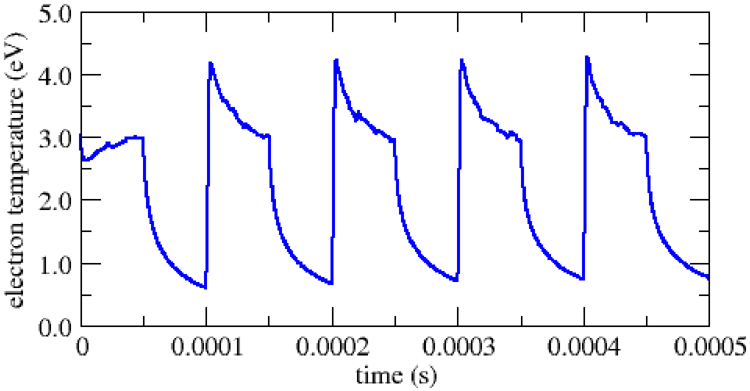

- **small “ripples” on Te are numerical due to finite energy resolution in the Boltzmann solver**

- **I=100A, low current operation: plasma does not reach steady state during active phase**

50 μs pulse, low coil current: power on

RF Power deposition

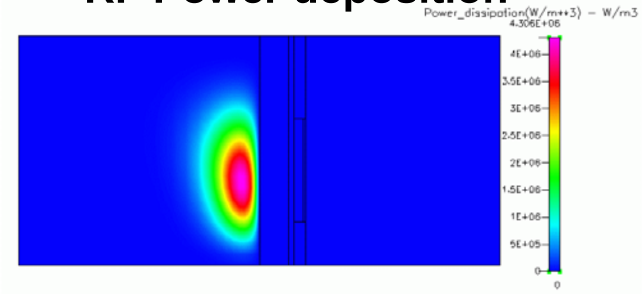

Electron density

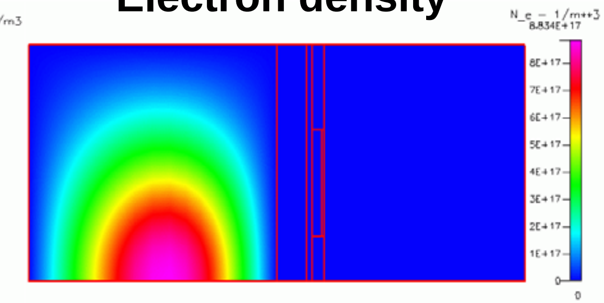

Electron temperature

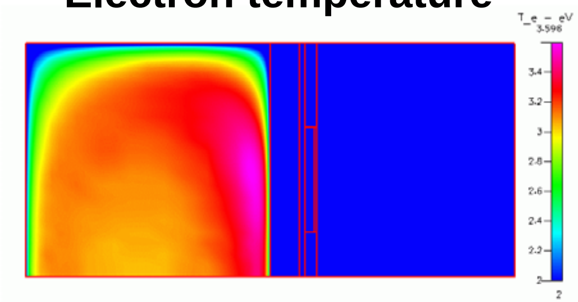

Electric potential

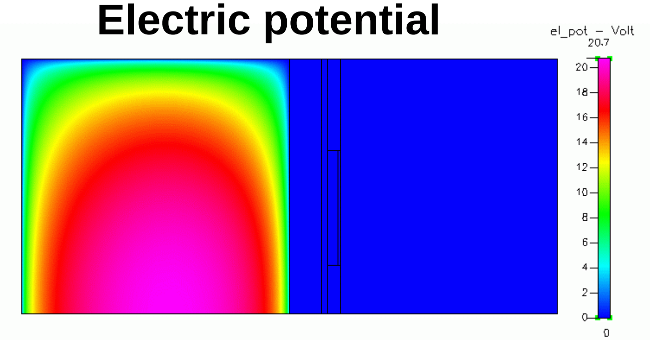

EEDF at 3 locations along axis at r=4 cm

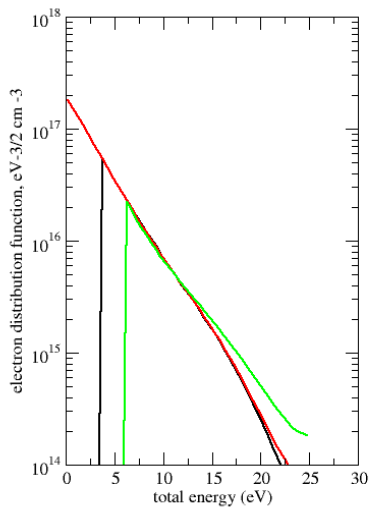

- **EEDF body is Maxwellian**
- **EEDF is enriched by fast electrons near coils (green line)**
- **EEDF is depleted for energies larger first excitation potential**

50 μs pulse, low coil current: power off

Electron density

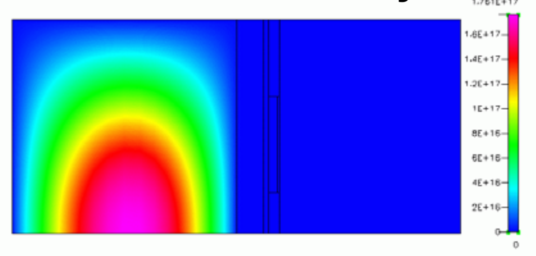

Electron temperature

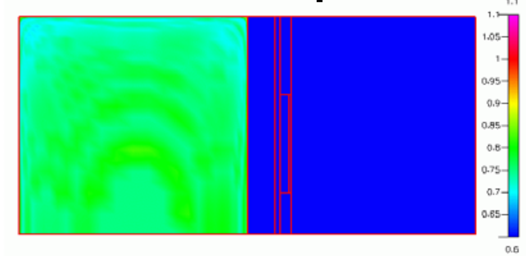

Electric potential

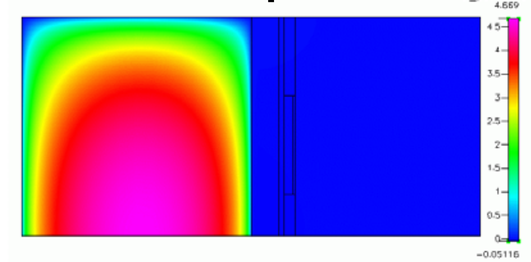

EEDF @ different locations

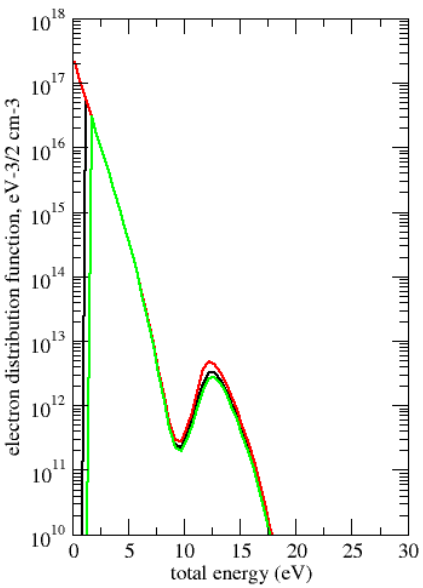

- **EEDF body is Maxwellian in afterglow**
- **EEDF is depleted at energies higher wall potential (~4.5 V)**
- **There is a well pronounced peak @ ~12eV due to fast electron production in collisions of slow electrons with metastables**

Summary for ICP Simulations

- Hybrid kinetic/fluid simulation of ICP in Argon have performed in a wide range of discharge conditions to investigate the importance of different model assumptions on plasma properties

- The key features of the model include:

  deterministic Boltzmann solver for electrons
  non-uniform grid to resolve potential drops in the sheaths
  ion inertia effects
  gas heating with velocity slip and temperature jumps at the walls
  gas flow to maintain constant pressure in the reactor

- Known limitations of the electron kinetic model:

  no magnetic field effect on electron kinetics
  no stochastic heating and anomalous skin effect

Kinetic simulations of capacitively coupled plasmas with external circuit

Ar, 400 mTorr, 400 V

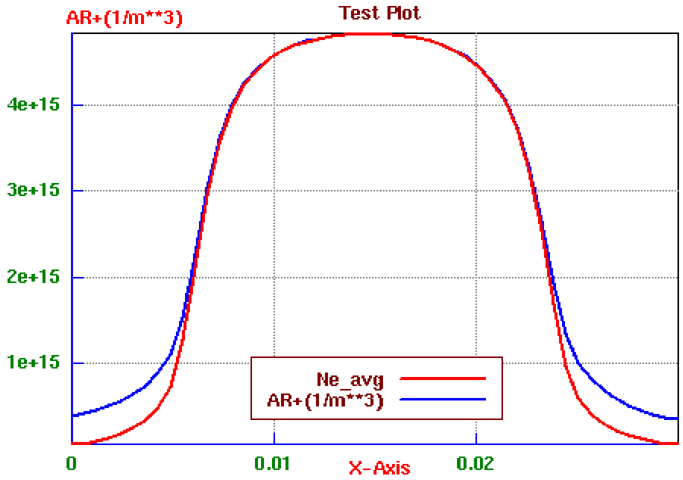

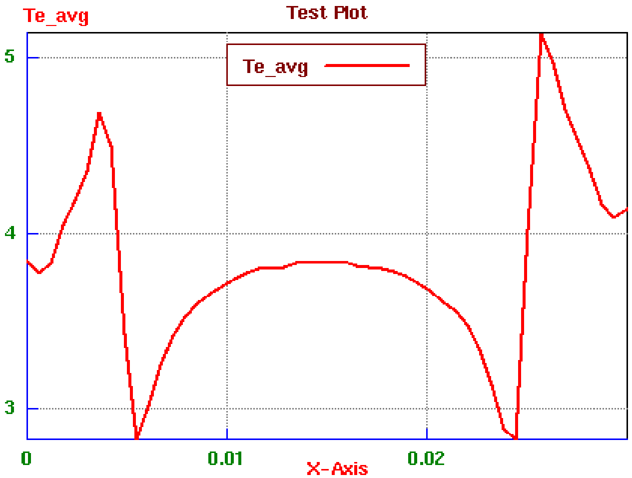

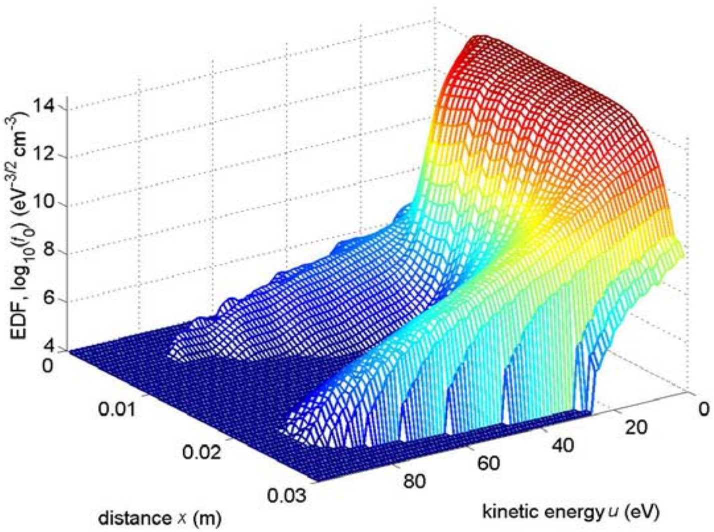

- higher pressures $\Rightarrow$ the plasma density profile is broader
- The average electron temperature decreases from the plasma center towards the RF sheathes, and then increases in the sheathes
- The temporal evolution of the EDF is small during one RF cycle

Ar, 100 mTorr, 300 V

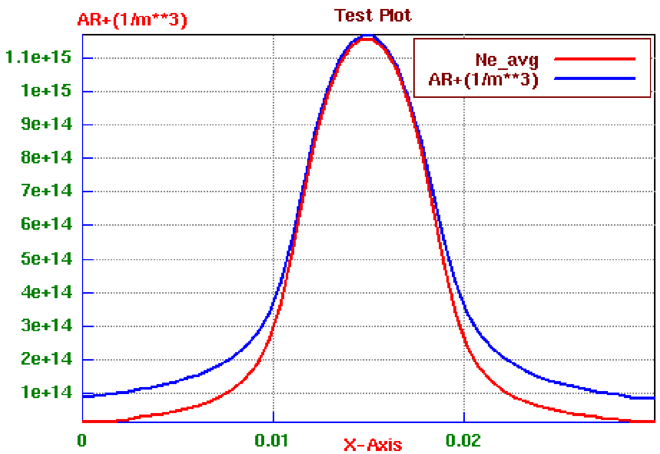

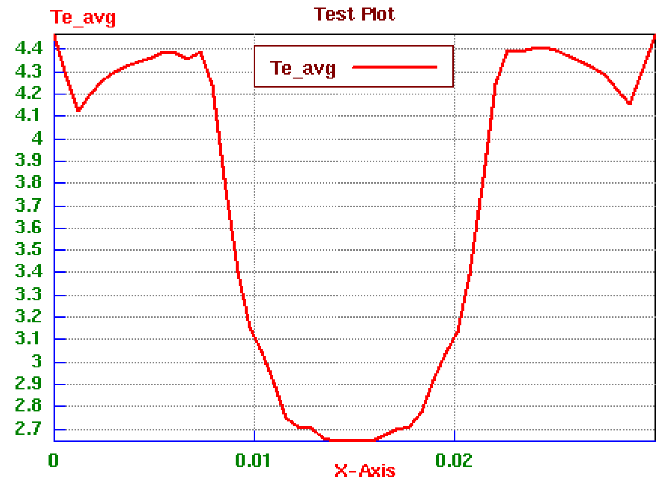

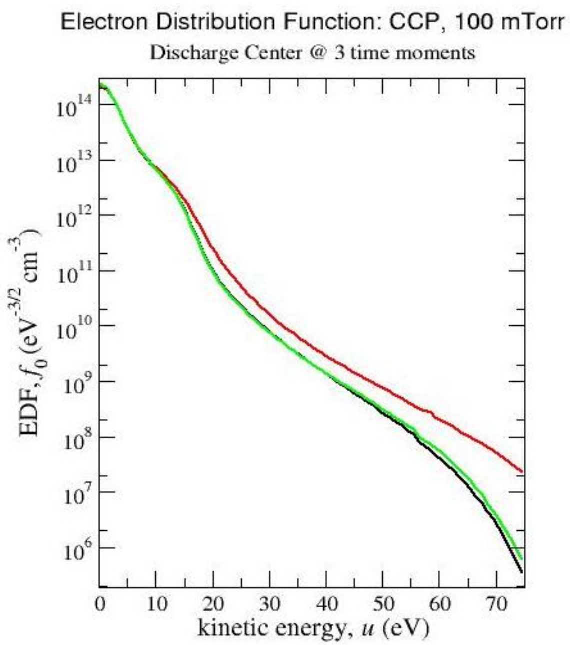

- nonlocal Boltzmann equation for electrons

- The low-energy peak of the EDF is responsible for the <u> profile: low <u> in center is indication of nonlocal regime

- The bulk EDF shows almost no time evolution, the high energy tail oscillates significantly

Results for CH_4 CCP Discharges

- Discharge gap 3 cm, gas pressure 140 mTorr, RF voltages 50-400 V

- Compare results with Ivanov *et al* paper

[1] V. Ivanov, O. Proshina, T. Rakhimova, A. Rakhimov, D. Herrebout and A. Bogaerts, "*Comparison of a one-dimensional particle-in-cell–Monte Carlo model and a one-dimensional fluid model for a CH4/H2 capacitively coupled radio frequency discharge*," J. Appl. Phys. **91**, 6296 (2002).

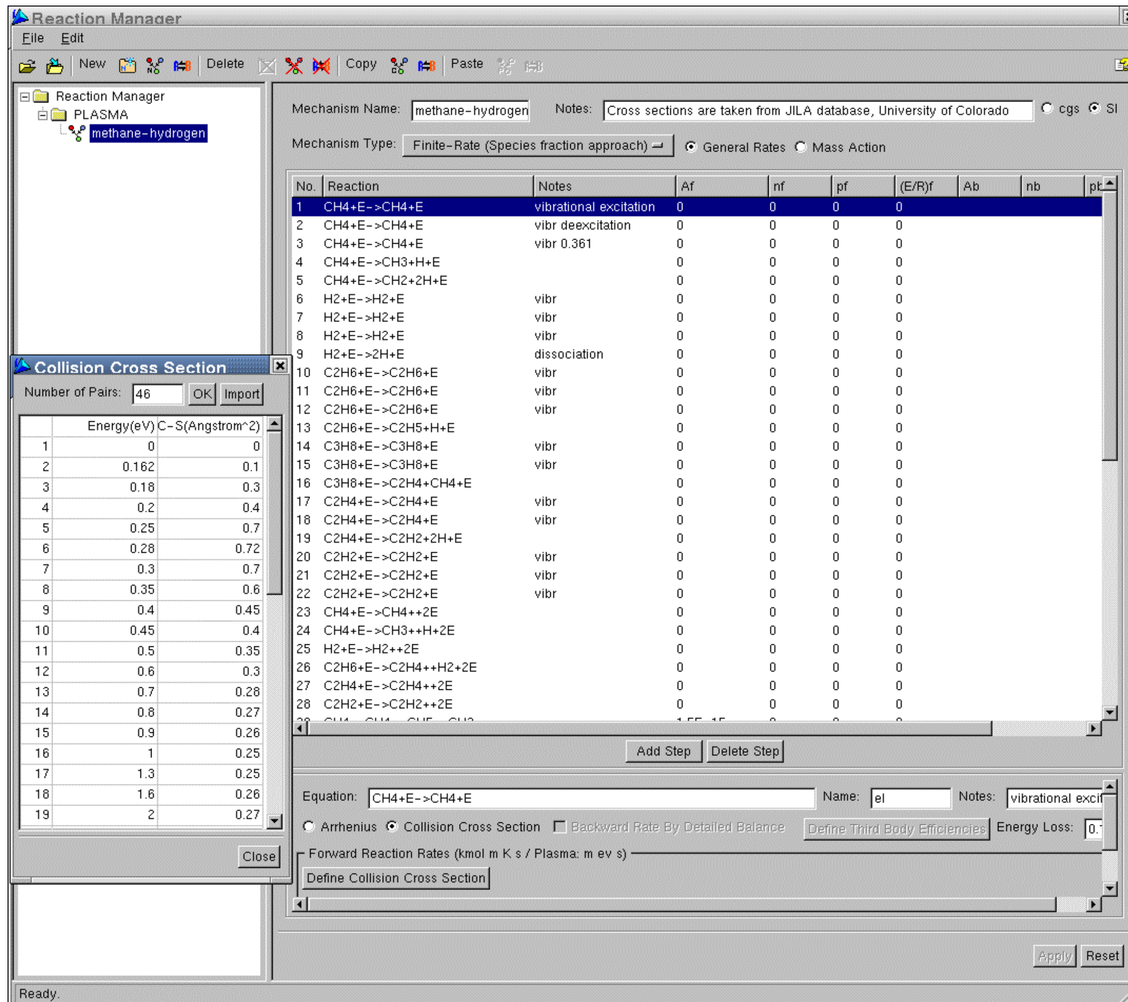

- 54-step reaction mechanism with 33 species

CH_4 , 140 mTorr, 400 V

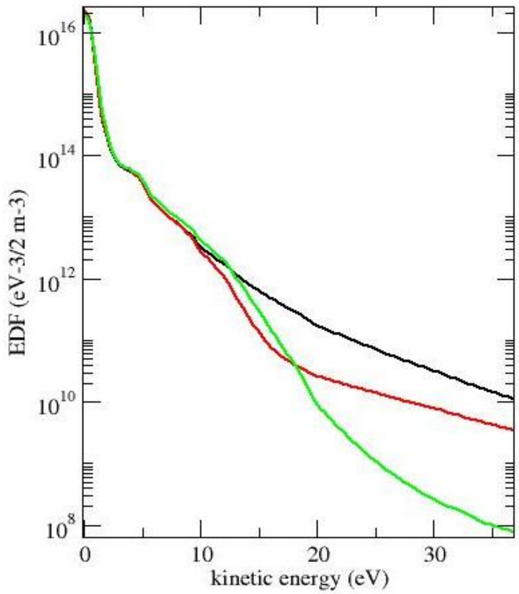

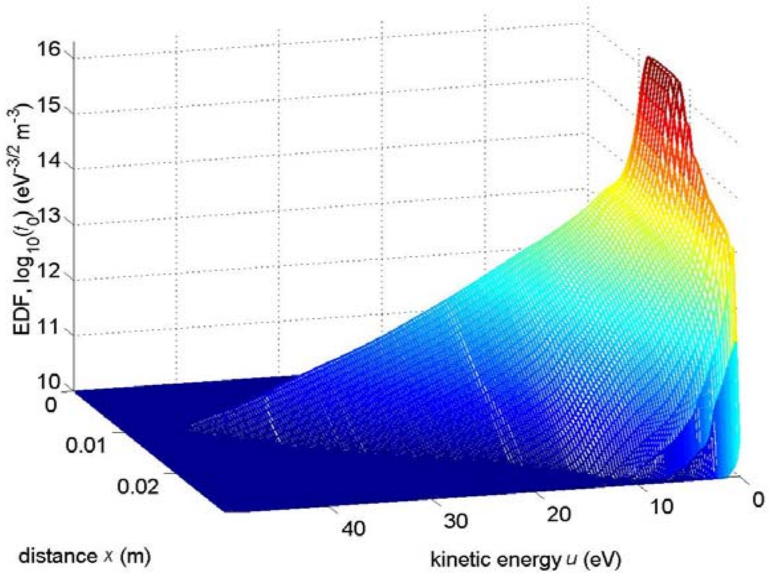

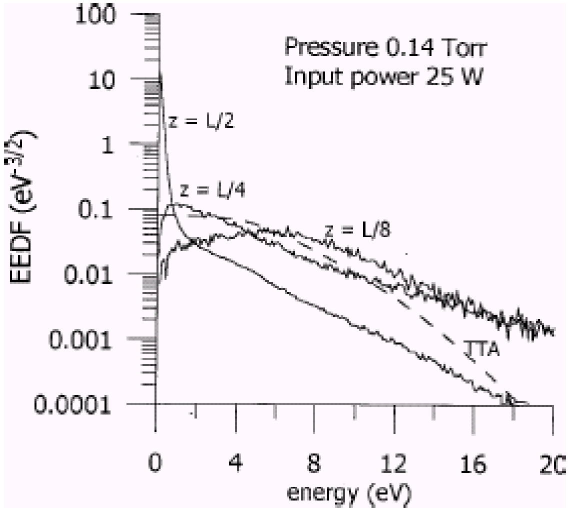

FIG. 3. EEDF at different distances between the electrodes at a pressure of 0.14 Torr and an input power of 25 W, calculated with the PIC–MC model (solid lines) and as a result of solving the homogeneous Boltzmann equation in the two-term approximation, used in the fluid model (dashed line) at an average electron energy of 5 eV.

- The calculated EEDF has a low-energy peak formed by electrons trapped in the ambipolar potential well.

- The low-energy peak of the EEDF is more pronounced in Ivanov *et al*, which is most likely to be due to the absence of electron-electron collisions in the model in Ivanov *et al*.

Unified Flow Solver

Boltzmann Equation

Direct Simulation Monte-Carlo (DSMC)

Direct Numerical Solution

Domain Decomposition

Coupling Algorithm

Continuum Kinetic Schemes

***<u>Direct Numerical Solution</u>* of the Boltzmann equation is preferable to DSMC for coupling kinetic and continuum models**

<u>Unified Flow Solver with AMAR</u>

- **Cartesian mesh with embedded solid boundaries**
- **Tree based adaptation of the mesh to the solution and geometry**
- **Automatic switching based on a continuum breakdown criteria**

Unified Flow Solver

low pressure high pressure

density

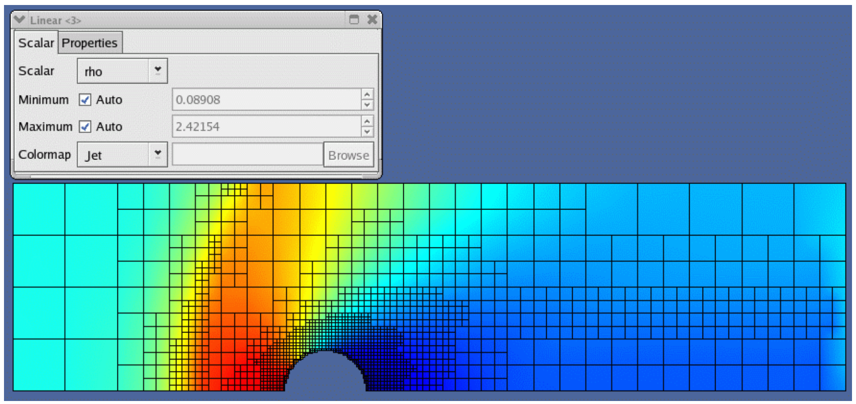

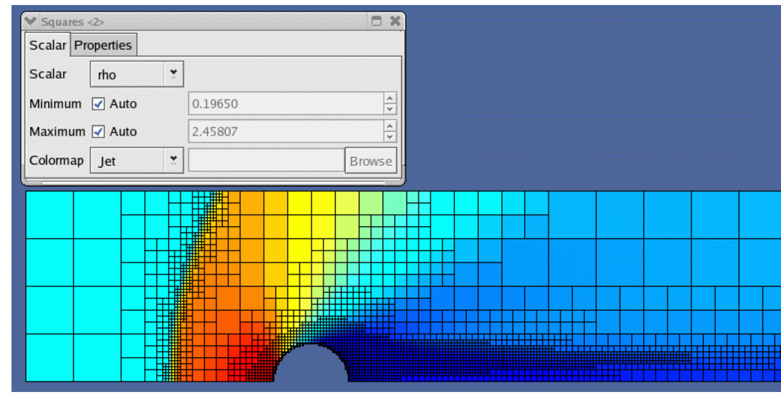

Kinetic region

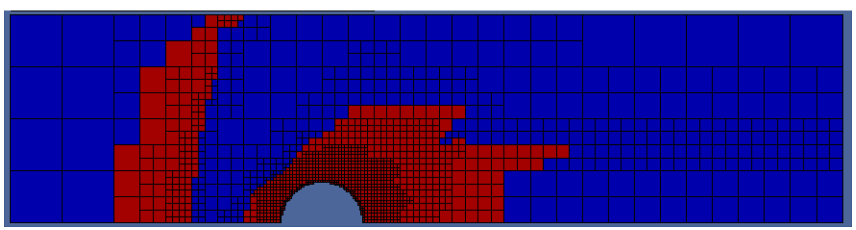

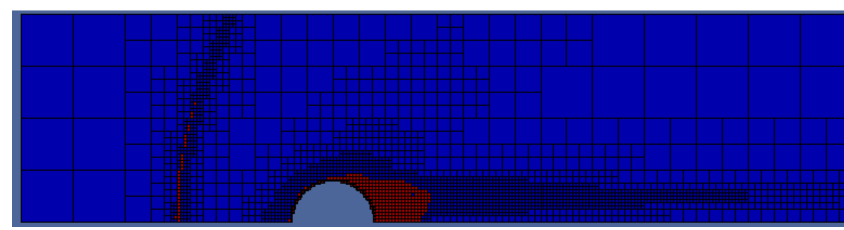

UFS extensions for plasma simulations

• **We have added to UFS a Poisson solver that has the automatic mesh refinement etc.** The figure below shows the solutions of the Poisson equation with a fixed BC at the left boundary = 100 V, and the rest BCs are zero BCs

• **We have implemented a simple plasma model, which includes Poisson equation + 3-momentum equations for electrons + 1st momentum for ions:**

- ions are assumed to be frozen.
- energy equation for electrons is not solved: constant Te = 1 eV is assumed and ionization is calculated as a function of local E/N.

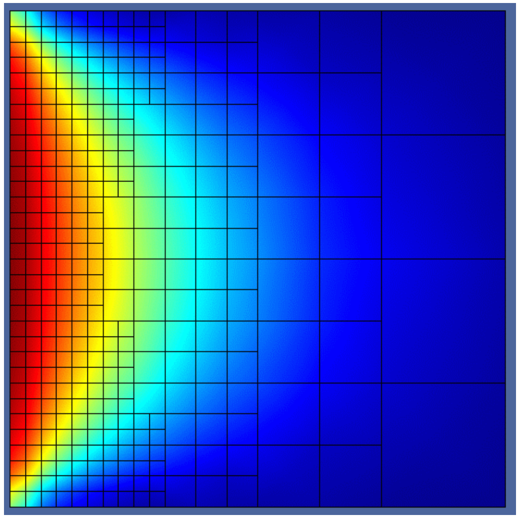

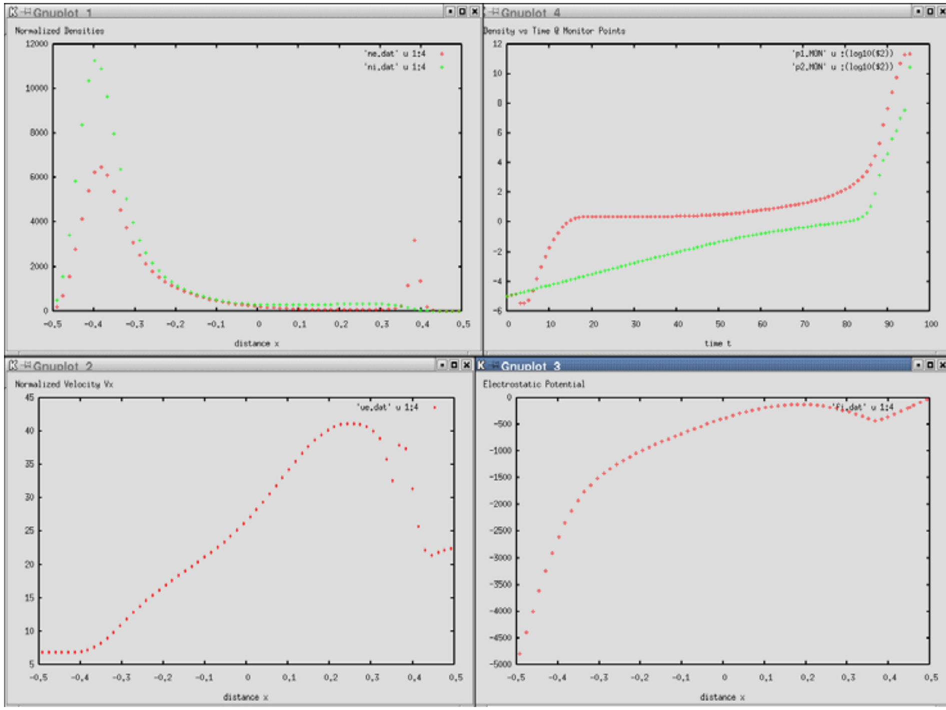

Simulations of collisionless effects

- **Vlasov equation is solved numerically**

$$\frac{\partial f}{\partial t} + v_x \frac{\partial f}{\partial x} - \frac{eE(x,t)}{m}\frac{\partial f}{\partial v_x} = 0$$

- **Simple model of collisionless sheath is considered: electric field is**

$$E(x,t) = \begin{cases} A(x-s) & x < s(t) \\ 0 & x < s(t) \end{cases} \qquad s(t) = \overline{s}_0 - s_0 \cos(\omega t)$$

- **Particles are injected from one (left) side with a given distribution function:**

  Electrons: half-Gaussian, *n=1* and *T=1*,

  Ions: Maxwellian (Gaussian) shifted by Bohm velocity

Electron distribution in the sheath: $\nu = 0.1$

density vs time

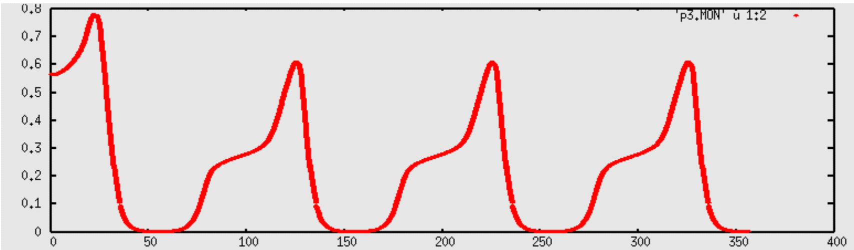

x = 15, inside the sheath

Distribution function $f(v_x, v_y, t)$

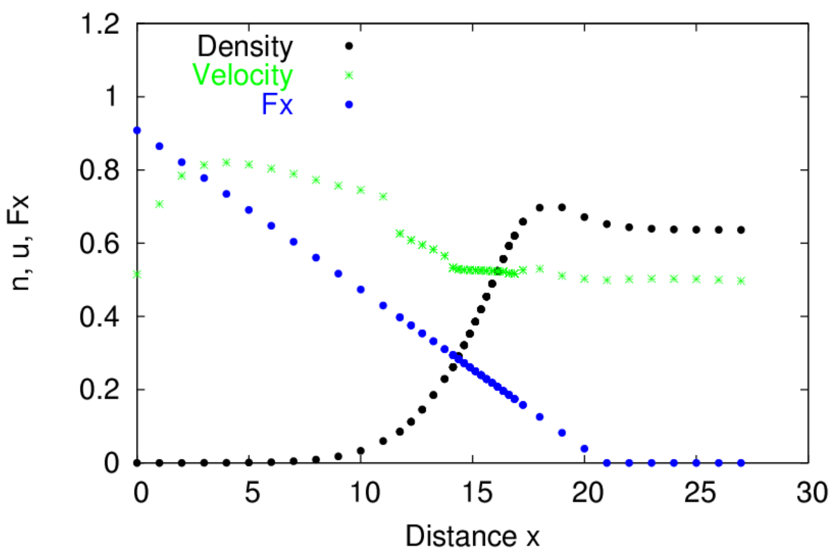

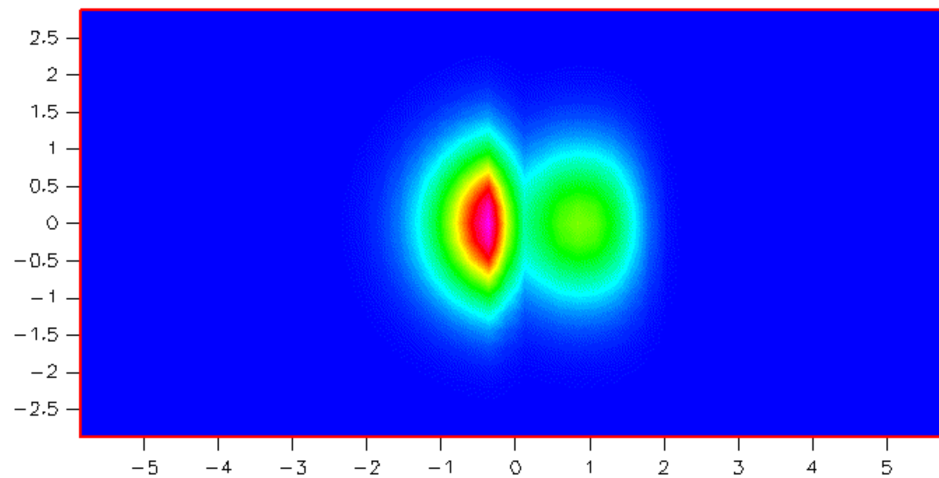

Grid adaptation in physical space based on density gradient

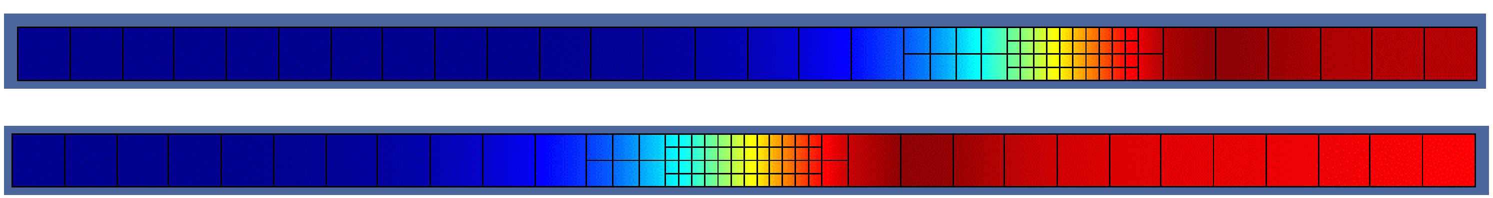

Frequency dependence of electron distribution function

$$E(x,t)=\begin{cases}\dfrac{a}{s_m}(x-s) & x<s\\ 0 & x<s\end{cases}$$

$$s_m = 23; a = 3$$

$\nu = 1$

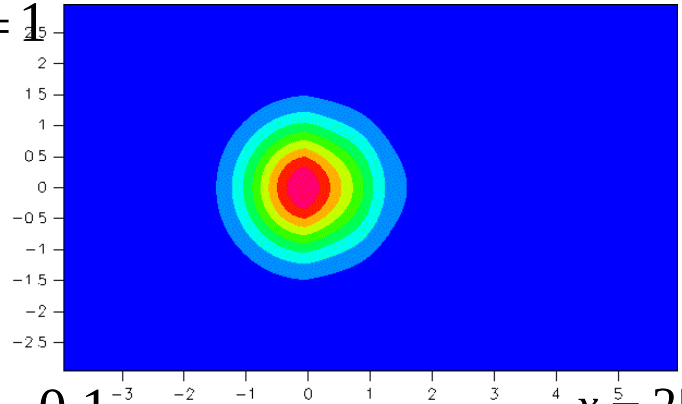

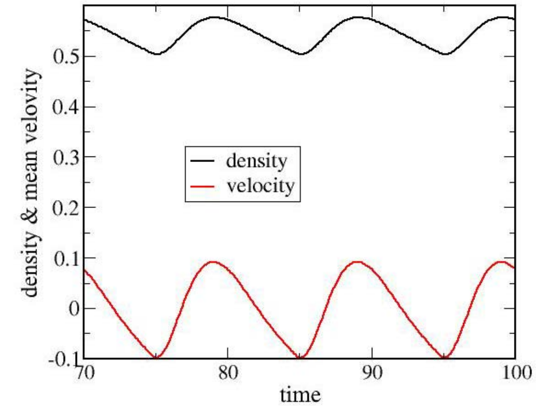

$x = 0$

$\nu = 0.1$

$x = 25$

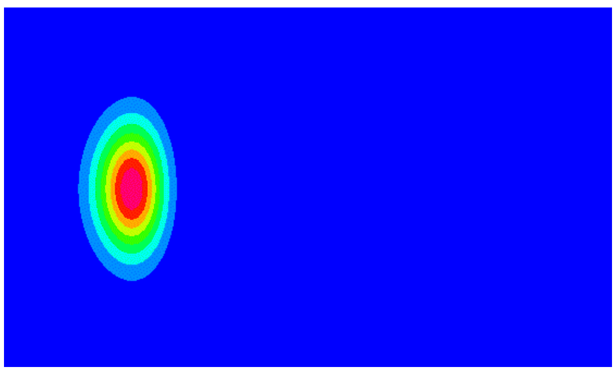

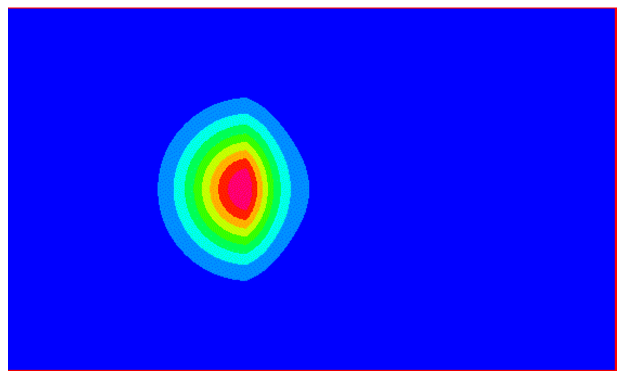

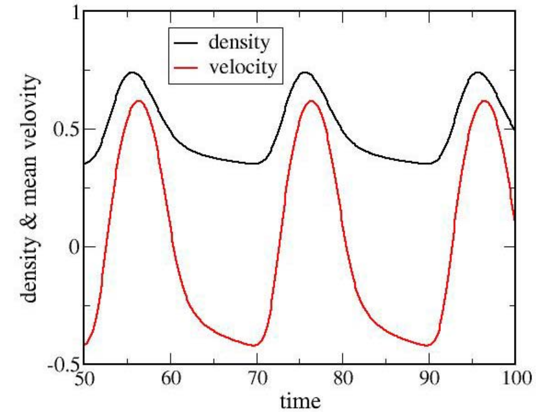

$\nu = 0.01$

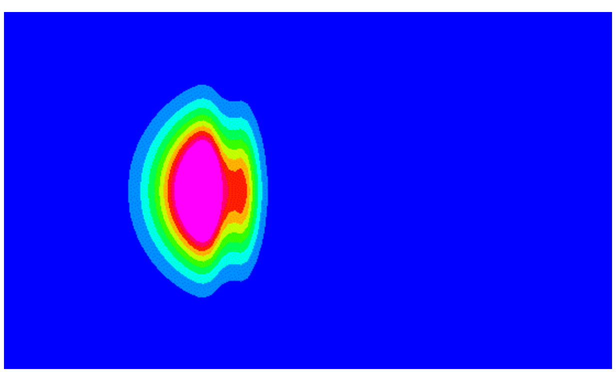

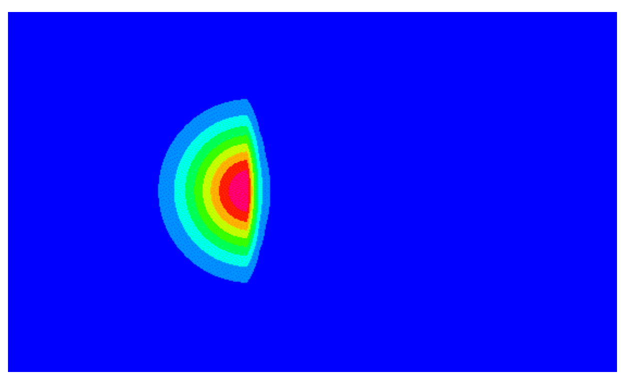

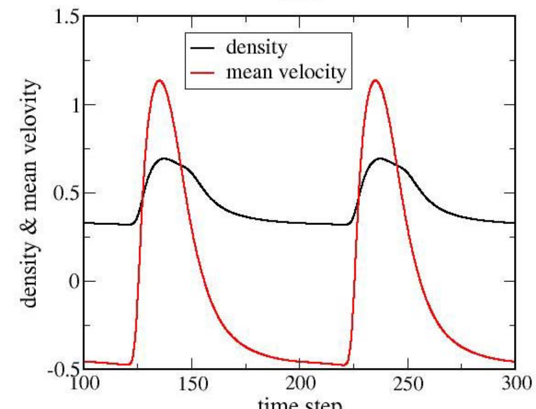

Electron distribution function (continued)

$$E(x,t) = \begin{cases} \dfrac{a}{s_m}(x - s) & x < s \\ 0 & x < s \end{cases}$$

$$s_m = 23; a = 1$$

$x = 25$

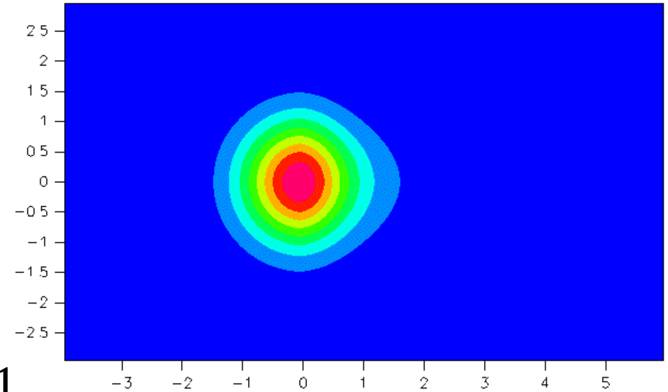

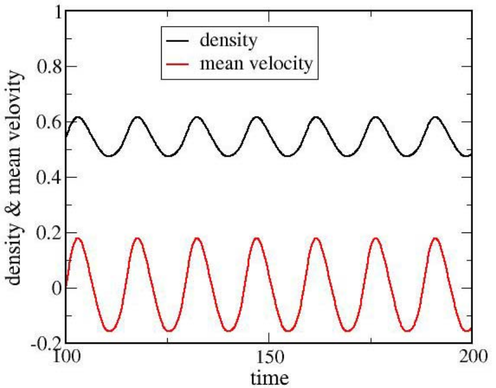

$\nu = 0.1$

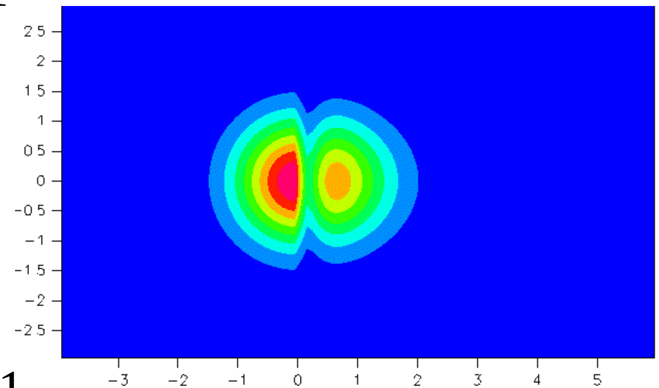

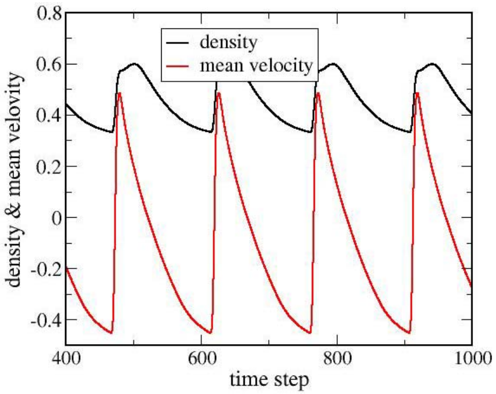

$\nu = 0.01$

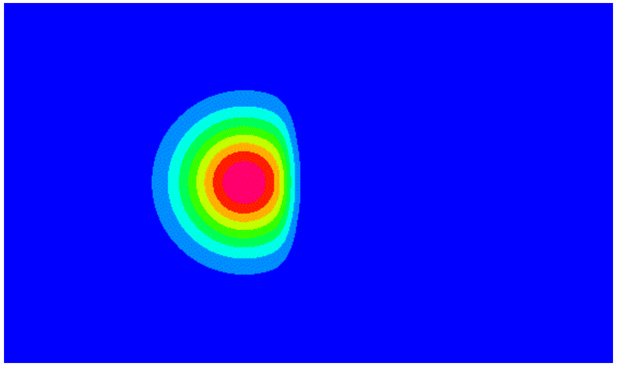

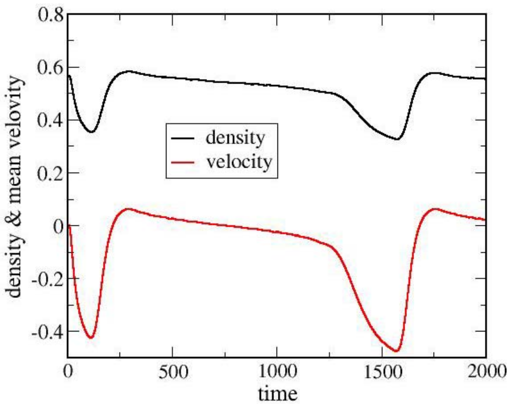

$\nu = 0.001$

Ion distributions in the sheath

$\nu = 1$ $x = 0$

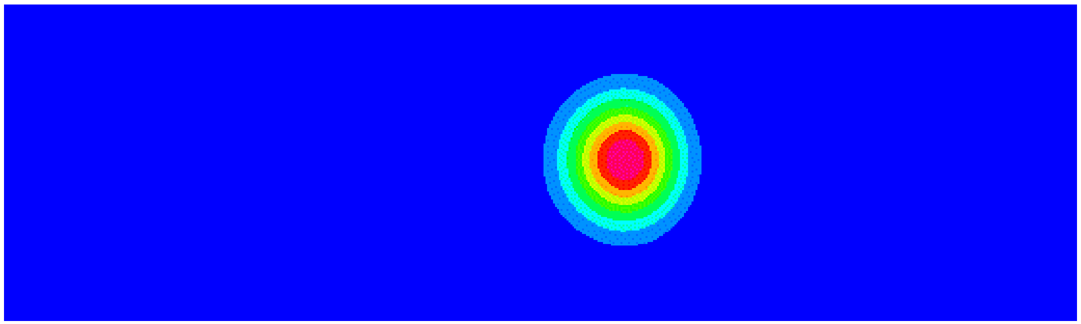

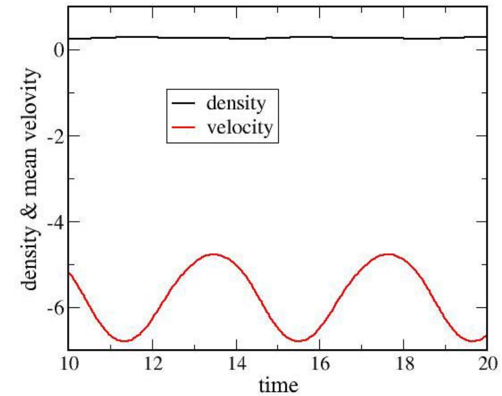

$\nu = 0.1$

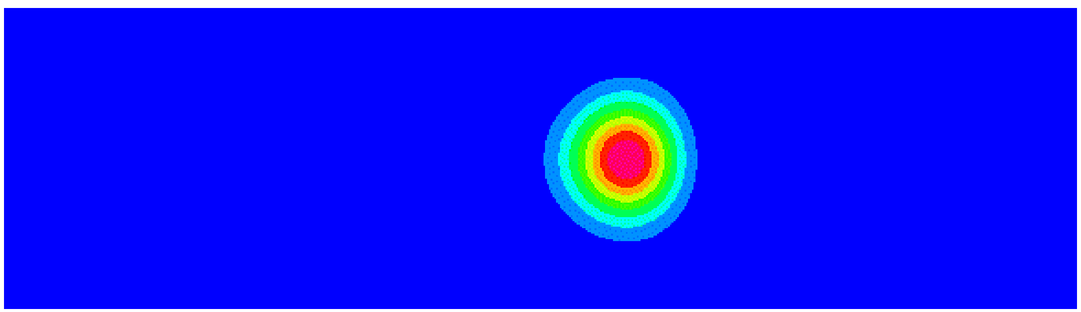

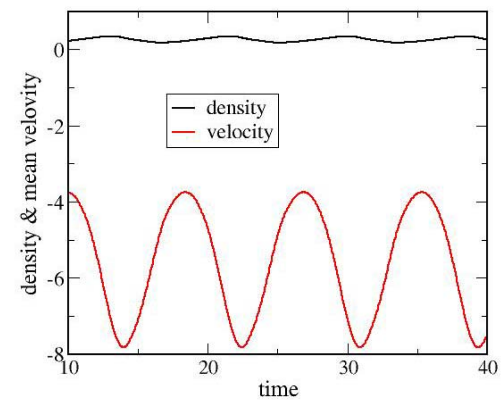

$\nu = 0.01$

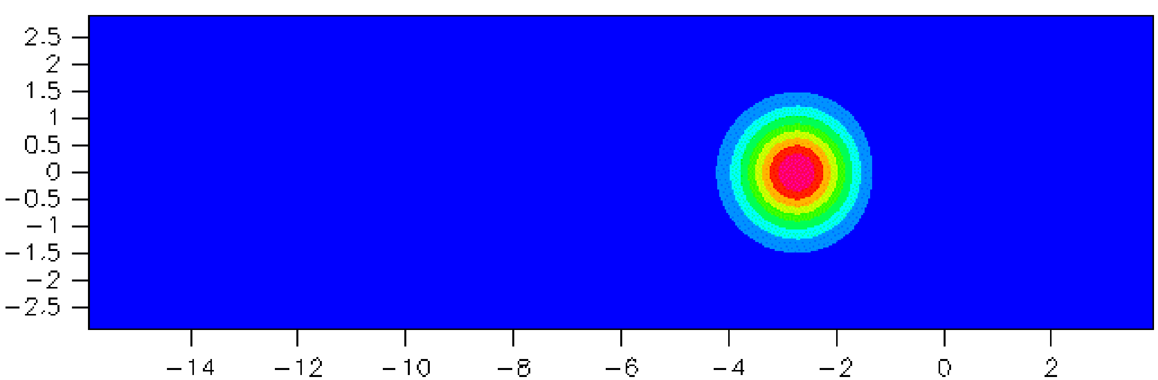

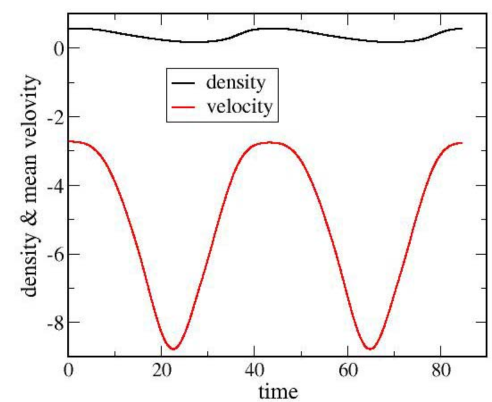

Summary and outlook

- CFD-ACE+PLASMA has been used for simulations of different plasma devices and processes. The Plasma Technologies Branch at CFDRC continues to develop advanced plasma models and customize CFD-ACE for user’s needs

- There are several limitations of the physical model and numerical algorithms implemented in CFD-ACE
    - Rarefied Gas Dynamics effects can not be calculated
    - Solution Adaptive Grid capabilities
    - Collisionless phenomena and fast plasma processes related to electron inertia effects can not be simulated
    - Rarefied Gas Dynamics
- We have started R&D work to expand our Unified Flow Solver for Plasma Simulations

Acknowledgements

- **Drs N.Zhou, A.Vasenkov, D.Sengupta at CFDRC**

- **Drs A.Kudriavtsev, E.Bogdanov & Mr E.Toinov at St Petersburg University, and Prof Lev Tsendin at St Petersburg Technical Uni.**

- **Prof Mark Kushner at the University of Illinois**
- **Prof Mounir Laroussi at the Old Dominion University**

- **National Science Foundation**
- **Air Force Office of Scientific Research**
- **The Next Step to Market Program of the US Dept. of Commerce**
- **The SABIT Program of the US Dept. of Commerce**
- **A number of industrial companies supported plasma development at CFDRC**

10mT, 6.8 MHz

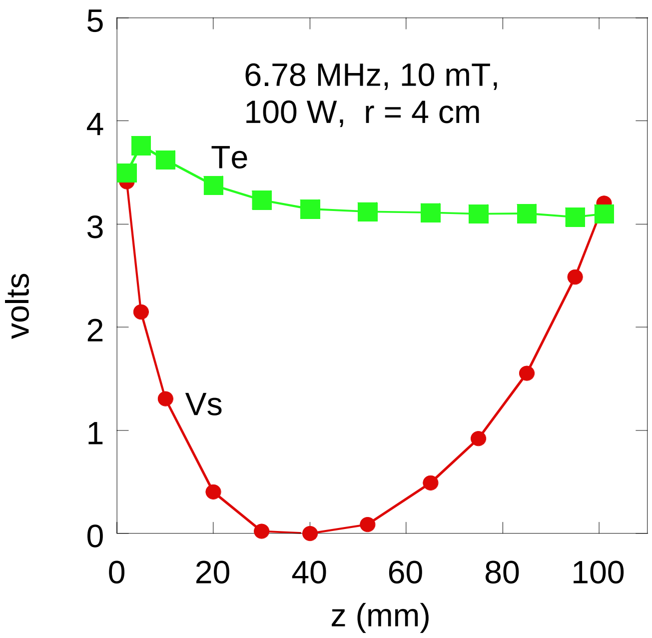

6.78 MHz, 10 mT,
100 W, r = 4 cm
Te
Vs
volts
z (mm)

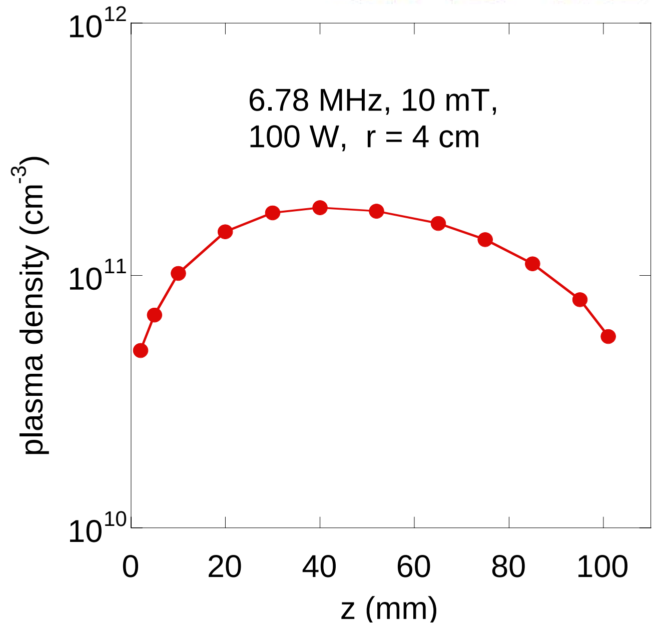

6.78 MHz, 10 mT,
100 W, r = 4 cm
plasma density (cm^{-3})
z (mm)

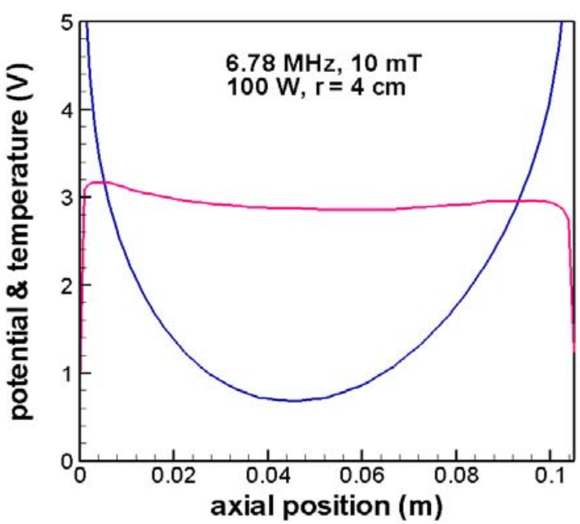

6.78 MHz, 10 mT
100 W, r = 4 cm
potential & temperature (V)
axial position (m)

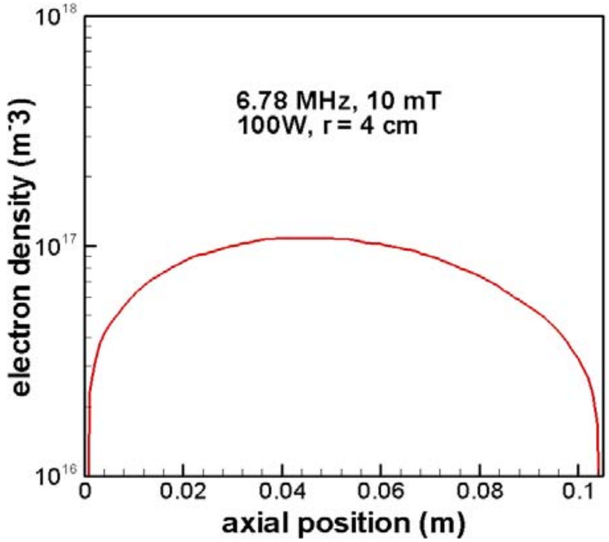

6.78 MHz, 10 mT
100W, r = 4 cm
electron density (m^3)
axial position (m)

10mT, 6.8 MHz, No Gas Heating

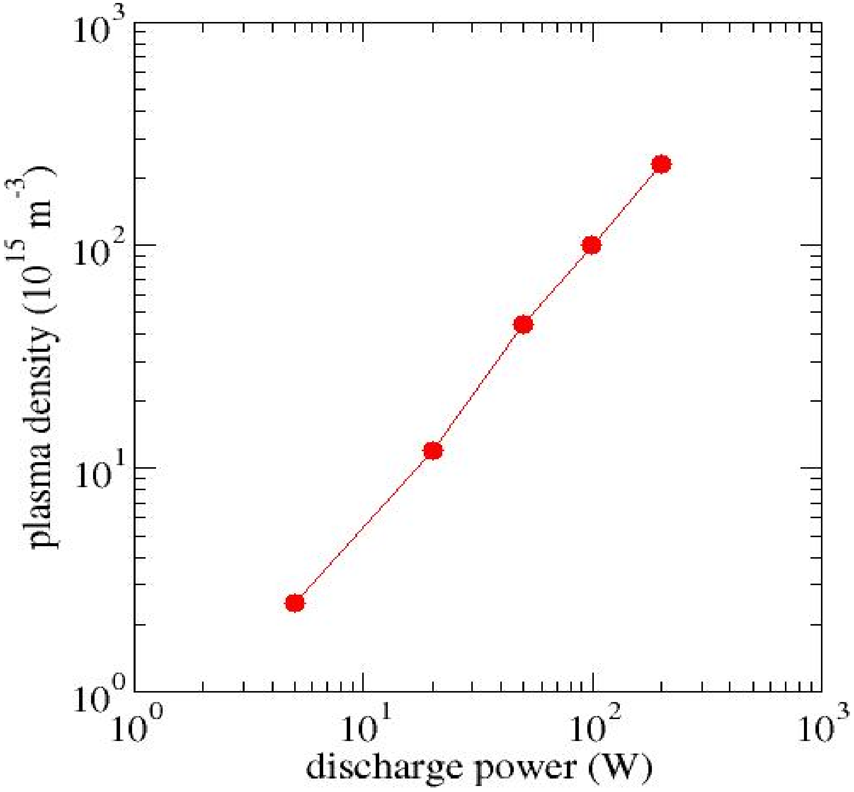

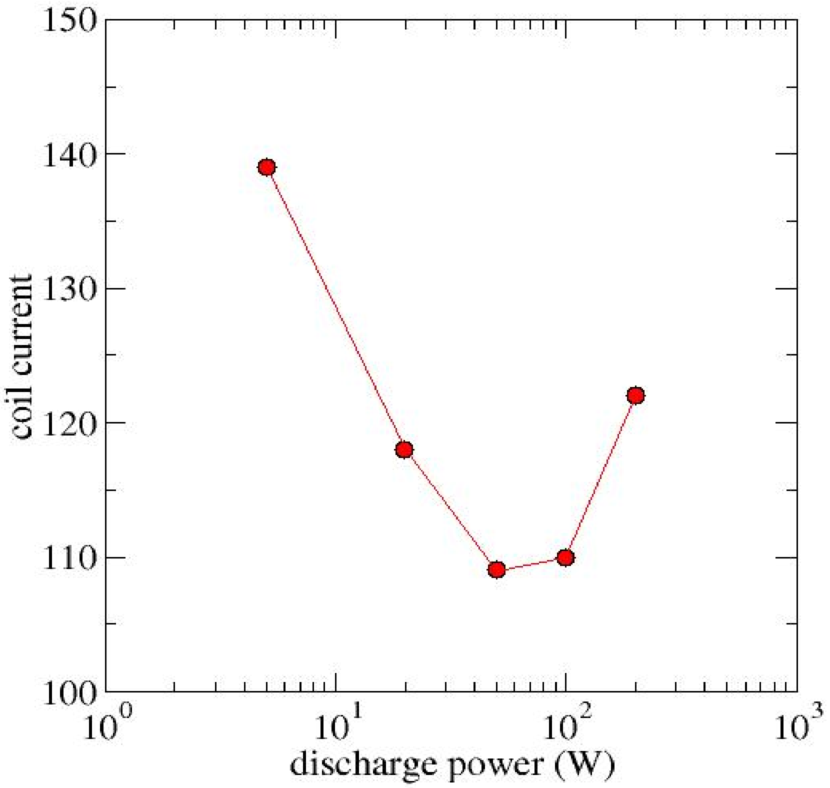

100mT, 6.8 MHz

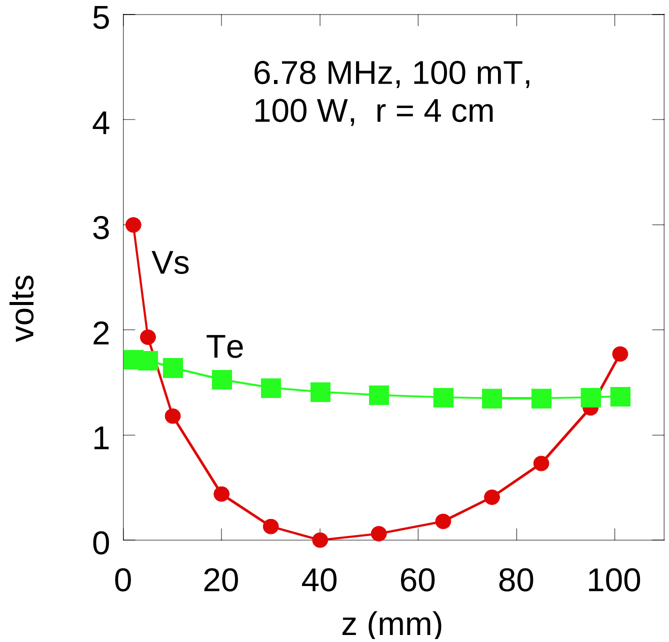
6.78 MHz, 100 mT,
100 W, r = 4 cm
volts
Vs
Te
z (mm)
0
1
2
3
4
5
0
20
40
60
80
100

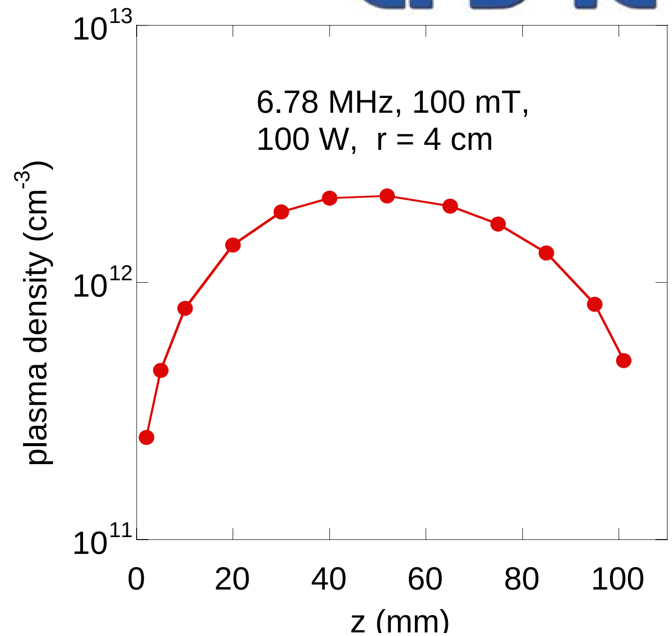
6.78 MHz, 100 mT,
100 W, r = 4 cm
plasma density (cm^{-3})
10^{13}
10^{12}
10^{11}
z (mm)
0
20
40
60
80
100

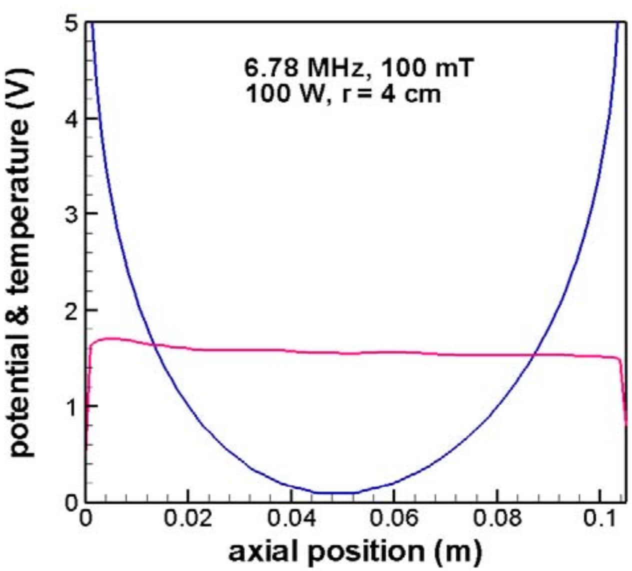
6.78 MHz, 100 mT
100 W, r = 4 cm
potential & temperature (V)
axial position (m)
0
1
2
3
4
5
0
0.02
0.04
0.06
0.08
0.1

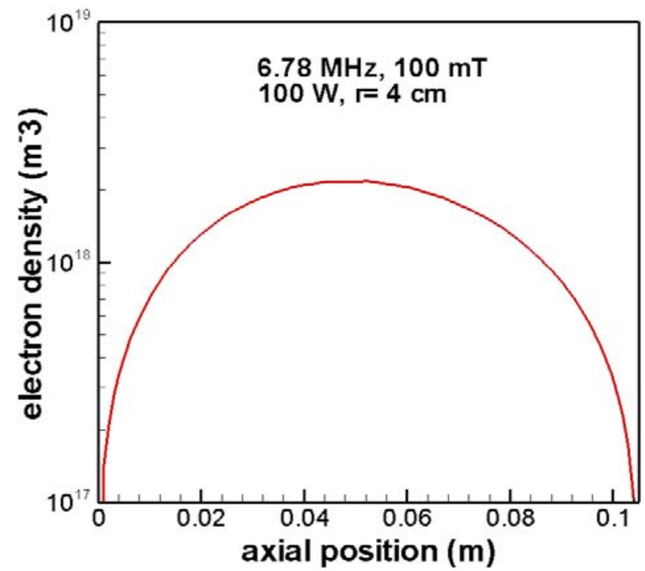
6.78 MHz, 100 mT
100 W, r= 4 cm
electron density (m^-3)
10^{19}
10^{18}
10^{17}
axial position (m)
0
0.02
0.04
0.06
0.08
0.1

1 mT, 100 W, With Gas Heating

Gas Temperature

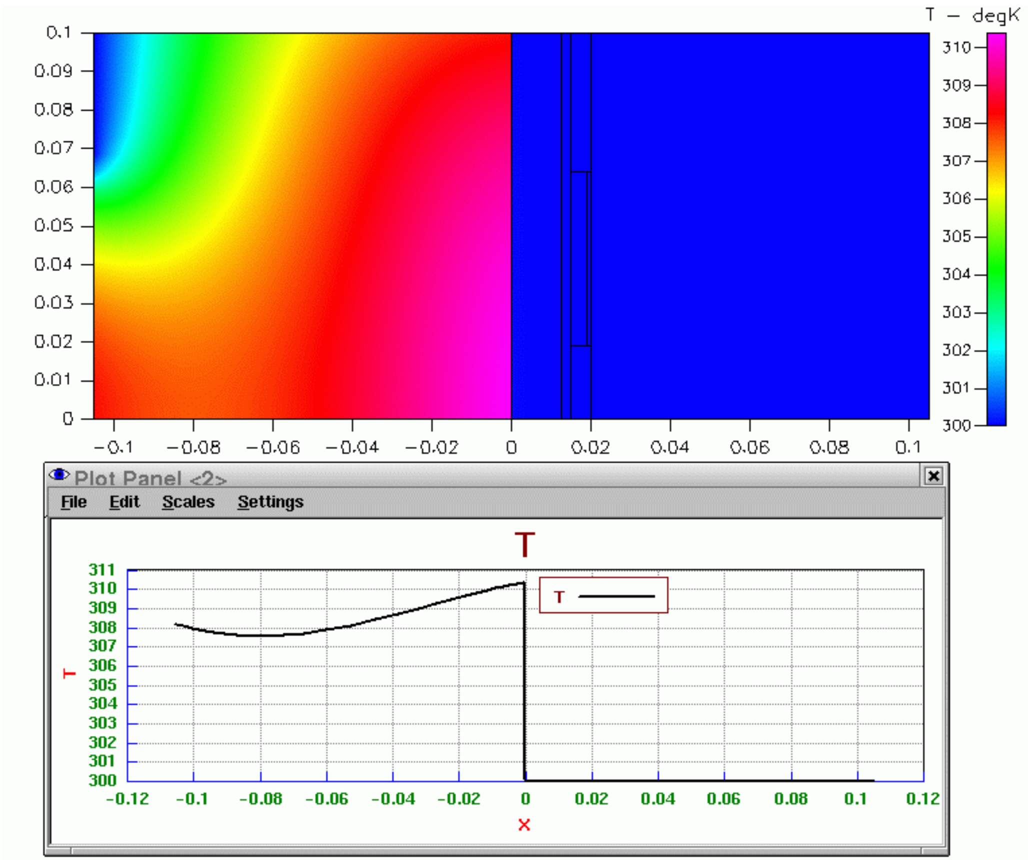

Electron density

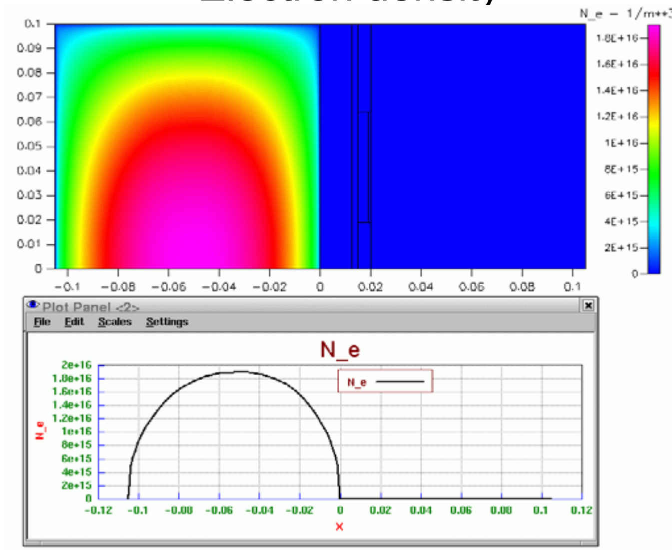

Electron temperature

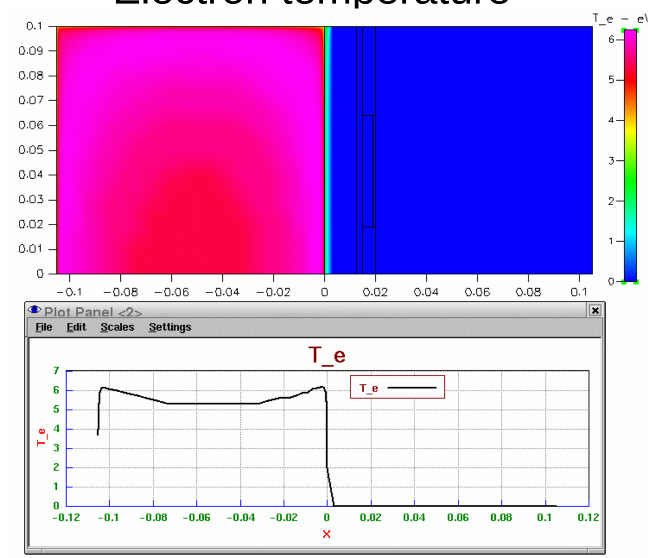

There is strong temperature jump (slip wall)

Temperature at outlet is = room temperature

Outlet is important for maintaining constant pressure

10 mT, 100 W, With Gas Heating

Gas Temperature

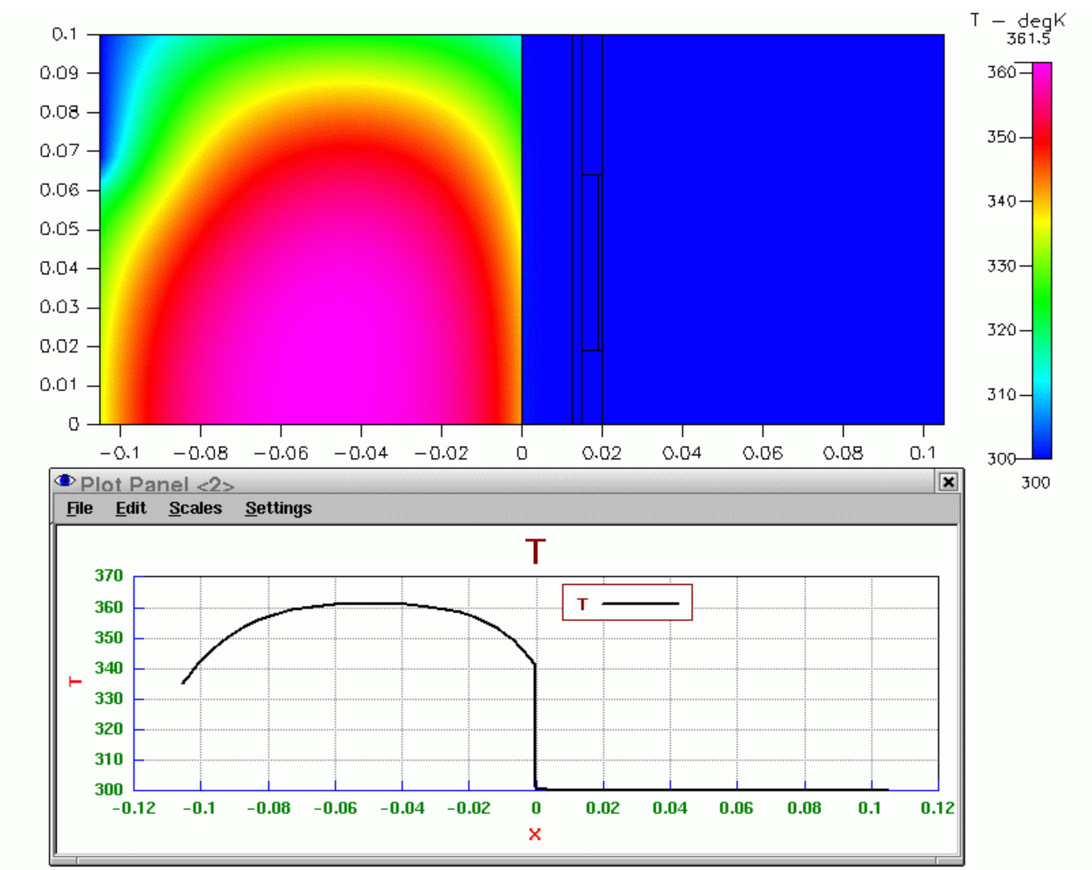

Electron density

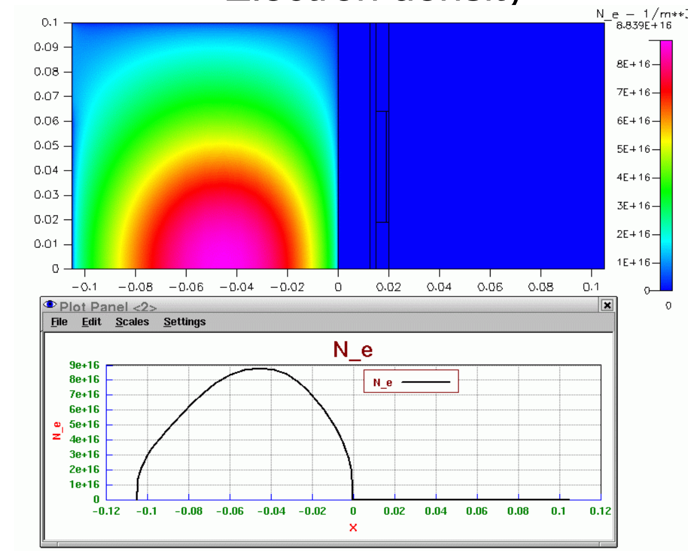

Electron temperature

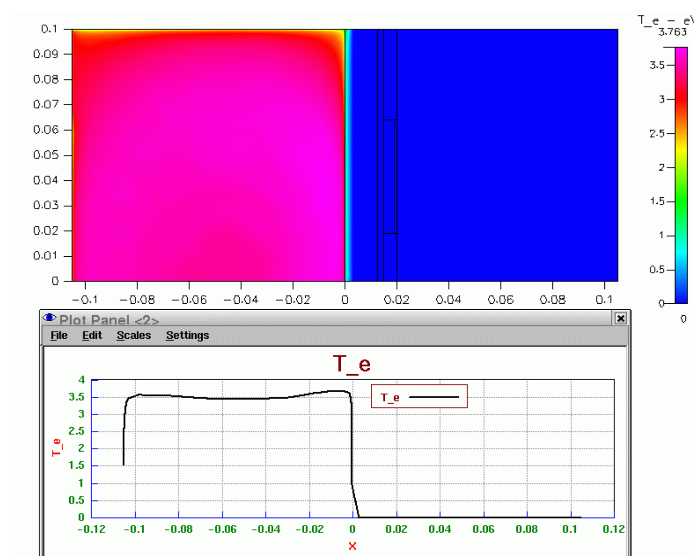

Temperature jump is smaller than @ 1mTorr

Temperature at outlet is room temperature

100 mT, 200 W, With Gas Heating

Gas Temperature

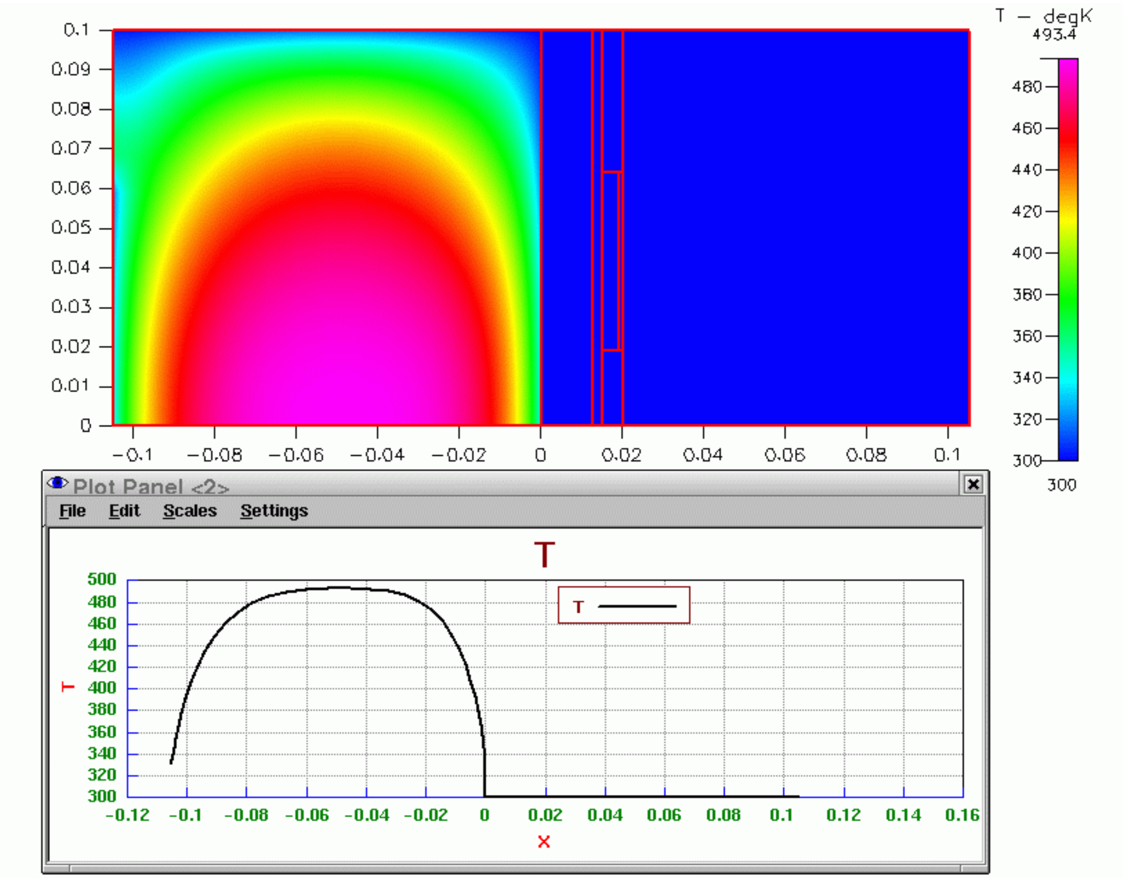

Electron density

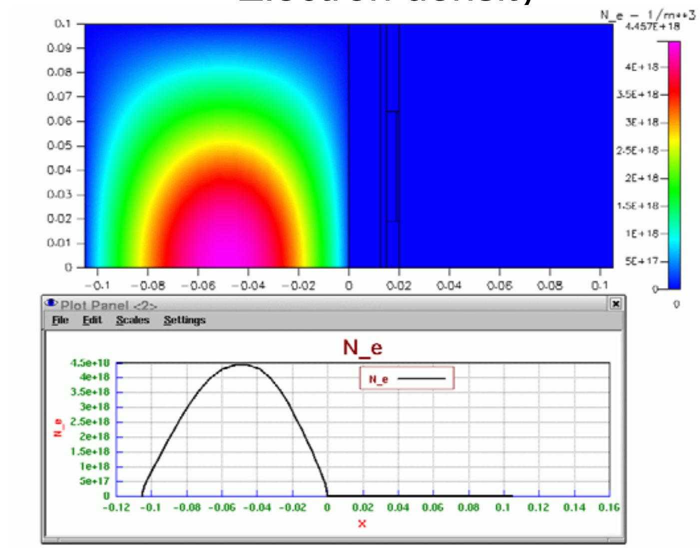

Electron temperature

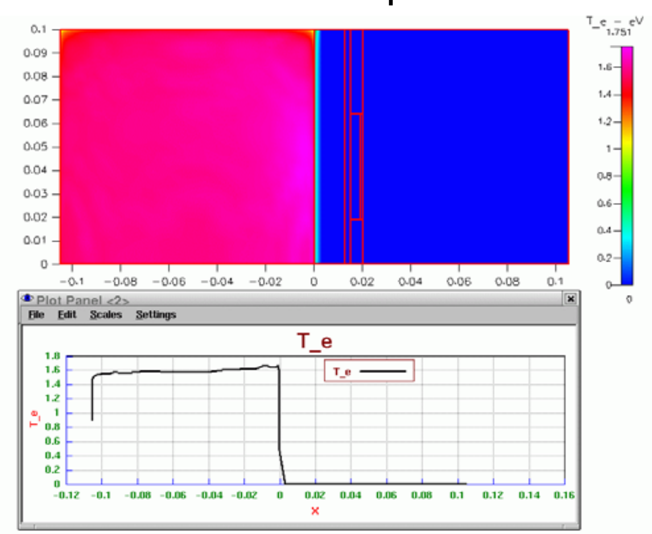

Temperature jump is small at this pressure

Summary of Results with Gas Heating

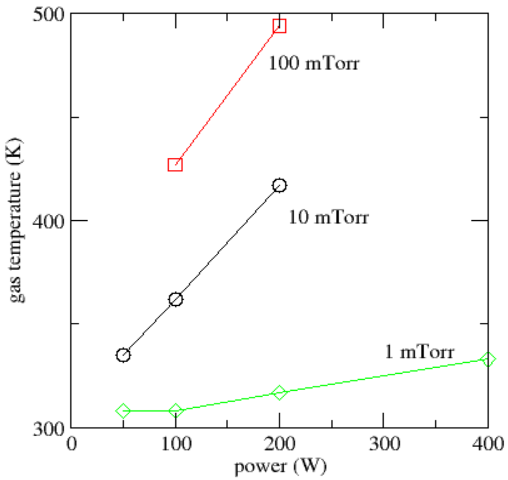

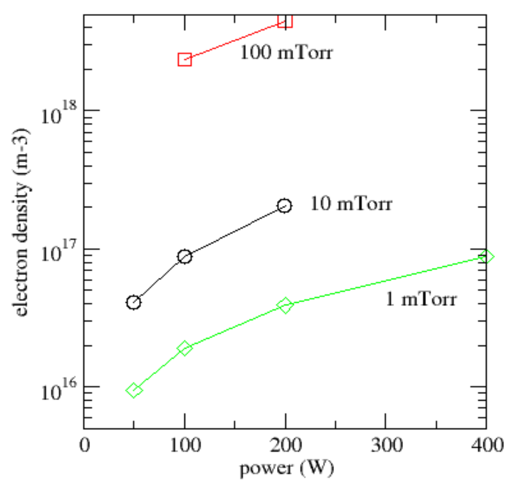

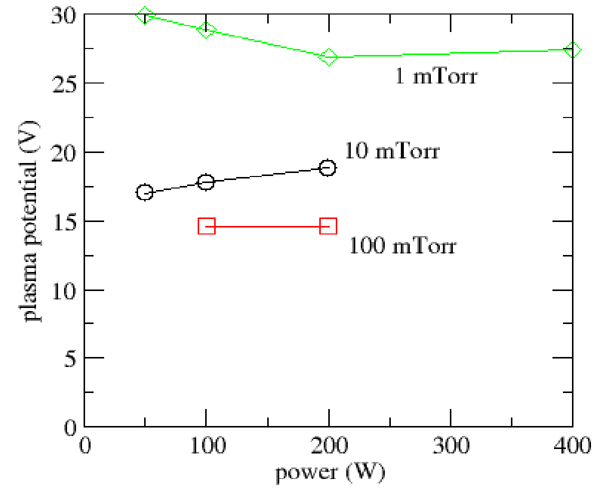

Gas heating is maximum at higher pressures

Electron density agrees rather well with experiments

Plasma potential is larger at lower pressures

Time-resolved ICP Simulations: Model

- **fluid model for heavy particles (ions and neutrals)**
- **Boltzmann solver (2D space and 1D energy) for electrons. Total energy formulation is used. Instantaneous RF heating (energy diffusion coefficient) is used in order to resolve electron kinetics during RF cycle**
- **Electromagnetic Module both in frequency and time domains**

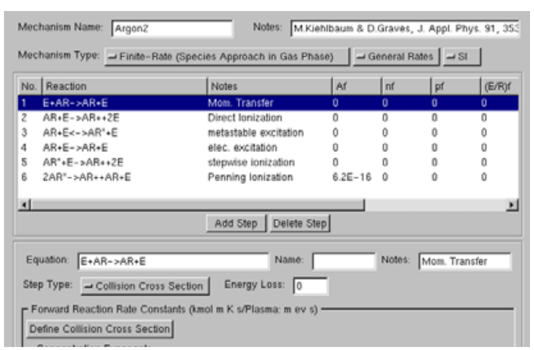

- **5-step mechanism with Ar ions and metastables.**
- **simulations take 1-2 days of computational time on 1 GHz processor**

Boltzmann Equation with Time-Dependent RF Heating

$$\underset{(a)}{\frac{\partial}{\partial t}(\upsilon f)} - \underset{(b)}{\frac{\partial\phi}{\partial t}\frac{\partial}{\partial\varepsilon}(\upsilon f)} - \underset{(c)}{\nabla\cdot\chi\nabla f} - \frac{\partial}{\partial\varepsilon}\left[\underset{(d)}{Y_{ee}\left(Cf + D\frac{\partial f}{\partial u}\right)} + \underset{(e)}{\upsilon V_T f} + \underset{(f)}{\upsilon D_E\frac{\partial f}{\partial u}}\right] = \underset{(g)}{\nu S}$$

a) Transient
b) Convection due to time-varying electrostatic potential
c) Transport in configuration space
d) Coulomb collisions
e) Quasi-elastic collisions
f) Heating by alternating electromagnetic fields
g) Inelastic Collisions

Total Energy Formulation

$$\varepsilon = u - \phi(\vec{r}, t)$$

Energy Diffusion Coefficient Due to instantaneous RF field:

$$D_E = \frac{1}{6}\frac{\tilde{E}_{rf}^2(\vec{r})}{1+(\omega/\nu)^2}\frac{\upsilon^2}{\nu}\left[1+\cos(2\omega t)+\frac{\omega}{\nu}\sin(2\omega t)\right]$$

$\tilde{E}_{rf}(\vec{r})$ - amplitude of RF field (real+imaginary)

Time resolved ICP: time evolutions

Electron density, reactor center

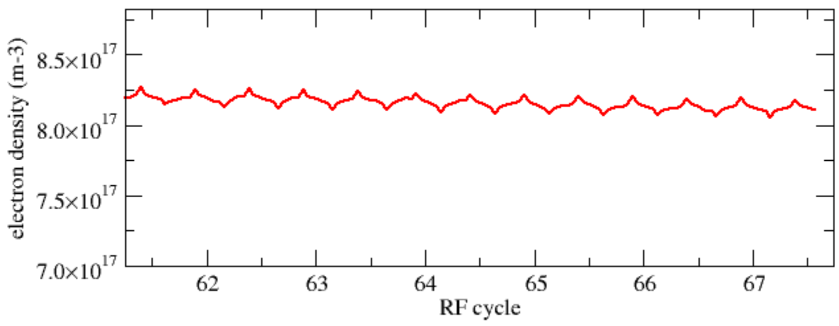

Electron temperature, reactor center

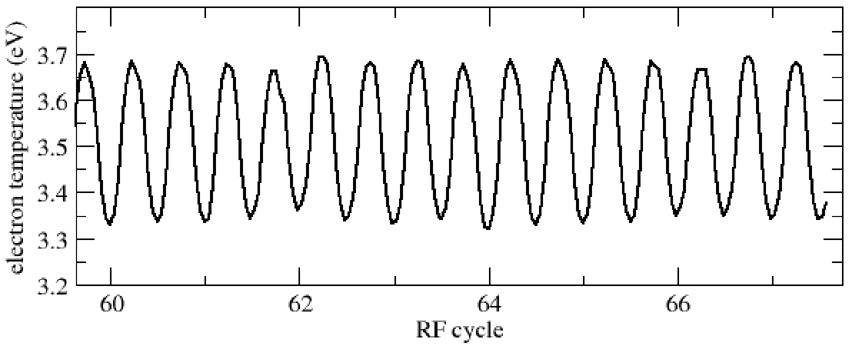

Electron density, near coil

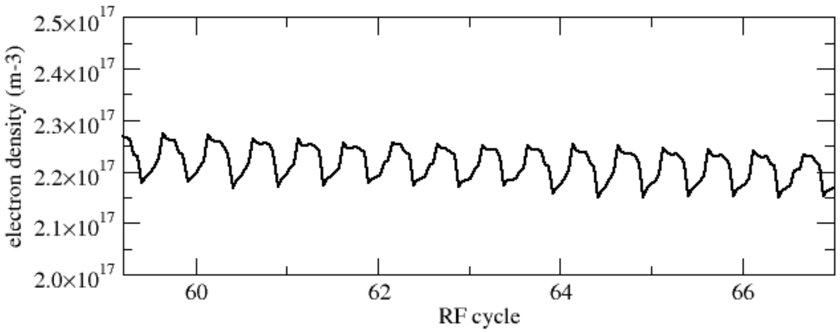

Electron temperature, near coil

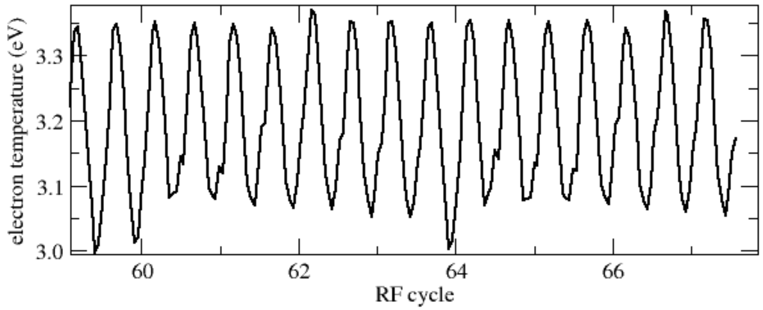

- **modulation of ne and Te takes place at second harmonic of main frequency 450 kHz**

Time resolved ICP: EEDFs

reactor center

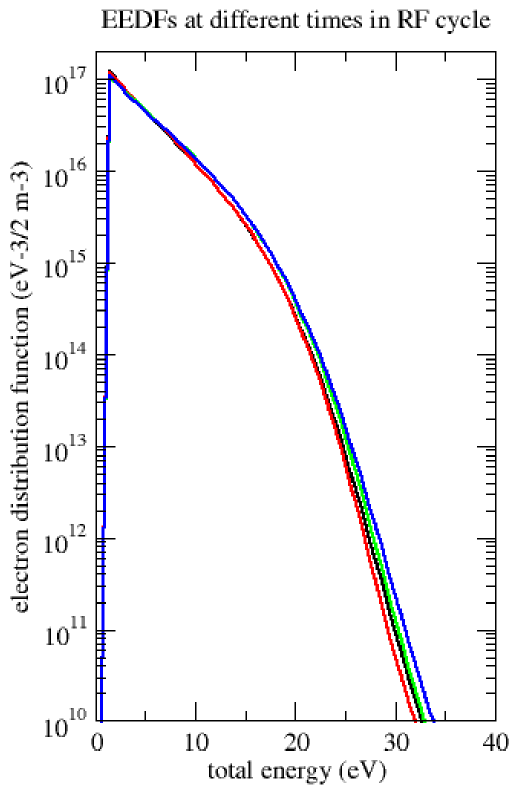

near coil

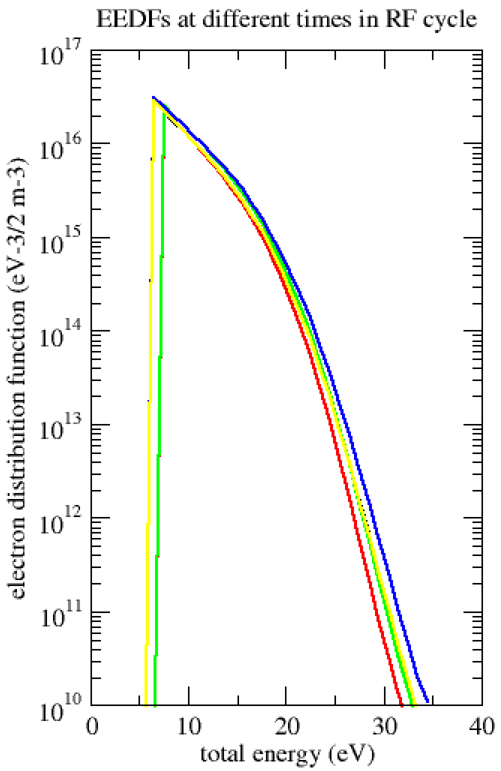

- **modulation of EEDF mainly in the tail portion**
- **modulation of EEDF stronger near coils**

Time resolved ICP: 2D instantaneous profiles in RF cycle

Electron density

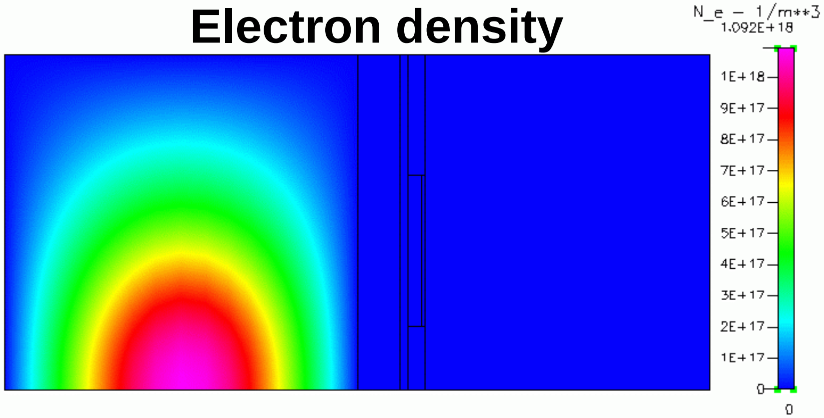

Electron temperature

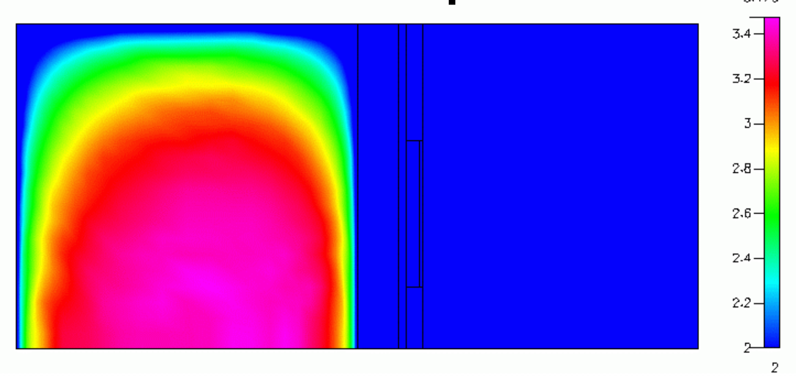

Electrostatic potential

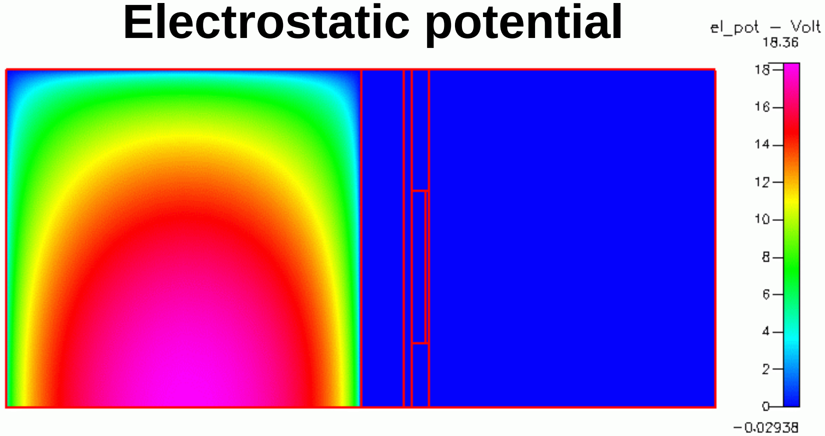

RF power

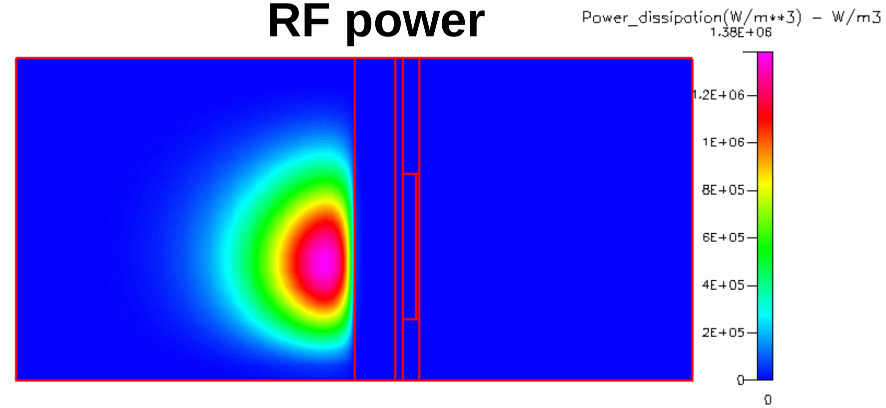

- **modulation of electrostatic potential follows that of Te**

Modeling of DC Micro Discharges

- Used in various applications such as MEMS technology
- p=1-10 Torr, U =300-500V, d = 1-10mm
- gas air, pure nitrogen

Experimental results ⇒

High Voltage Limits for Electrostatic Transducers: On the Role of Ambient Pressure and Device Dimension in MicroDischarges

Chester G. Wilson[1], Amy E. Wendt[1], and Yogesh B. Gianchandani[1,2]
[1]Department of Electrical and Computer Engineering, University of Wisconsin, Madison, WI 53706
[2]EECS Department, University of Michigan, Ann Arbor, MI 48109

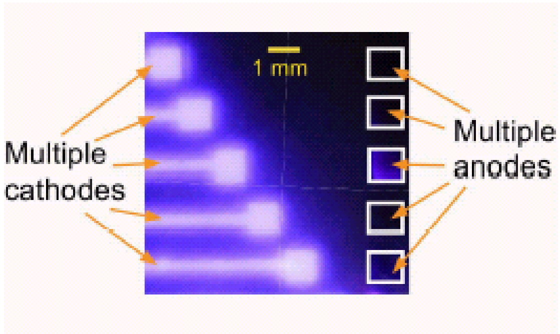

Fig. 5: Air microplasmas with varying electrode spacing show that the glow exists only over the cathode, and is independent of spacing, but dependent upon pressure and power density.

- modeling shows similar picture

electron density

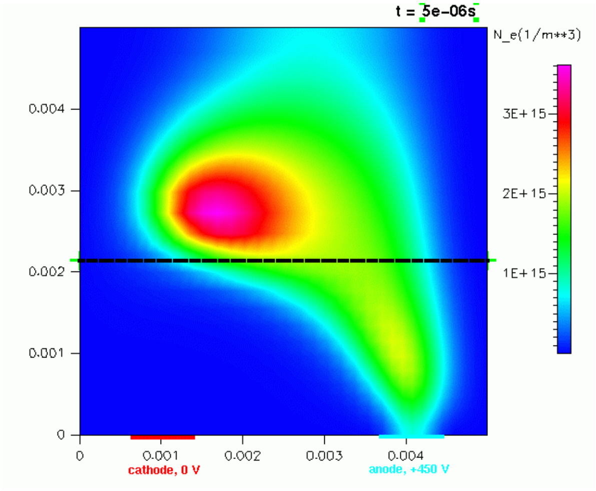

1.2 Torr, 450 V, N_2

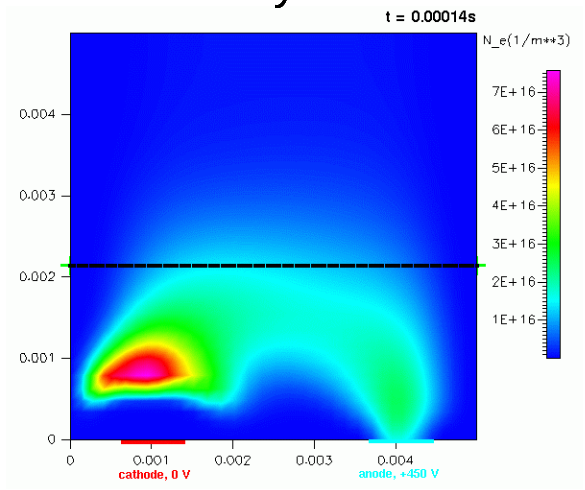

4 Torr, 450 V, N_2

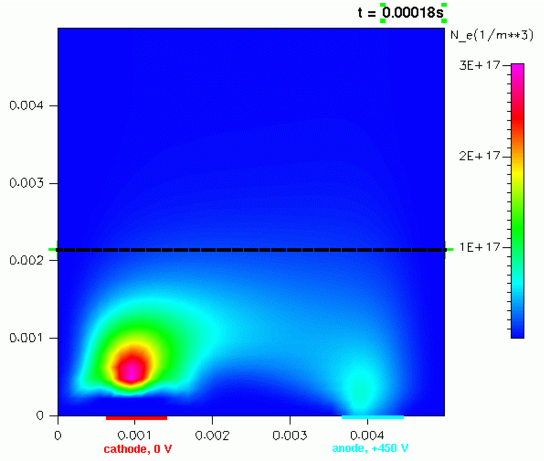

6 Torr, 450 V, N_2

Micro Discharge: Calculation of the EDF

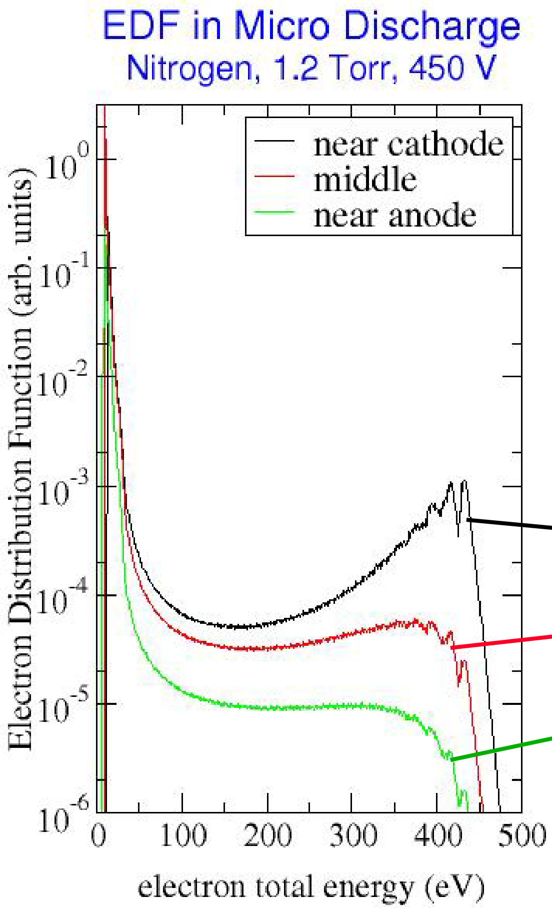

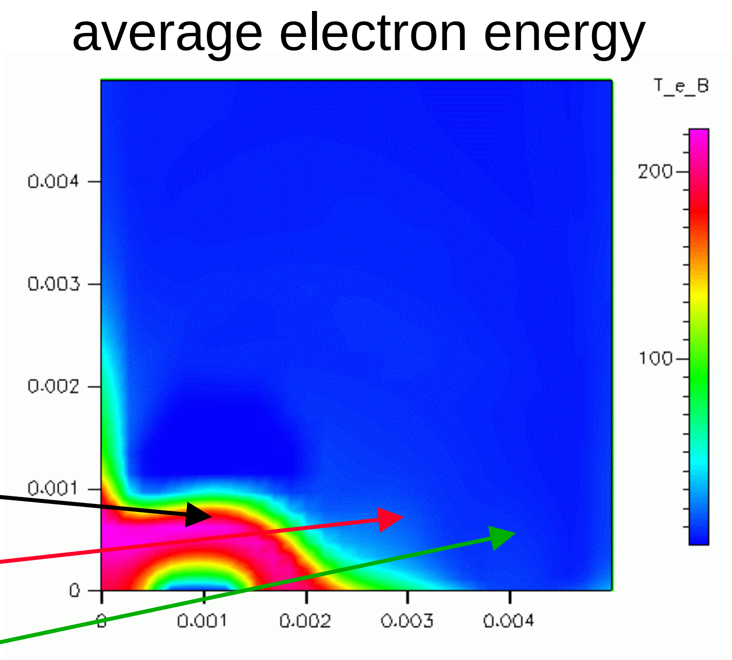

C.G.Wilson et al., J. Appl. Phys. 94, 2845 (2003)

- predicted EDF shows typical behavior in DC glow discharge
- tail of EDF formed by progeny electrons ejected from cathode
- body of EDF formed by elastically scattered electrons

DC Discharge with Ring Anode

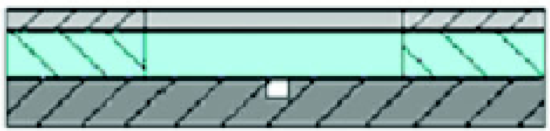

Simulations by E.Toinov using CFD-ACE

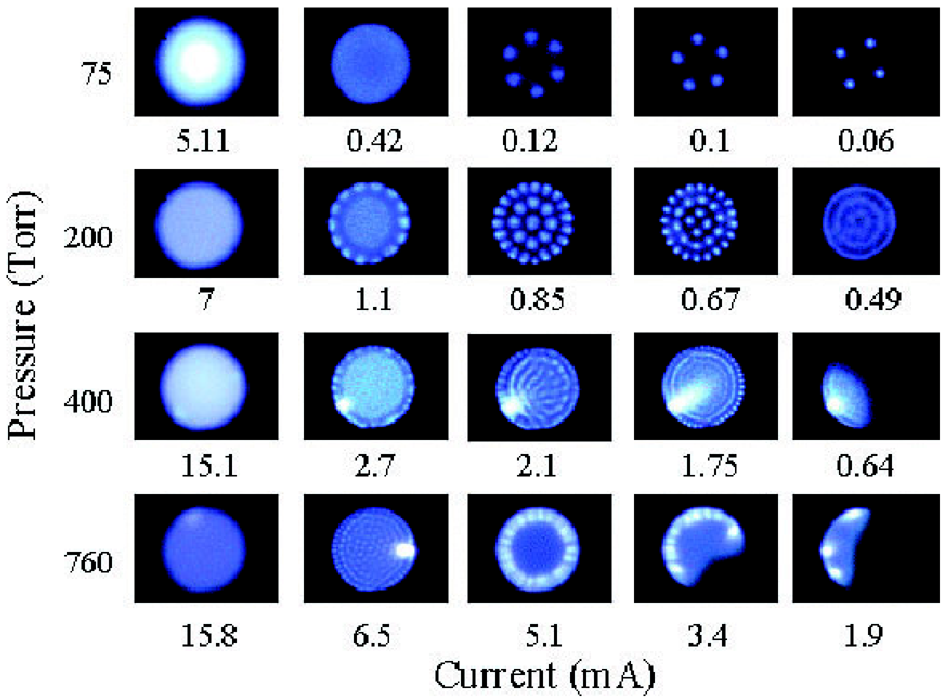

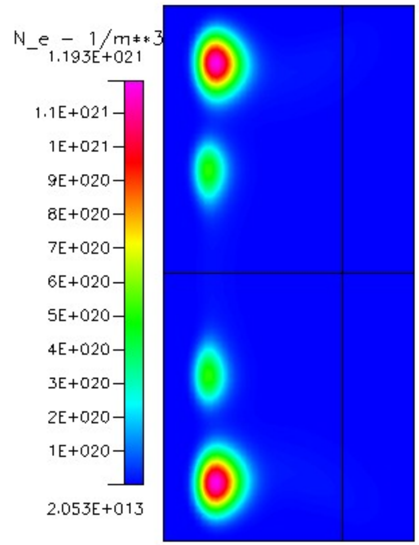

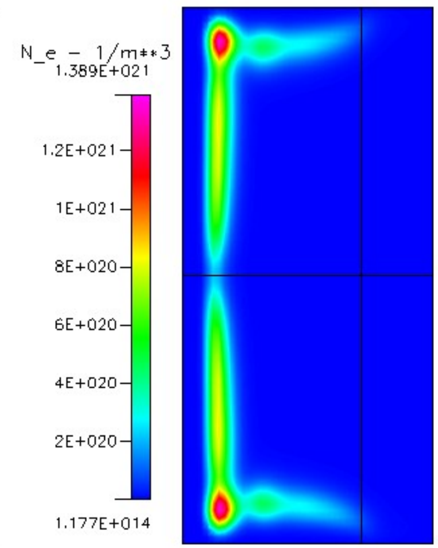

U=279V, I=4mA

U= 381V, I=19mA

Experiment by K.Schoenbach et al.
PSST 13, 177 (2004)

Xenon, P=100Torr, Gap=250micron, R=375micron
Initial voltage =400V, gas heating, Gamma=0.002

Experimentally observed cathode spots arranged in concentric circles have been obtained in two-dimensional simulations of high-pressure DC micro discharges with ring anode in Xenon

Plasma Display Simulations

Fujitsu Unveils New Type of Plasma Technology for 100-Inch-Plus Flat-Screen Displays

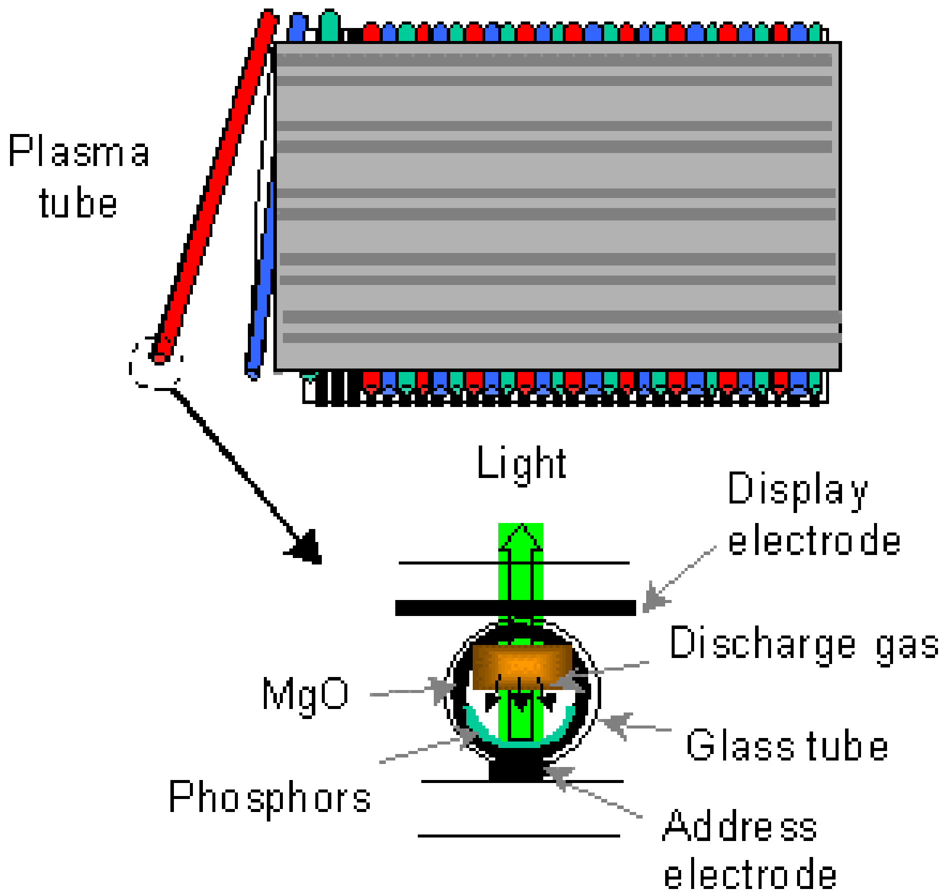

CFD-ACE+ simulations by E.Toinov

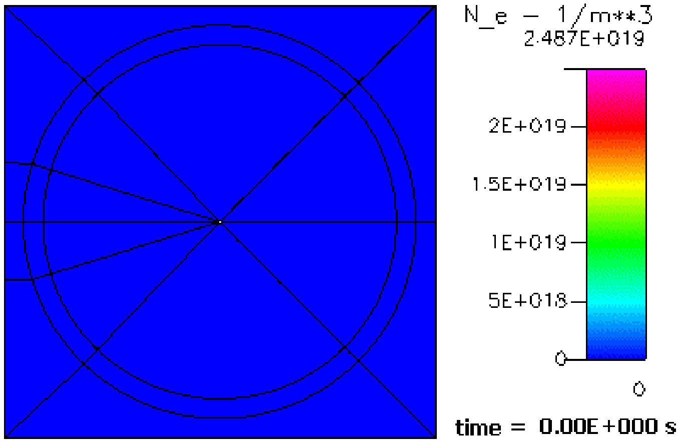

Discharge conditions: Helium, P=400torr, Pulse 6kV/50ns, R=0.5mm

This technology has the following features:

1. Ultra-lightweight, flexible screen size & shape
2. High luminous efficiency
3. Low-cost production

What have we learned ?

- Positive Column is the most studied object in gas discharge physics. It is unexpected to find a new physical effect in such a system
- We have first discovered a paradoxial non-monotonic distribution of excitation rates and excited species densities in simulations
- This effect has been later understood and confirmed by theoretical analysis and there is some experimental evidence
- Further experimental studies are required to observe this effect in real systems
- The effect has its origin in the kinetics of electrons and gives another evidence of the importance of electron kinetics in gas discharges
- Simulations become a predictive tool for studies of plasma systems

Dielectric Barrier Discharges

Plasma Optimization for Efficient Generation of UV Radiation and Active Radicals

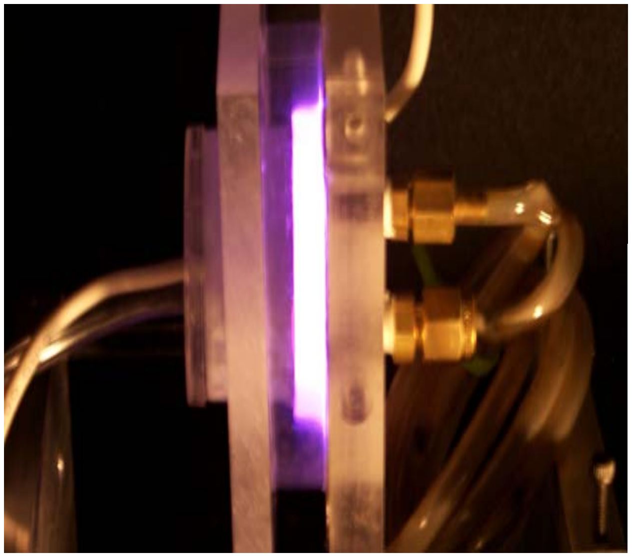

Pulsed power DBD in atmospheric pressure:.pulse frequency is 1kHz, the pulse width is 400ns, and the amplitude is 8kV (experiments by M.Laroussi)

The **goal of this project** is to optimize the pulsed-power atmospheric pressure non-equilibrium plasma sources for efficient generation of UV radiation and active radicals using a combination of experimental studies and advanced plasma simulations to explore whether the added complexity of fast risetime pulsed circuits has a payoff in terms of UV radiation output and overall chemical-processing efficiency

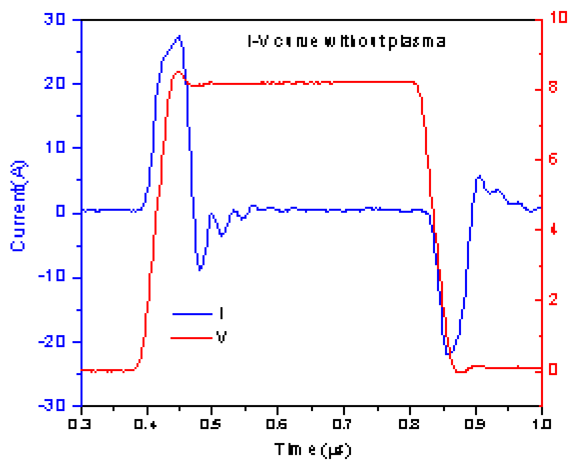

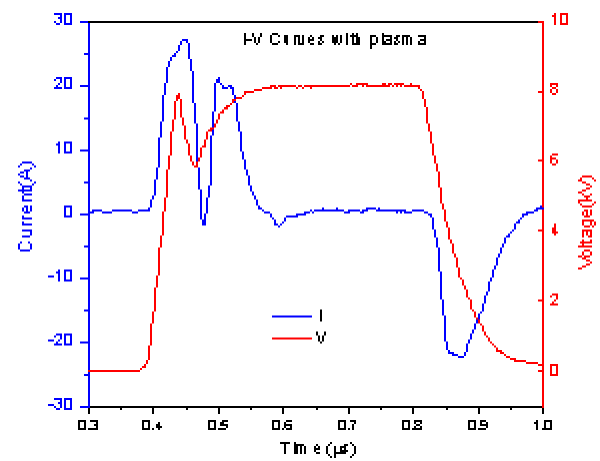

Measured current and voltage curves without (left) and with (right) the presence of plasma.

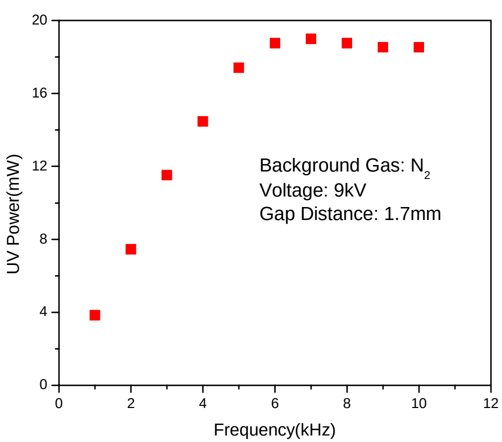

Total emitted UV power versus pulse frequency. The pulse width is 500ns, background gas N_2, applied voltage 9kV, and gap distance 1.7mm.

M.Laroussi et al., J. Appl. Phys. 96, 3028 (2004)

Plasma Optimization for Efficient Generation of UV Radiation and Active Radicals

Simulations of pulsed DBD in He-N_2-Air Mixtures

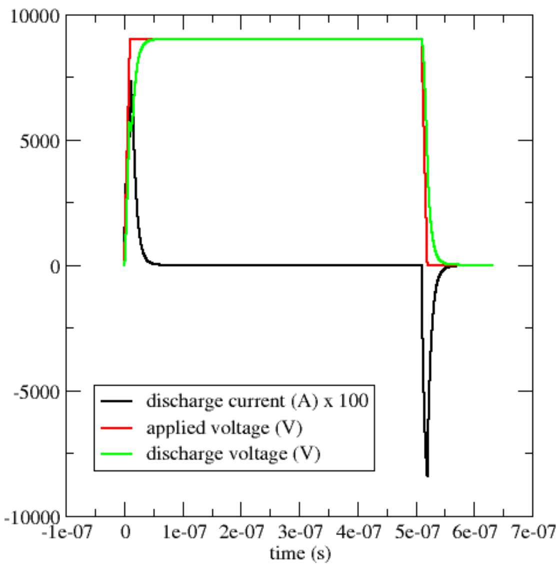

Discharge voltage and current for 9 kV, 500ns pulses

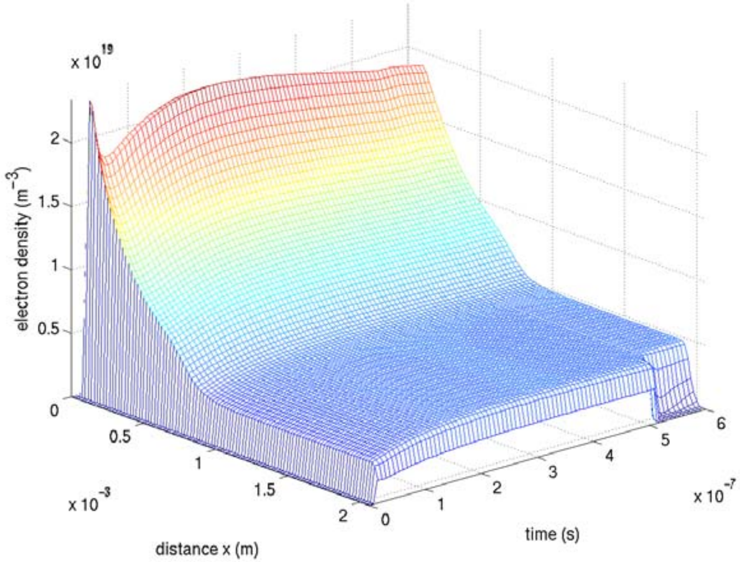

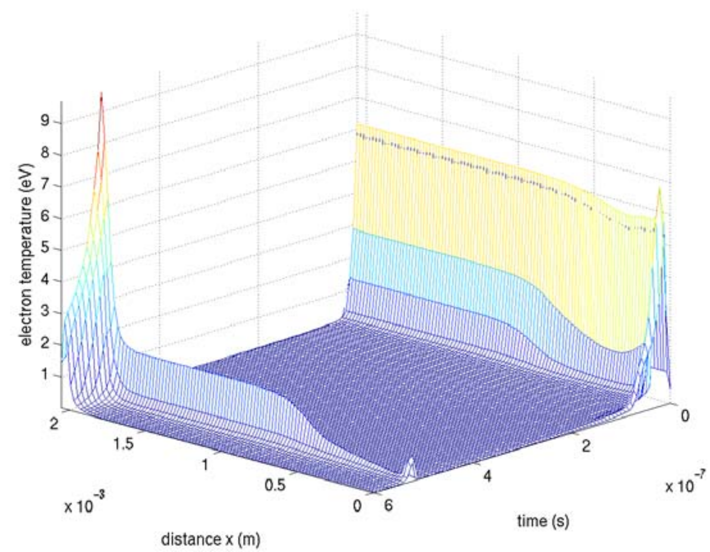

Electron density and temperature during active pulse of DBD plasma with 9 kV pulses

Simulation of pulsed dielectric barrier discharge xenon excimer lamp

Breakdown stage

Excimer lamps are efficient sources of non-coherent ultraviolet (UV) or vacuum ultraviolet (VUV) radiation generated by rare gas dimers and rare gas halides.

The dielectric barrier discharges (DBD) are ideally suited to induce excimer formation

To understand qualitatively the increased efficiency in the pulsed operating regime, a comprehensive numerical model of pulsed DBD for excimer lamps has been developed

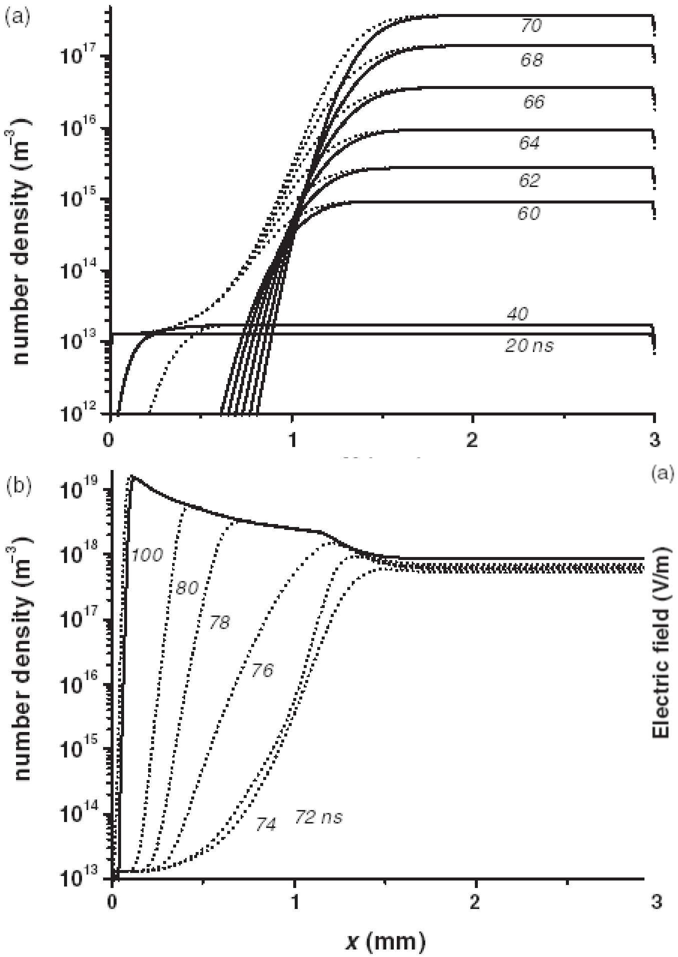

Spatial distributions of electron and ion densities and electric field at different times during gas breakdown stage

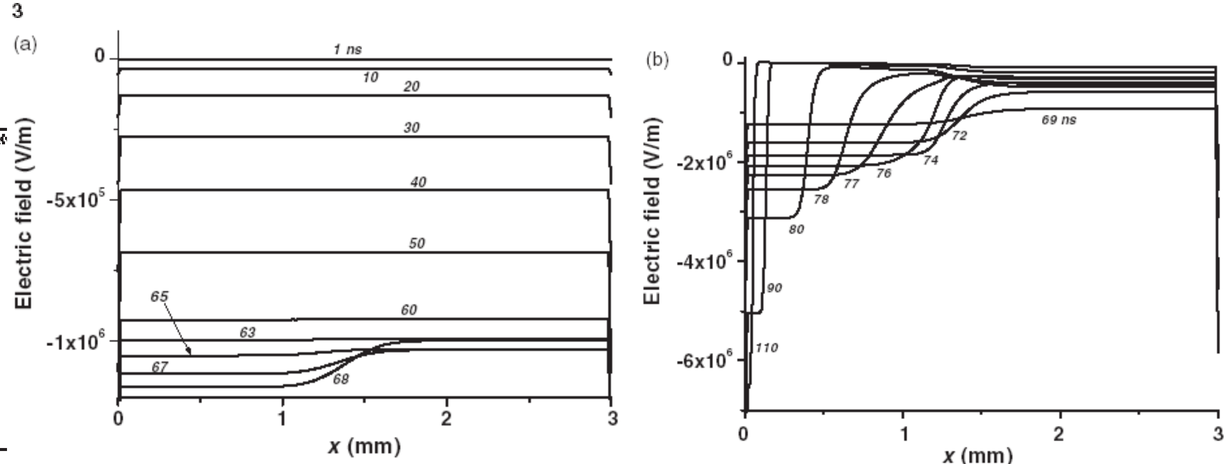

E.Bogdanov et al., J. Phys. D 37, October (2004)

Simulation of pulsed dielectric barrier discharge xenon excimer lamp

Afterglow stage

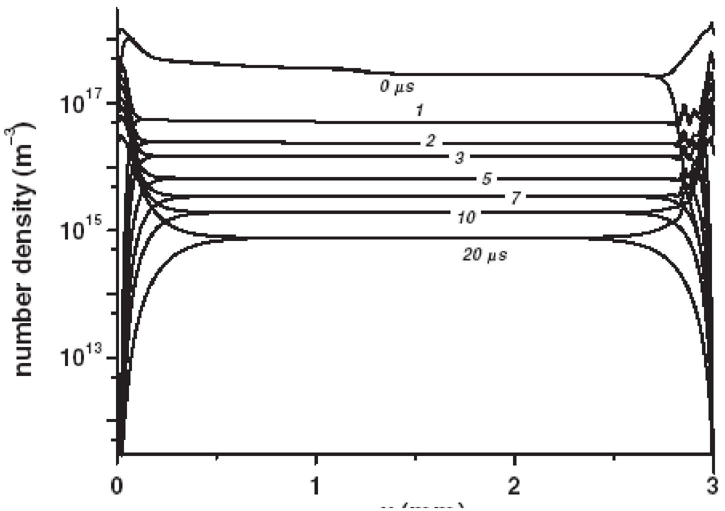

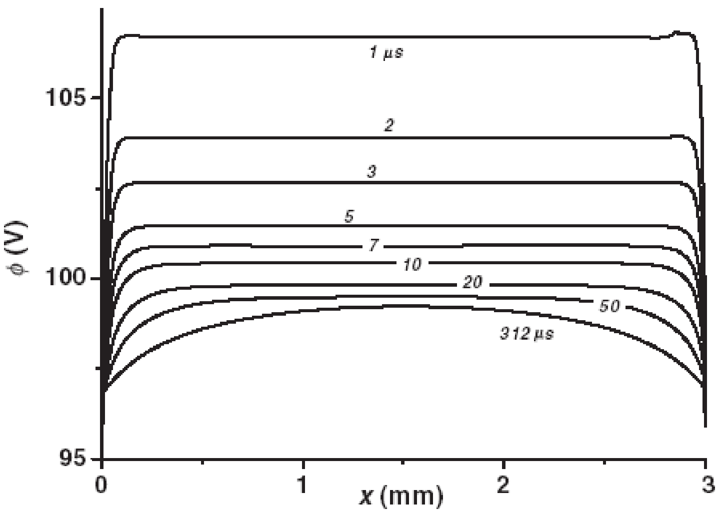

Plasma decay during the afterglow defines the breakdown dynamics which depends significantly on whether the gas is initially ionized or not. .

High over-voltages applied on non-ionized gas result in streamers, whereas the discharge development of initially ionized gas can take place under uniform conditions.

It is hence very important to model correctly the whole discharge pulse including both the breakdown and the afterglow stages.

Spatial distributions of electron and ion densities and electrostatic potential at different times in the afterglow.

It is seen that plasma remains quasi-neutral during the afterglow stage (ion and electron densities have the same values) with except of the sheath areas.

E.Bogdanov et al., J. Phys. D 37, October (2004)

Conclusions about DBD simulations

• Simulations helped us to understand the important features of DBD operation in pulsed power regime and clarify optimization scenarios for improvements of plasma sources for generation of active radicals and UV output.

• Two distinct stages. In the first, fast stage, the power deposition takes place over a short time period of the order of several 10s ns. This phase is the most crucial for DBD optimization. By tailoring the electron spectrum one can affect the efficiency.

• The "afterglow" stage defines the plasma composition, determines how the next current pulse will occur.

• Simulations have confirmed that electron emission at dielectric surfaces plays minor role in the discharge dynamics - distinguish it from traditional (slow) breakdown that occurs in DBDs driven by low frequency RF sources

Conclusions

- **CFD-ACE+PLASMA has reached the state of maturity and has been used for simulations of different plasma devices and processes**

- **The Plasma Technologies Branch at CFDRC continues to develop advanced plasma models and customize CFD-ACE for user's needs**

- **Potential Research and Development areas include (but not limited to)**
  - **Radiation Transport in Plasma Sources**
  - **Microwave Plasmas**
  - **Multi Scale Simulations for Nano-Technologies**
  - **Rarefied Gas Dynamics**

FPE & its Numerical Solution

$$\frac{\partial f}{\partial t} + \nabla \cdot \left[D_r \nabla f + \mathbf{V}_r f \right] + \frac{1}{\chi(u)} \frac{\partial}{\partial u} \left(\chi(u) \left[D_u \frac{\partial f}{\partial u} + V_u f \right] \right) = S$$

Operator splitting technique

$$\frac{\partial f}{\partial t} = \mathrm{F_r} + \mathrm{F_u}$$

introduce a residual function $\mathrm{R}(f) = \mathrm{F_r} + \mathrm{F_u} - \frac{\partial f}{\partial t}$ and use the iterative method

To find the value of f^{n+1} for the next iteration, we first solve for f* in physical space

$$\left(\frac{1}{\Delta t} - \theta(1 + \beta \delta_{ij}) \mathrm{F_r} \right) f' = \mathrm{R}(f^{(n)}) \qquad f^* = f^{(n)} + \alpha f'$$

Then we solve for f^{**} in the energy space

$$\left(\frac{1}{\Delta t} - \theta(1 + \beta \delta_{ij}) \mathrm{F_u} \right) f^{**} = \mathrm{R}(f^*) \qquad f^{(n+1)} = f^* + \alpha f^{**}$$

Here α is a linear relaxation parameter ($0 < \alpha < 1$), and β is the inertial relaxation parameter

Visualization of Simulation Data

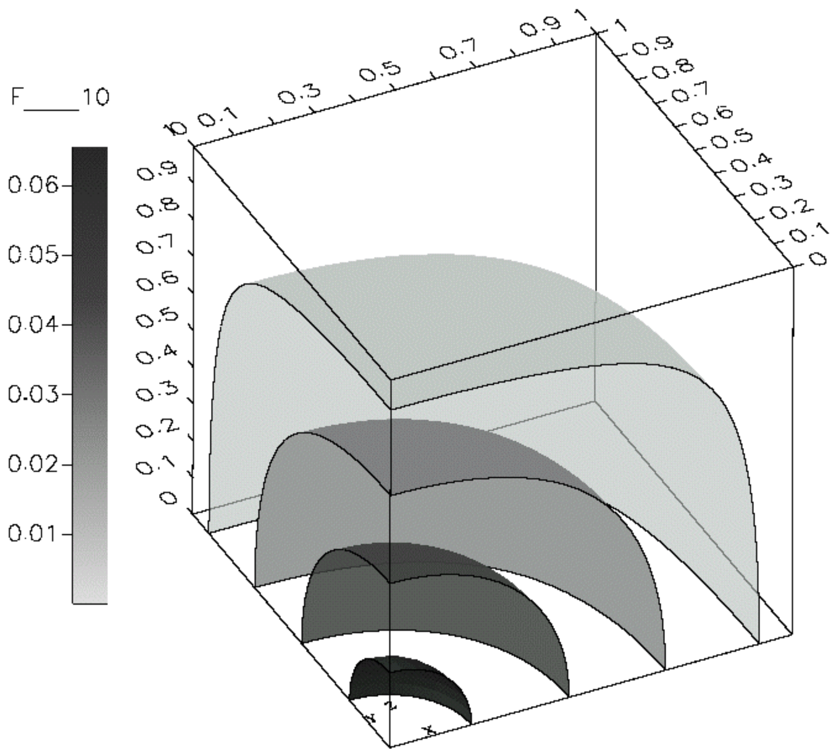

boundary conditions

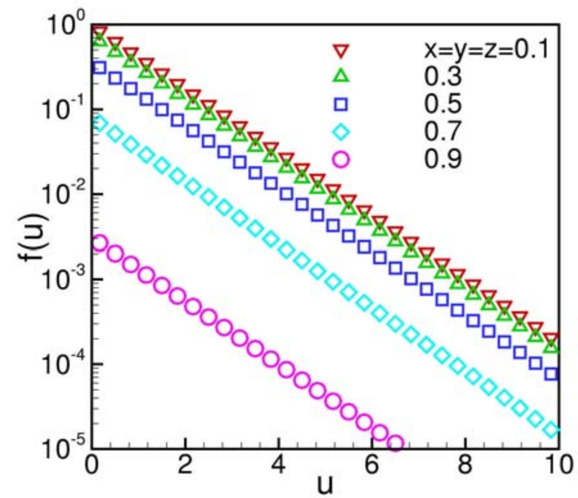

4D box: 0<x<1, 0<y<1, 0<z<1, 0<u<10

$$\chi(u) = 1 \quad D_r = 1 \quad V_r = 0 \quad D_u = 10 \quad V_u = 0 \quad S = 0$$

$$f(x, y, z, u = 0) = \cos(\frac{\pi x}{2})\cos(\frac{\pi y}{2})\cos(\frac{\pi z}{2}) \qquad \frac{\partial f}{\partial u} = -\alpha f \qquad \text{at u=10}$$

$$\frac{\partial f}{\partial n} = 0 \qquad \text{at x=0, y=0, z=0,}$$

$$f(x, y, z, u) = 0 \qquad \text{at x=1, y=1, or z=1.}$$

$$f(x, y, z, u) = \cos(\frac{\pi x}{2})\cos(\frac{\pi y}{2})\cos(\frac{\pi z}{2})\exp(-\alpha u)$$

$$\alpha = \frac{\pi}{2}\sqrt{\frac{3}{10}}$$

Structure of Plasma Simulators

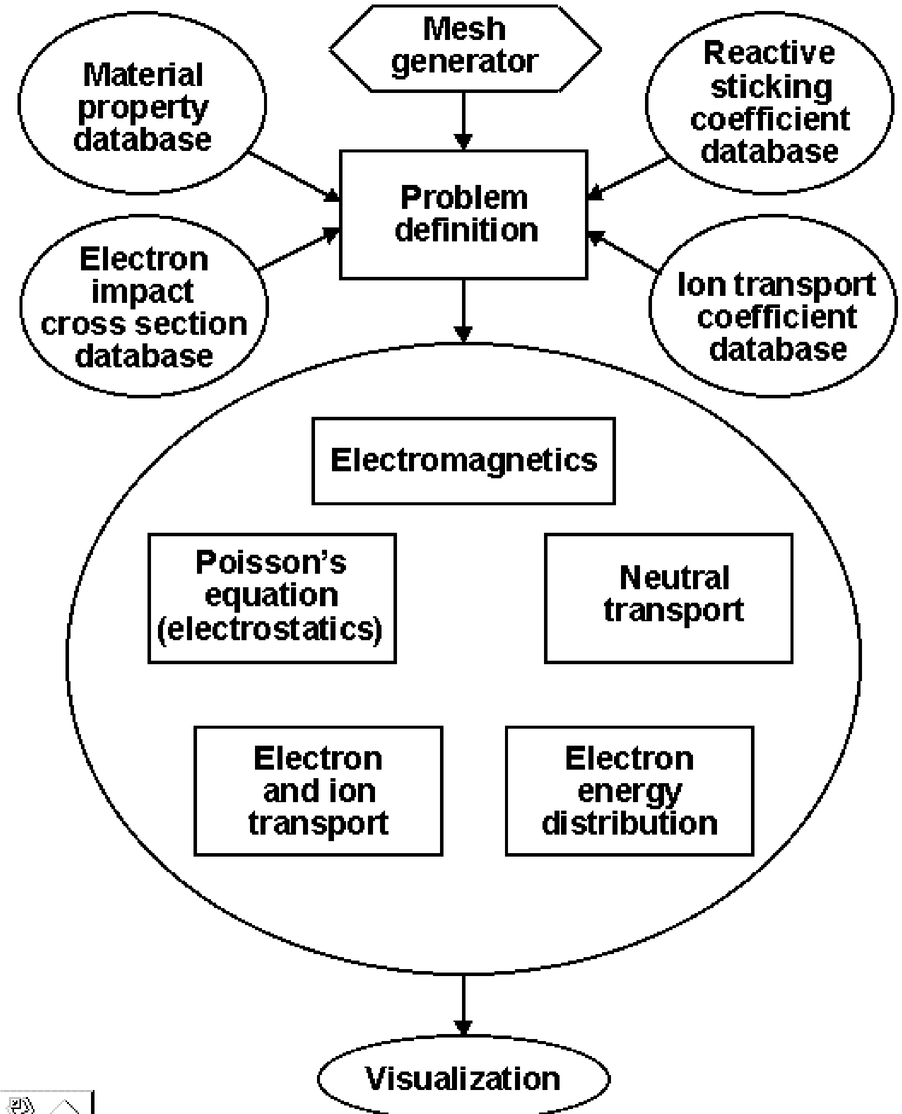

f_0

Coupling electron kinetics and electro-magnetics

- Having solved FPE for electron energy distribution function, we calculate macroscopic properties of electrons (mobility and diffusion coefficients) and rates of electron induced chemical reactions

- We solve the electron density balance together with the kinetic equation using the electron production rate and electron flux provided by the kinetic module.

- The electron number density calculated in such a way is used in Poisson and Maxwell equations for calculation of electrostatic and electromagnetic fields.

Choosing the right physical model

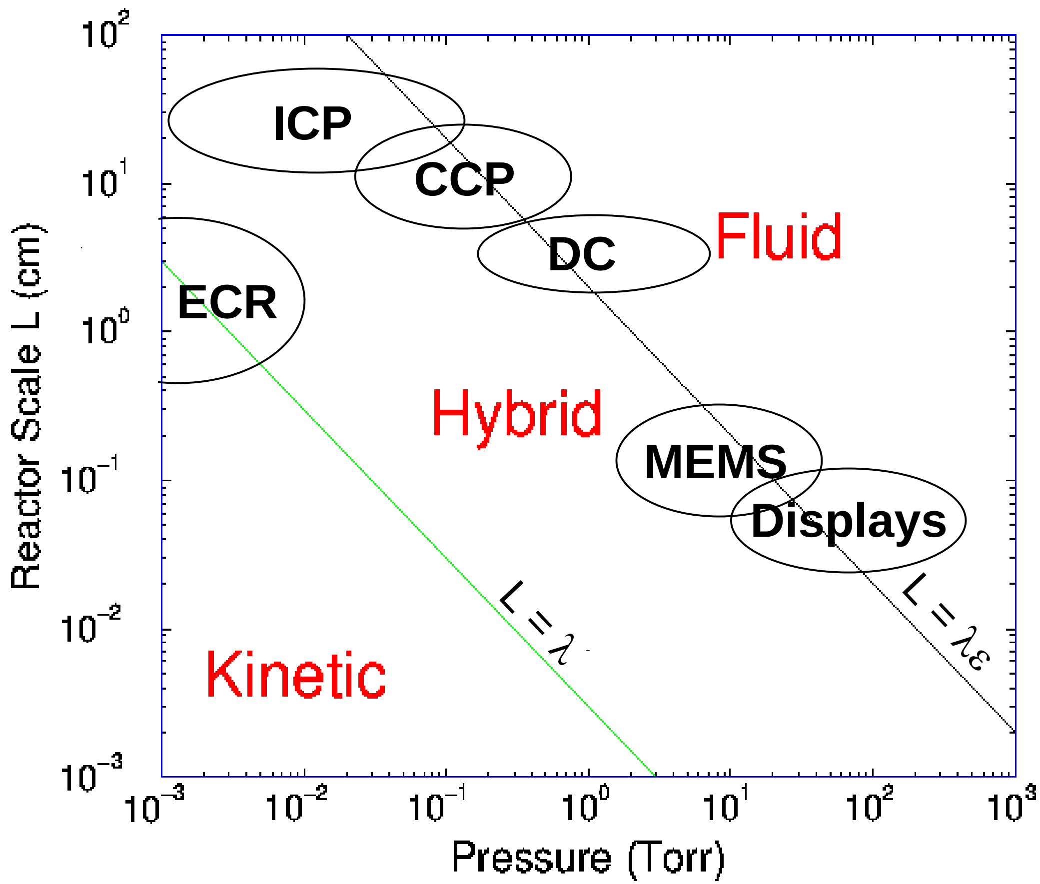

•***Fluid models:*** Conservation of density, momentum and energy for electrons, ions and neutral species

•***Kinetic models:*** Solving Boltzmann equation for the particle distribution function

•***Hybrid models:*** Fluid model for heavy species and kinetic model for electrons

He, 100 mTorr, 200 V

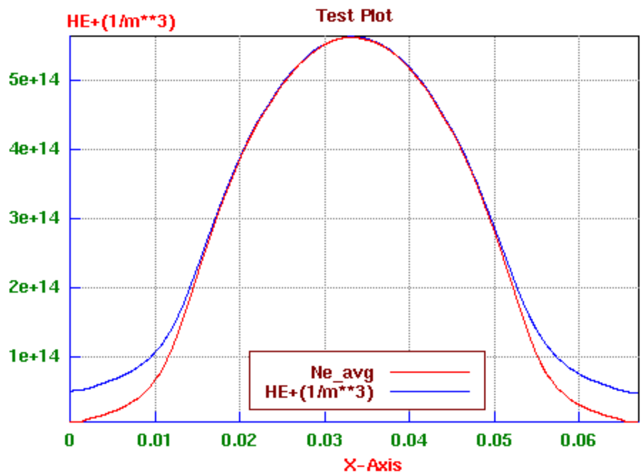

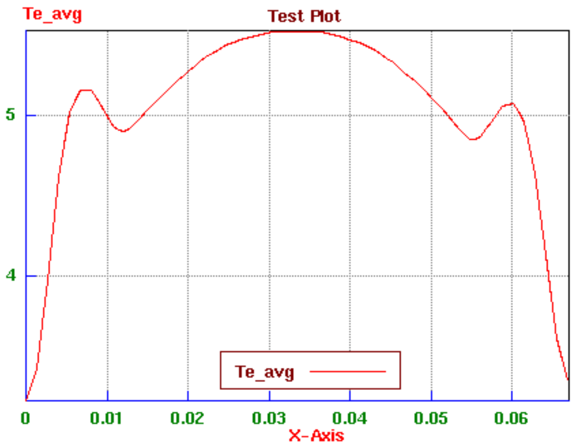

- predicted current density is about 0.8 mA/cm^2 for these conditions
- The central electron density predicted by CFD-ACE+Plasma is about 5.6×10^8 cm^{-3}.
- data in Ref. [1]: electron density varies from 4.5×10^8 cm^{-3} to 1.6×10^9 cm^{-3} for different models
- T_e varies from 2.4 to 6.7 eV in Ref. [1]. CFD-ACE+Plasma predicts the (effective) electron temperature of 5.5 eV.

EEDF Maxwellization & Reaction Rates

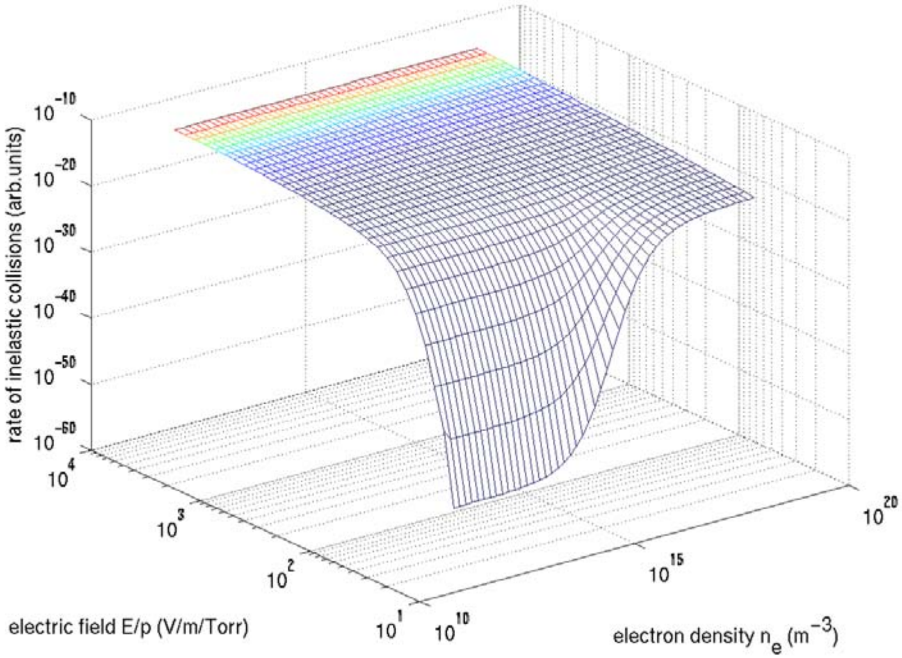

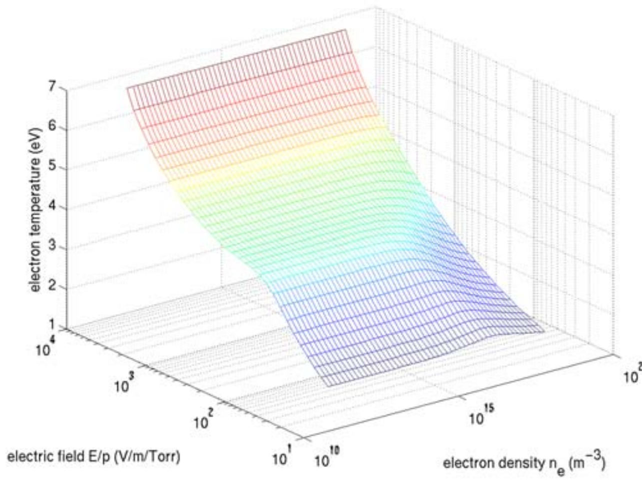

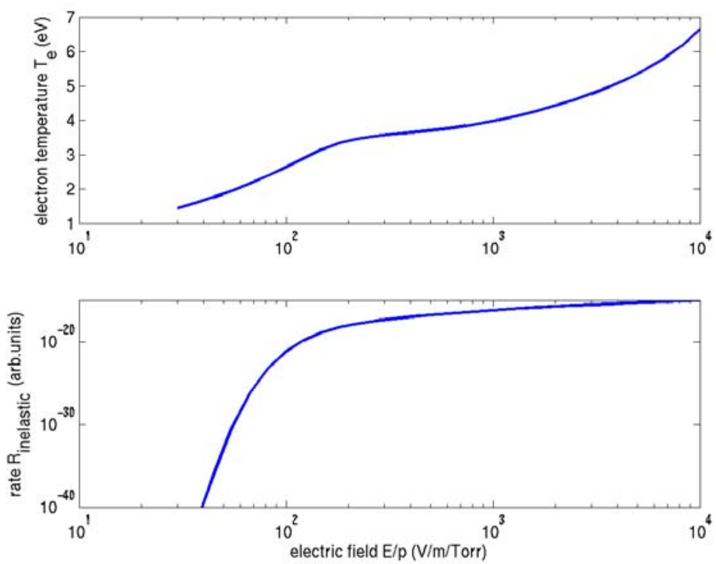

- EEDF Maxwellization due to Coulomb collisions among electrons results in a strong dependence of inelastic collision rates on electron density
- This effect is most pronounced for the elastic energy balance of electrons

50 μs pulse, high coil current: time evolution

Electron density, reactor center

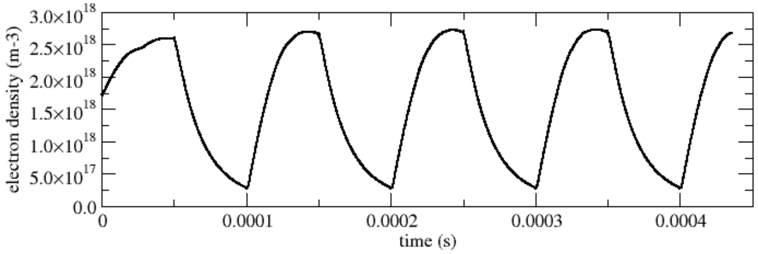

Electron temperature, reactor center

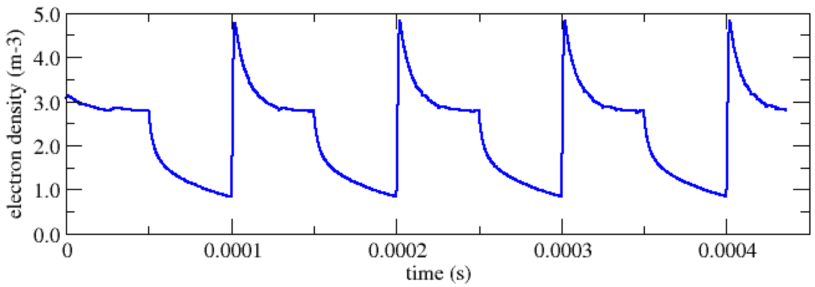

- **small “ripples” on Te are numerical due to finite energy resolution in the Boltzmann solver**

- **high current operation: plasma reaches steady state during active phase**

30 μs pulse, low coil current: time evolution

Electron density, reactor center

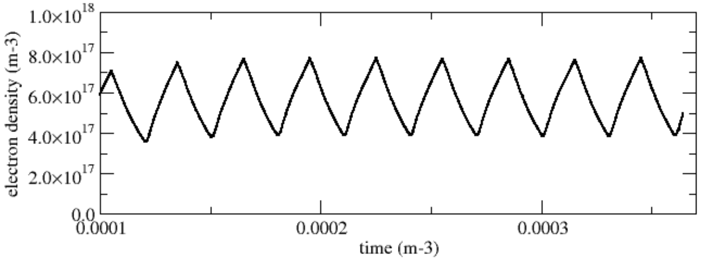

Electron temperature, reactor center

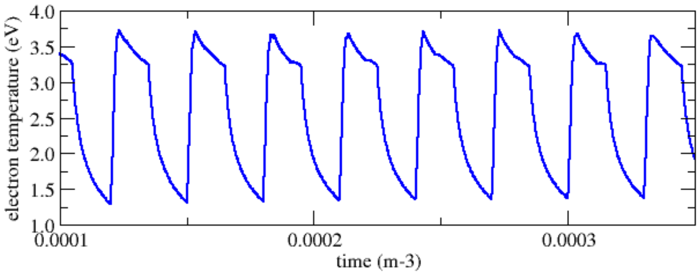

- **small "ripples" on Te are numerical due to finite energy resolution in the Boltzmann solver**

- **short-length pulse operation: plasma does not reach steady state during active phase**

Non-monotonic excitation profiles explained

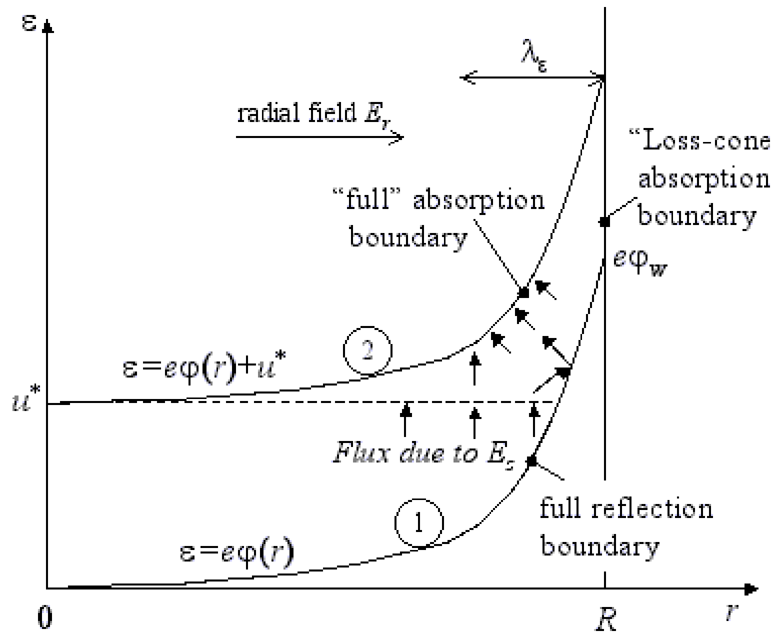

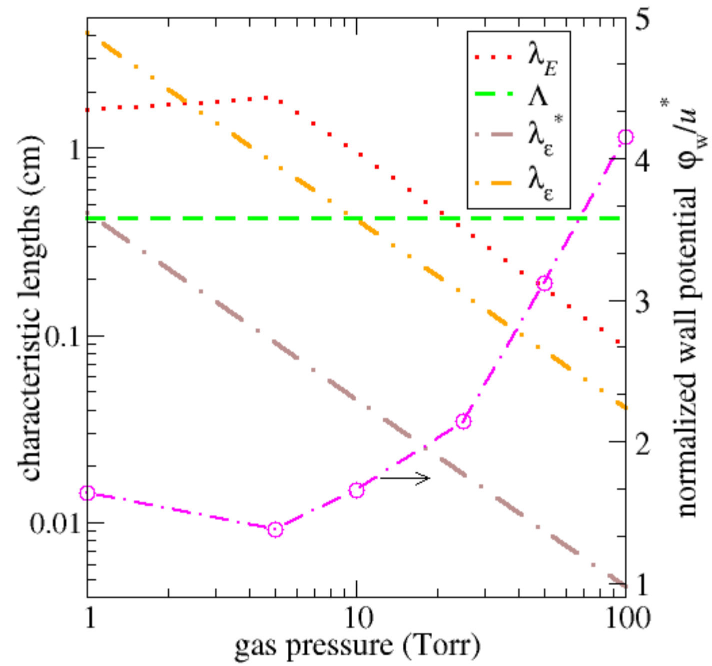

PC was simulated in a wide range of pressures (0.1-100 Torr) and currents μA-0.1A in Ar and He gases

♦The predicted flux of electrons shown schematically by arrows is directed towards the discharge center. The electron flux to boundary 2 (where $u = u^*$) defines the rates of inelastic processes.
♦ The increased radial flux of electrons at this boundary is responsible for the enhancement of inelastic collision rates at the discharge periphery.

R.Arslanbekov et al., Applied Physics Letters 85 (15), October (2004)

140 mTorr and 50 V RF voltage

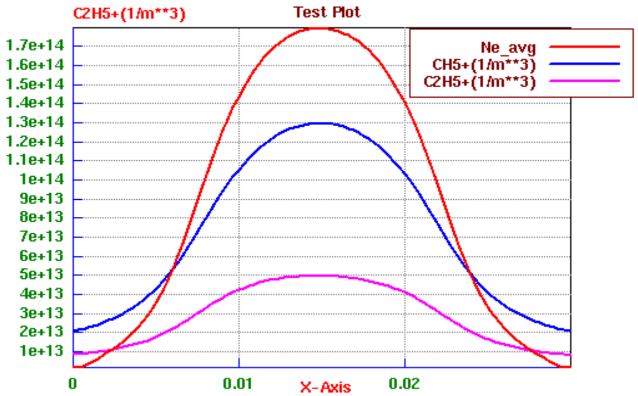

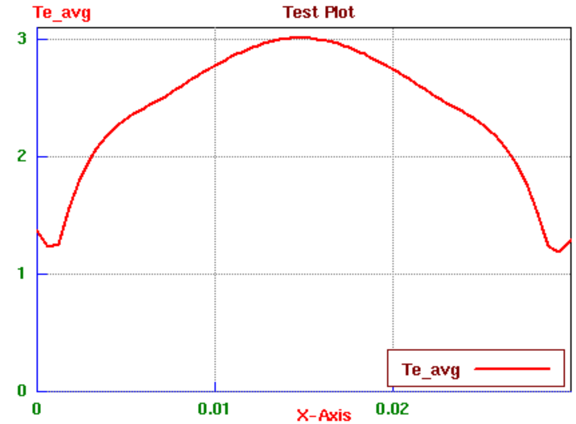

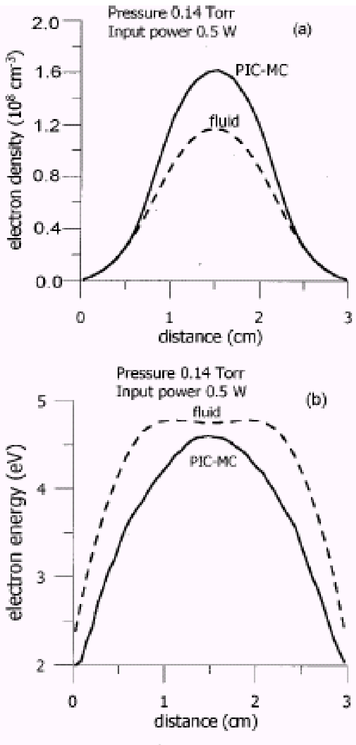

FIG. 4. Stationary state spatial distributions of: (a) the electron density and (b) the electron energy at a pressure of 0.14 Torr and an input power of 0.5 W, averaged over a rf cycle, calculated with the PIC–MC model (sold lines) and the fluid model (dashed lines).

- electron temperature profile is drastically different from that obtained in the high current density case (with 400 V RF voltage)
- discharge current density predicted by CFD-ACE+Plasma is about 0.25 mA/cm^2 (0.22 mA/cm^2 in Ivanov *et al*.).
- charged-particle's profiles, as well as the (effective) electron temperature profiles are close to those obtained in Ivanov *et al*.

CH_4 , 140 mTorr, 400 V RF

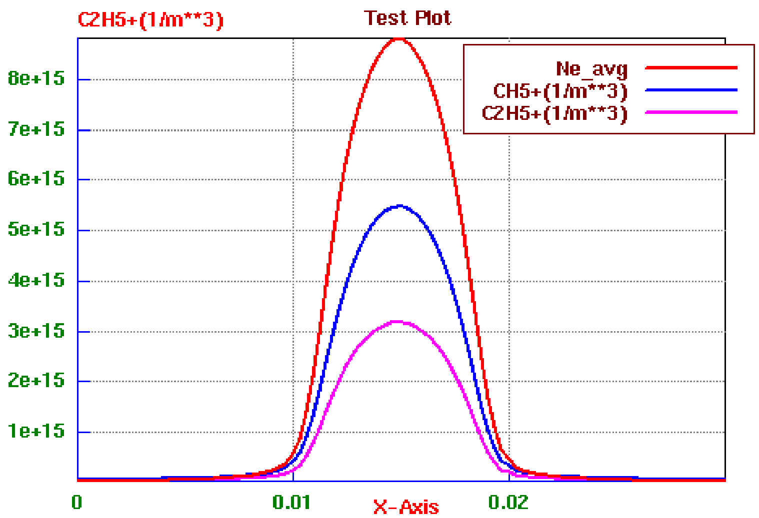

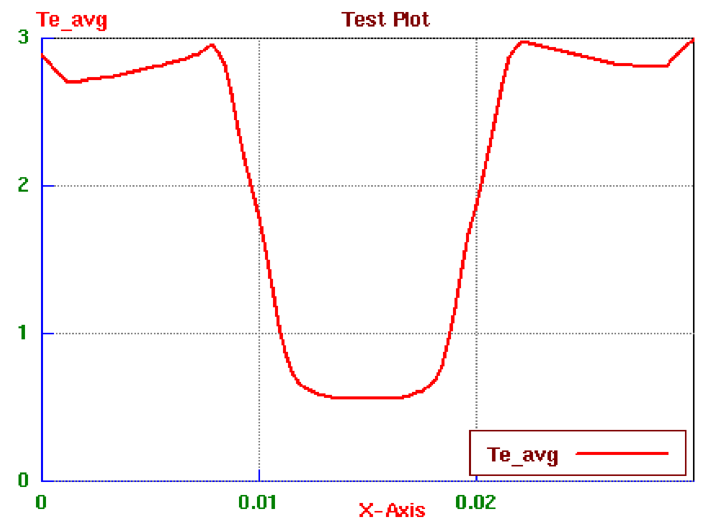

- current density predicted by CFD-ACE+Plasma is about 2 mA/cm^2, which agrees well with that of 2.2 mA/cm^2 obtained in Ivanov *et al*

- the charged-particle's profiles, as well as the (effective) electron temperature profiles are close to those obtained in Ivanov *et al*

- the electron energy profiles feature a strong dip in the plasma center due to the cold peak on the EDF.

- The electron density predicted by CFD-ACE+Plasma is lower than in Ivanov *et al* (~10^{10} cm^{-3} vs ~3×10^{10} cm^{-3}), which most likely due to different ion mobilities used in the two codes.